Aus dem Institut für Virologie
des Fachbereichs Veterinärmedizin
der Freien Universität Berlin

Attachment of stearic acid to the Hemagglutinin-Esterase-Fusion (HEF) protein of influenza C virus affects membrane fusion and virus replication

Inaugural-Dissertation
zur Erlangung des Doctor of Philosophy (Ph.D.)-Grades
in Biomedical Sciences
an der
Freien Universität Berlin

vorgelegt von

Mingyang Wang

aus der Volksrepublik China

Berlin 2015

Journal-Nr.: 3818

Gedruckt mit Genehmigung des Fachbereichs Veterinärmedizin

der Freien Universität Berlin

Dekan:	Univ.- Prof. Dr. Jürgen Zentek
Erster Gutachter:	PD Dr. Michael Veit
Zweiter Gutachter:	Prof. Dr. Andreas Herrmann
Dritter Gutachter:	Univ.- Prof. Dr. Klaus Osterrieder

Deskriptoren (nach CAB-Thesaurus):
Influenza C virus, glycoproteins, spikes, hemagglutinins, esterases, fusion proteins, modification, fatty acids, stearic acid, mutational analysis, growth curve, transport, protein composition, electron microscopy, hemolysis

Tag der Promotion: 18.09.2015

Bibliografische Information der *Deutschen Nationalbibliothek*
Die Deutsche Nationalbibliothek verzeichnet diese Publikation in der Deutschen Nationalbibliografie; detaillierte bibliografische Daten sind im Internet über <http://dnb.ddb.de> abrufbar.

ISBN: 978-3-86387-652-4
Zugl.: Berlin, Freie Univ., Diss., 2015
Dissertation, Freie Universität Berlin
D188

Choriner Str. 85 - 10119 Berlin
verlag@menschundbuch.de – www.menschundbuch.de

Abstract

The only spike of Influenza C virus, the hemagglutinin-esterase-fusion glycoprotein HEF combines receptor binding, receptor hydrolysis and membrane fusion activities. HEF is S-acylated, but in contrast to HA of Influenza A and B virus, it contains just one acylation site, a cysteine located at the cytosol-facing end of the transmembrane region which contains stearic acid. Previous studies established the essential role of S-acylation of HA for replication of Influenza A and B virus by affecting budding and/or membrane fusion, but the function of acylation of HEF was hitherto not investigated.

Using reverse genetics we rescued a virus containing non-stearoylated HEF, which was stable during serial passage and showed no competitive fitness defect, but the growth rate of the mutant virus was reduced by one log. Acylation of HEF does neither affect the kinetics of its plasma membrane transport nor the protein composition of virus particles. Cryo-electron microscopy showed that the shape of viral particles and the hexagonal array of spikes typical for Influenza C virus were not influenced by this mutation indicating that virus budding was not disturbed. However, the extent and kinetics of hemolysis were reduced in mutant virus suggesting that non-acylated HEF has a defect in membrane fusion.

Key words: influenza C virus, reverse genetics, HEF, acylation, stearoylation, membrane fusion

Zusammenfassung

Die Anheftung von Stearinsäure an das Hämagglutinin-Esterase Fusionsprotein (HEF) von Influenza C virus beeinträchtigt die Membranfusion und die Virusreplikation

Die einzige Spikeprotein der Influenza C Viren, das sogenannte Hämagglutinin-Esterase-Fusionsglycoprotein (HEF) besitztrezeptorbindende, rezeptorzerstörende und membranfusionierende Aktivität. Es vereint damit die Aktivitäten der beiden Membranproteine Hämagglutinin (HA) und Neuraminidase (NA) der Influenza A und B Viren. HEF ist kovalent mit Fettsäuren modifiziert, aber im Gegensatz zum HA besitzt es nur eine Acylierungsstelle, nämlich ein Cystein lokalisiert an dem Cytosol-zugewandten Ende seiner Transmembranregion. Zudem wird HEF mit Stearinsäure, und nicht, wie die meisten anderen acylierten Proteine, mit Palmitinsäure modifiziert. Frühere Studien etablierten die essentielle Rolle der Acylierung des HA für die Replikation von Influenza A und B Viren, wobeientweder der Viruseintritt durch Membranfusion oder die Virusfreisetzung gestört war. Die Funktion der Acylierung von HEF wurde bisher noch nicht untersucht.

Mit Hilfe der reversen Genetik habe ich ein rekombinantes Virus hergestellt, welches nicht-acyliertes HEF enthält. Die eingefügte Mutation ist stabil während einerseriellen Viruspassage und die mutierten Viren zeigten keinen Fitnessdefekt, aber die Wachstumsrate der mutierten Virenwar um etwa eine Zehnerpotenz gegenüber dem Wildtyp-Virus reduziert. Die Acylierung des HEF hat weder Einfluss auf die Kinetik seines Transportes zur Plasmamembran noch auf die Proteinzusammensetzung von Viruspartikeln. Kryo-Elektronenmikroskopie zeigte, dass die Morphologie der Viruspartikel und auch die für Influenza C Viren typische hexagonale Anordnung der Spikeproteine von der Mutation nicht beeinflusst wurden. Jedoch zeigten mutierte Viren eine reduzierte Hämolyseaktivität, was darauf hindeutet, dass der virale Zelleintritt mittels Membranfusion gestört ist.

Schlagwörter: Influenza-C-Virus, reverse Genetik, HEF, Acylierung, Stearoylierung, Membranfusion

Abbreviations

bis-ANS	1,1'-bis (4-anilino) naphthalene-5,5'-disulfonic acid
bp	Base pair
C, Cys	Cystein
CM2	Influenza C ion-channel matrix protein 2
CPE	Cytopathogenic effect
Cs	non-acylation mutant (mutate stearoylated Cysteine into Serine)
CoV	Coronaviruse
CT	Cytoplasmic tail
DMEM	Dulbecco's Modified Eagle Medium
DNA	Deoxyribonucleic acid
DOPC	1, 2 - Dioleoyl - sn - Glycero-3 - Phosphocholin
E.coli	*Escherichia coli*
ER	Endoplasmic reticulum
FCS	Fetal calf serum
GFP	Green fluorescent protein
HA_0	Hemagglutinin precusor
HA_1, HA_2	Hemagglutinin subunits
HEF	Hemagglutinin-esterase-fusion protein
HEF_1, HEF_2	Hemagglutinin-esterase-fusion protein subunits
HI	Hemagglutination inhibition experiment
IP	Immunoprecipitation

kDa	Kilo dalton
LB	Luria –Bertani
mAb	Monoclonal antibody
MDCK- I	Madin- Darby canine kidney cell type I
M1	Matrix protein 1
MOI	Multiplicity of infection
NA	Neuraminidase
ORF	Open reading frame
Opti-MEM	Opti-MEM® I Reduced Serum Medium
pal	Palmitate
PBS	Phosphate – buffered saline
p.i.	Post-infection
RBC	Erythrocyte
RNA	Ribonucleic acid
rpm	Revolutions per minute
RT	Room temperature
RT - PCR	Reverse transcription polymerase chain reaction
TMD	Transmembrane domain
S, Ser	Serine
SDS-PAGE	Sodium dodecyl sulfate polyacrylamide gel electropheresis
TCID50	50% tissue culture infective dose
TPCK-trypsin	Tosyl-phenylalanine chloromethyl-ketone treated trypsin

Vero	African green monkey kidney epithelial cell
WB	Western blot
Wt	Wild type
9-O-Ac-NeuAc	9-O-Acetyl-N-acetylneuraminic acid

Table of contents

List of Figures

1. Introduction

1.1 Epidemiology and pathology of influenza C virus

Influenza C virus was first isolated from throat washings of patients during epidemics of respiratory illness in 1947, which were found to be hemagglutinating viruses (1-3). In a serial hemagglutination inhibition (HI) experiments, this virus and corresponding antiserum showed no cross reaction with influenza A and B viruses and corresponding antiserum, therefore it was identified as a new genus in Orthomyxoviridae and named influenza C virus (1).

Influenza C virus usually causes upper respiratory tract inflammation but sometimes causes lower respiratory infection, especially in children from infants under 2 years old to children up six years old (4-6). Clinical symptoms as cough, fever, malaise are typically mild, but occasionally cause bronchitis, bronchiectasie and broncho-pneumonia (4-7). Though influenza C viruses occur primarily in a pattern of sporadic cases or in limited outbreaks of mild illness involving children or young adults (8, 9), serological studies indicated that this virus is widely distributed around the world and that the majority of humans acquire antibodies against the virus early in life (7, 10). In a serological study carried out in France in 1992, 61 to 70% of the population was found to have been previously exposed to the virus, the highest rates for positive samples being found in the 16- to 30-year-old group. In a 6-year tracking study in hospitalized children in Spain, influenza C infections accounted for 13.3% of influenza-positive cases (11). The results indicated intense circulation of influenza C virus in the population (12).

Human beings are thought to be the primary hosts and reservoir of influenza C virus, but there is some evidences that this virus possess the ability to infect animals (13) (Figure 1.1). Serological studies showed that influenza C virus antibodies are widely present in pigs and dogs (14-20). In 1981, a number of influenza C virus strains were isolated from pigs in Beijing and these strains could be transmitted from pig to pig under experimental condition (21). The existing strains are divided into 6 genetic and antigenic lineages according to phylogenetic analysis on HEF genes (Taylor/1233/47, Aichi/1/81, Sao Paulo/378/82, Kanagawa/1/76, Yamagata/26/81 and Mississippi/80) (22-24). We aligned these six lineages to show the homology and other common characteristics (supplemental material) and there is very little sequence variation. Therefore, influenza C virus was considered to be monosubtypic and stable in evolution. The evolutionary rate of the virus is much lower than

that of influenza A virus (22, 25). Though influenza C virus was considered to be stable in evolution and monosubtypic, reassortment events between strains within genus occur frequently and this leads the appearance of new strains better adapted to the host (23, 26). In 2011, an influenza C-like virus was isolated from clinically ill pigs exhibiting influenza-like symptoms (C/Oklahoma/1334/2011) and subsequently also from cattle (D/bovine/Oklahoma/660/2013) which subsequently turned out to be the main reservoir of this newly discovered virus (27-29). Phylogenetic analysis showed that these strains with 50% overall homology to human influenza C viruses. The divergence between these viruses and human influenza C viruses are similar to that observed between influenza A and B viruses (27). No cross reactivity was observed between these strains and human influenza C viruses in hemagglutination inhibition (HI) assays and serological typing by agar gel immunodiffusion (AGID). This new strain has a broader cell tropism than human influenza C virus and is capable of infecting and transmitting by direct contact in both pigs and ferrets. It also encodes a novel mechanism for generating the M1 protein and, importantly, is unable to reassort with human influenza C virus and generate viable progeny. Based on these differences to influenza C virus it was suggested that this virus warrants classification as a new genus of influenza virus, named influenza D virus (27, 28).

1.2 Evolutionary relationship of influenza C with other viruses

Influenza C virus possesses all the characteristics of Orthomyxoviridae family: the genome consists of single-stranded, negative-stranded, segmented RNA, and the nucleocapsid is wrapped by an envelope membrane (13, 30). The major difference between influenza A (B) virusparticle and influenza C viral particle is, that influenza A and B virus contain two spike proteins, Hemagglutinin (HA) and Neuraminidase (NA), while influenza C virus possess only one spike, designated Hemagglutin-Esterase-Fusion (HEF) protein, which combines both the functions of HA (receptor binding, membrane fusion) and NA (receptor destroying). Phylogenetic analyses of nucleoproteins and polymerase proteins indicated that all Influenza viruses have a common ancestor, but influenza A and B viruses are more closely related to each other than to influenza C virus (31-33). Phylogenetic analysis showed that the divergence between the HA gene of influenza A and B virus occurred later than the divergences between some HA-subtypes of influenza A virus subtypes (34). Based on the rate of amino acid substitutions in human influenza A virus HA genes, the earliest divergence time between subtypes of influenza A HA genes was estimated to be 200-300 years ago (35). The rate of amino acid substitution for influenza A virus HAs from duck, a natural virus

reservoir, was estimated to be 3.19×10−4 per site per year, which was slower than that for human and swine Influenza A virus HAs (0.56-2.03×10−3 per site per year), but similar to that for influenza B (5.3×10−4 per site per year) and C virus HEFs (2.3×10−4 per site per year). Based on this estimated substitution rate from duck, the divergences between different subtypes of Influenza A virus HA genes occurred several thousand to several hundred years ago. The earliest divergence time was estimated to be about 2000 years ago and the influenza A HA gene diverged from influenza B HA gene about 4000 years ago and from the influenza C virus about 8,000 years ago (36).

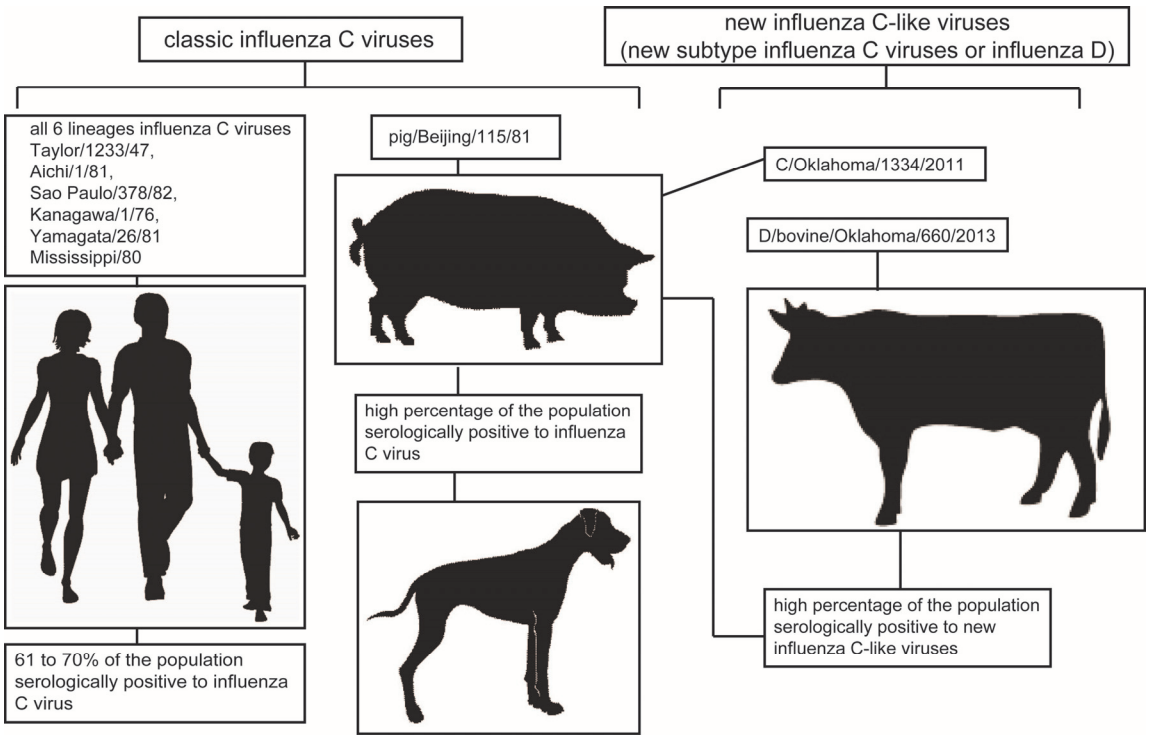

FIG 1.1 Host specificity of influenza C virus. Human beings are the major host and reservoir of influenza C virus. All viruses strains from six genetic and antigenic lineages were isolated from human being and serological studies indicated that this virus is widely distributed around the world and that the majority of humans acquire antibodies against the virus early in life; Serological studies showed that influenza C virus antibodies are widely observed in pigs and dogs,and 1 strain of influenza C virus was isolated from pigs in Beijing; From the year 2011, new influenza C-like orthomyxoviruses were isolated from pigs and cattle. Serological studies showed these new viruses (designated new subtype influenza C virus or influenza D virus) widely spread in pigs and cattle population.

1.3 Viral particle and genome structure of influenza C virus

Influenza C virus particles exhibit two morphologies, either spherical with a diameter of 80-120 nm or filamentous with the same diameter but with lengths in μm range (37). Already during the budding process at the plasma membrane, filamentous particles may aggregate via

their long axes into 500 µm long cord-like structures, which are all covered by a layer of surface projections (38). Studies using reverse genetics showed that an amino acid exchange at residue 24 of the M1 protein (Ala to Thr) that reduces membrane association of this intrinsically hydrophobic protein, eliminates cord formation and also affects virus morphology (39, 40). Another unique characteristic of influenza C virus particles observed by electron microscopy is a reticular hexagonal structure, which is formed by the HEF protein and discussed in more detail below (41-43).

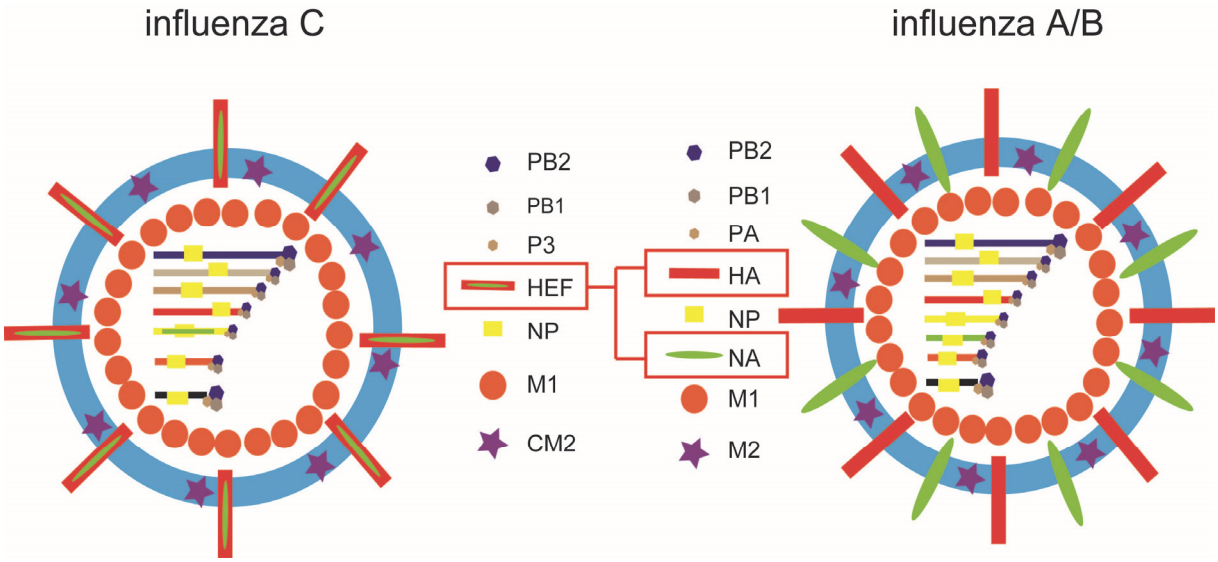

FIG 1.2 Scheme of influenza C virus and Influenza A/B virus particles. Proteins having the same function are depicted with the same symbol. Note that influenza C virus has only one spike protein, the hemagglutinin-esterase-fusion glycoprotein HEF that combines the functions of both hemagglutinin (HA) and neuraminidase (NA) from influenza A and B virus. PB1, PB2, P3 and PB1, PB2, PA are the polymerase proteins of influenza C virus and influenza A/B virus, respectively, that build together with the nucleoprotein NP and the viral RNA-segments the ribonucleoprotein complexes (vRNP). M1 is the matrix protein and M2 and CM2 the proton-channel.

The influenza C virus genome consistof negative-sense, single-stranded RNA (44), but in contrast to influenza A and B virus only seven (not eight) gene segments are present in virus particles (see Figure 1.2 for the structure of a virus particle and Figure 1.3 for the structure of viral genome segments). The longest three segments encode the proteins PB2, PB1 and P3 that form the heterotrimeric polymerase complex (45). The protein encoded by segment 3 is named P3 (instead of PA as in the case of influenza A virus) since it does not contain negative charges at neutral pH. The fourth segment encodes the glycoprotein HEF, the only spike of the viral membrane (46). The fifth segment encodes the nucleoprotein NP that associates with the viral genome segments along its whole length and builds, together with the polymerases the viral ribonucleoprotein complex (vRNPs) (47). The sixth segment encodes two proteins,

the matrix protein M1, a peripheral membrane protein that covers the viral envelope on its inside, and CM2, a short transmembrane protein supposed to exhibit proton-channel activity required for virus entry. M1 and CM2 are generated by alternative splicing, but in a different manner as described for influenza A virus. Whereas in influenza A virus M1 is translated from a unspliced mRNA, M1 of influenza C virus is generated from a spliced mRNA. Removal of an intron generates the stop codon UGA such that a protein containing 242 residues is translated (48). The unspliced mRNA encoding CM2 translates into a long precursor protein (374 residues), named p42. P42 contains an internal signal peptide (residues 239-259) which co-translationally targets the protein from the cytosol to the ER and presents it to the translocon. Here residues C-terminal to the signal peptide are translocated into the lumen of the ER until translocation is stopped by a second hydrophobic region (residues 285-308) that functions as the transmembrane region (TMR) of CM2. The signal peptide is then cleaved by signal peptidase yielding the CM2 protein (115 residues) and the p31 protein (259 residues). P31, which is identical in sequence to M1 (except the 18 C-terminal amino acids), is rapidly degraded after cleavage from p42 suggesting that it does not plays any functional role for the viral life cycle (49, 50). Whether CM2 is a proton channel has not been directly demonstrated by biophysical assays, but it alters the intracellular pH in transfected cells and its transmembrane domain can substitute for that of the influenza A virus M2 protein(51). The seventh vRNA encodes the two non-structural proteins NS1 and NS2 that are also generated via mRNA splicing (52, 53). The unspliced mRNA is translated into the NS1 protein (246 residues) and the spliced mRNA translates the shorter NS2 protein (182 residues). The N-terminal 62 residues of NS1 and NS2 are identical in sequence, splicing then generates a shift in the ORF such that the remaining residues are translated from a different reading frame (54). All ORFs are flanked by non-coding (NC) sequences, which are more variable in length than those of influenza A and B virus (55). Non-coding sequences are divided into conserved and non-conserved sequences. The first twelve nucleotides at each 3' end (3'-UCGUU/CUUCGUCC-5') as well as the last eleven nucleotides at each 5' end (5'-AGCAGUAGCAA-3') are conserved between genome segments (44, 56) and are partially complementary to each other, which enables the single stranded RNA to form a "panhandle" structure (44, 57). This peculiar structure serves as the promotor for transcription of cRNAs and vRNAs, and is required for the endonuclease activity of the viral polymerase complex (55, 58, 59). A uridine-rich region located at position 17 to 22 at the 5' end of each segment is the template for the poly A tail present at the 3' end of each mRNA (44).

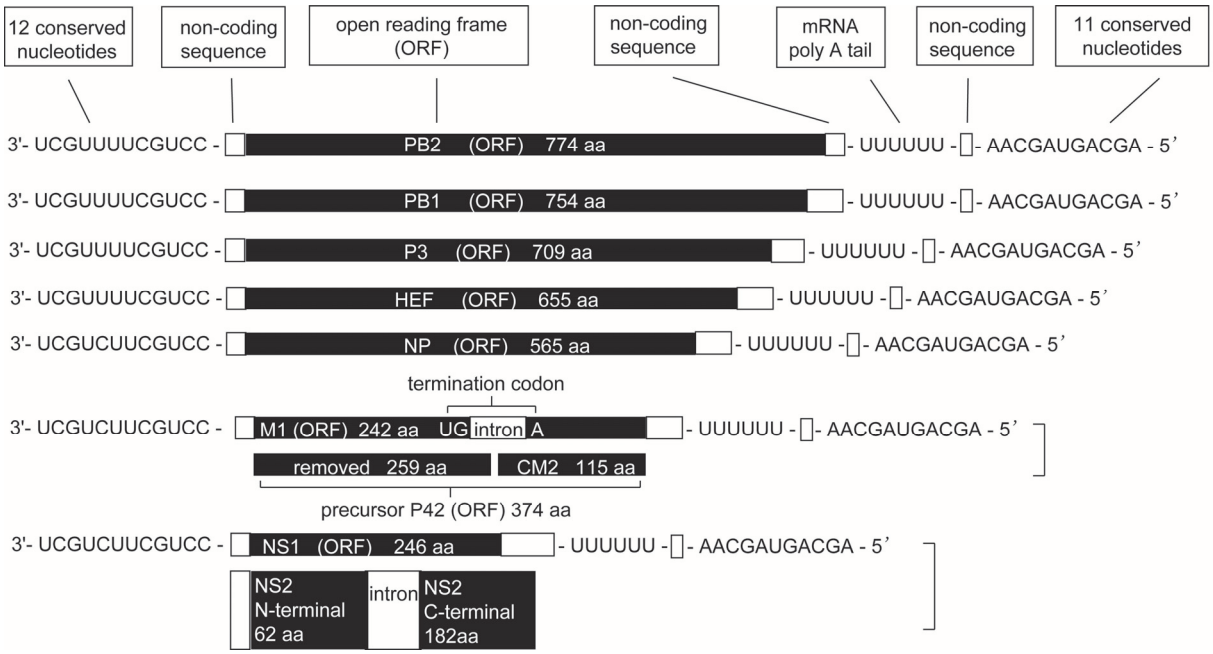

FIG 1.3 Structure of the seven influenza C virus genome segments. Open reading frames (ORFs) are indicated in black. Segment six and seven encode two proteins which are generated by splicing. Influenza C virus possesses 7 minus-senses, single-strand and segmented RNA. Each segment possesses 12 conserved nucleotides at 3' terminal and 11 conserved nucleotides at 5' terminal. A poly U motif is close to 5' terminal and it transcripts into mRNA poly A tail. Each of the longest 5 segments possesses only 1 open-reading-frame (ORF) and encodes PB2, PB1, P3, HEF and NP, respectively.

1.4 HEF protein of influenza C virus

While influenza A and B virus contain the two glycoproteins Hemagglutinin (HA) and Neuraminidase (NA) inserted into the viral membrane, influenza C virus possess only one spike designated Hemagglutinin-Esterase-Fusion (HEF) protein which combines the functions of both HA and NA (46, 60). Like HA, it recognizes and binds to a receptor on the cell surface to initiate virus entry. However, the receptor is not sialic acid, but an acetylated derivative, namely 9-O-acetyl-N-acetylneuraminic acid (61). HEF also catalyzes fusion of the viral envelope with endocytic vesicles by a mechanism that is believed to be similar to the well characterized fusion activity of HA. Finally, HEF is the receptor-destroying enzyme, which is the function of the neuraminidase (NA) in influenza A and B virus. HEF does not cleave the terminal neuraminic acid residue from carbohydrates, but has an esterase activity that removes acetyl from 9-O-Acetyl-N-acetylneuraminic acid(62). This function is probably required to release freshly budded virus particles from infected cells, which would otherwise be trapped at their plasma membrane if the receptor would still be present. Interestingly, HEF can substitute for both HA and NA to support influenza A virus replication if its gene is

equipped with the packaging signals from influenza A virus (63). After a description of the structure and the modifications of HEF its three functional activities will be discussed in more detail below.

1.4.1 Primary structure of HEF protein

All full-length HEF protein sequences present in the influenza virus database (http://www.ncbi.nlm.nih.gov/genomes/FLU/Database/nph-select.cgi) contain 641 amino acids (aa, excluding signal peptide), except HEF from one strain which is one amino acid shorter. HEF (like HA) is a typical type 1 transmembrane protein with a short N-terminal, cleavable signal peptide (14 amino acids), a long ectodomain (612 aa), a transmembrane region (26 aa) and a very short cytoplasmic tail (three aa). HEF present in infectious virus particles is composed of two subunits, the N-terminal 432 amino acids are the HEF1 polypeptide, the remaining sequence including the hydrophobic fusion peptide, the transmembrane domain (TMR) and the cytoplasmic tail is called HEF2 (64, 65). HEF proteins of the novel influenza C-like viruses (influenza D virus) contain a very similar number of amino acids (664 including signal peptide) as HEF from influenza C virus, are predicted to also adopt a type I membrane topology, but the amino acid identity with HEF is only ~53% (27).

We aligned the HEF sequences from the six Influenza C virus lineages to revealamino acid identity and other common characteristics (supplementary material). All residues important for the structure of HEF, such as glycosylation sites, cysteine residues (with one exception, Cys332 in the Taylor lineage), the N-terminal region of HEF2 containing the hydrophobic fusion peptide and the amino acids of the receptor-binding and receptor destroying domain of HEF are invariant. In general (and in contrast to the highly variable HA proteins of influenza A and B virus), only a few amino acid residues are not conserved through all lineages of HEF. 35 of them are located in HEF1 and seven in the smaller subunit HEF2. There are three small regions in HEF1 where many of the variable amino acids are clustered; residues 61-65 contain four amino acid substitutions, residue 165-172 six exchanges and residues 190-195 five substitutions (supplementary material). In the crystal structure of HEF the variable regions are located in loops at the surface of the trimer; the latter two near the receptor binding site at the top of the molecule and residues 61-65 near the esterase domain (Figure1.4). These amino acids have been shown to be antibody epitopes that gradually change due to antigenic drift (66).

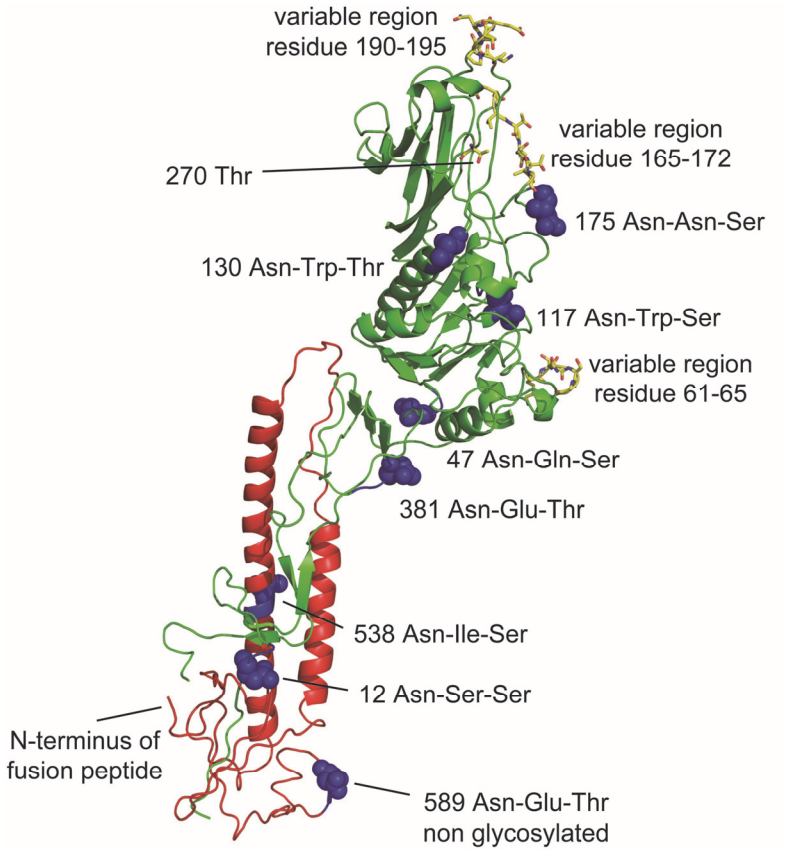

FIG 1.4 Location of N-Glycosylation sites and variable regions in the crystal structure of HEF. Asparagine residues of used and unused glycosylation sequons (Asn-X-Ser/Thr) are depicted in the secondary structure of a HEF monomer as highlighted as balls. Amino acids in the HEF protein from C/JHB/1/66, which vary in other influenza C virus isolates are marked as sticks (see supplementary table 1). Threonine residue 270, which is exchanged by isoleucine in a virus variant that has acquired the ability to grow in MDCKII cells, is also marked as sticks. Figure was created with PyMol from PDB file 1FLC.

1.4.2 Crystal structure of the HEF protein

Initial studies using electron microscopy showed that the HEF spike forms a mushroom-shaped trimer consisting of a membrane-near stalk and a globular head (43, 67). X-ray crystallography of the bromelain-cleaved ectodomain of HEF then revealed the high resolution structure (4.5Å) of the HEF trimer. Although there is only 12% amino acid identity between HA and HEF, the overall structure of both molecules as well as folds of individual segments are quite similar, except an additional bulge, which is located at the lower part of the globular domain and contains the esterase region that is not present in HA (Figure1.5). Similar to HA, the receptor-binding region is located at the top of the head domain, which consists only of HEF1 residues. The stalk is formed by three 60Å long α-helices that contain the whole HEF2 sequence and N-terminal residues 1-40 and C-terminal residues 367-432 of HEF1. The fusion peptide at the N-terminus of HEF2 is located around 35Å above the

membrane, but in contrast to HA, the first four residues are exposed at its surface and not buried within the trimer (68, 69). The detailed structure of the receptor binding site and the catalytic center of the esterase activity will be discussed in more detail in the last paragraph.

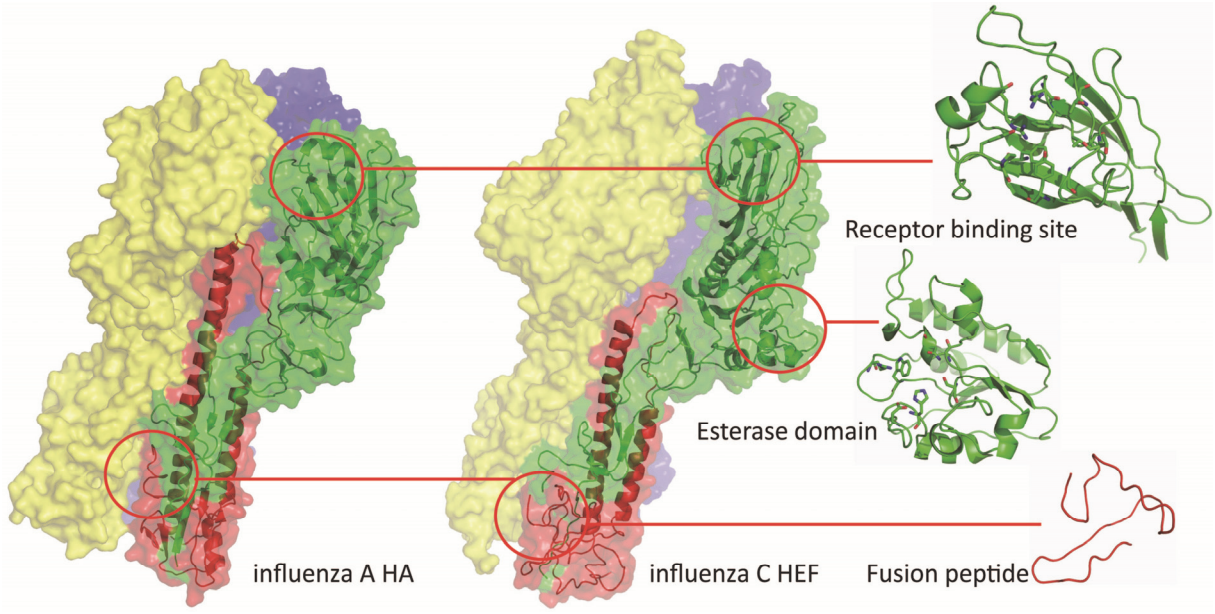

FIG 1.5 Comparison of the crystal structure of influenza C virus HEF protein and influenza A virus HA protein. Only the ectodomains of both proteins were amenable for crystallization. The viral membrane is located beneath the structure. Individual subunits of the trimeric spike proteins are drawn in different colors. The overall structure of both proteins is similar except an additional bulge in the head domain of HEF that contains the esterase activity which is not present in HA. The receptor binding region, esterase domain and the fusion peptide of HEF are enlarged. Figures were created with PyMol from pdb files 1RUZ (HA from Influenza A virus strain A/South Carolina/1/1918 (H1N1)) and 1FLC (HEF from Influenza C virus strain C/Jhb/1/66 strain)

1.4.3 Co-and post-translational modifications of HEF

HEF is synthesized on membrane-bound ribosomes and the primary translation product is subjected to a series of co- and posttranslational modifications, most of them are required for proper folding and/or functioning. Already during translocation of HEF into the lumen of the ER the N-terminal signal peptide is cleaved, carbohydrates are attached and intramolecular disulfide linkages are formed and probably remodeled. These co-translational modifications affect folding of the molecule and its trimerization, processes which are (at least in HA and other viral glycoproteins) a prerequisite for exit of cargo from the ER (70). Later on a long chain fatty acid is attached to a cysteine located at the end of the transmembrane region and HEF is proteolytically cleaved into the subunits HEF1 and HEF2, a process that is essential for virus replication.

1.4.3.1 Location of N-Glycosylation sites in the crystal structure of HEF

HEF, like HA, contains only asparagine-linked carbohydrates; O-glycosylation does not occur (60, 71). The composition of the carbohydrate chains has not been precisely determined, but apparently, some of them are not terminally glycosylated since they are not processed to an Endo-H resistant form (72). The location of the individual glycosylation sites in the crystal structure of HEF is depicted in figure 1.4. Seven of the eight highly conserved N-glycosylation sequons (Asn-X-Ser/Thr) are used. One is located in HEF2 and six in HEF1, three in the globular head and two in the hinge region that connects the stalk with the head. The site at position 589 is not glycosylated, probably because it is located too close to the membrane-spanning region and cannot be accessed by the oligosaccharide transferase (60, 64, 65) (Figure 1.4 and supplementary material). Although the position of carbohydrates attached to HA of Influenza A virus changes and their number increases during viral evolution (73), their distribution is quite similar to that of HEF, i.e. the majority is located in the larger subunit. Glycosylation of HEF is crucial for proper folding of the glycoprotein by protecting it from proteolytic degradation and hence important for the presentation of antigenic epitopes (74) .

1.4.3.2 Location of intramolecular disulfide bonds in the crystal structure of HEF

There are 15 cysteine residues in HEF1, twelve of them form six intrachain disulfide linkages that stabilize the globular head domain. Their location is depicted in the crystal structure of HEF in figure 1.6. Apparently not all of them are required for proper folding and functioning of HEF since cysteine 332 is exchanged by a tyrosine in the Taylor lineage of Influenza C virus. Two cysteines that do not form a disulfide linkage in the mature protein are located at the hinge that connects the globular head with the stalk region. The remaining cysteine in HEF1 forms an interchain disulfide bond with the only cysteine residue in the ectodomain of HEF2, which is located at the bottom of the trimer. A similar distribution of disulfide bonds is present in HA of influenza A virus, i.e. one disulfide bond connects HA1 with HA2; the majority are intrachain bonds, three or four in HA1 and just one in HA2 (73, 75). The rare occurrence of disulfide-bonds in HEF2 and HA2 allows this subunit to perform the large conformational changes that catalyze membrane fusion.

1.4.3.3 Folding and intracellular transport of HEF

HEF (at least from the strain C/JHB/1/66) is subject of a complicated folding procedure involving the formation and remodeling of intramolecular disulfide bonds. In virus-infected

cells freshly synthesized HEF has an apparent molecular weight (MW) of 80 kDa as demonstrated by both reducing and non-reducing SDS-PAGE. This corresponds to the predicted molecular weight of the glycosylated form of the protein. Subsequently HEF is converted to a form with a MW of 100kDa, which appears after non-reducing, but not after reducing SDS-PAGE, indicating that intramolecular disulfide-bond formation causes the decrease in electrophoretic mobility. Besides reduction of disulfide bonds, proteolytic cleavage also converts the 100 kDa into the 80 kDa form suggesting that the 100 kDa form possesses a strained conformation (43, 76-80).

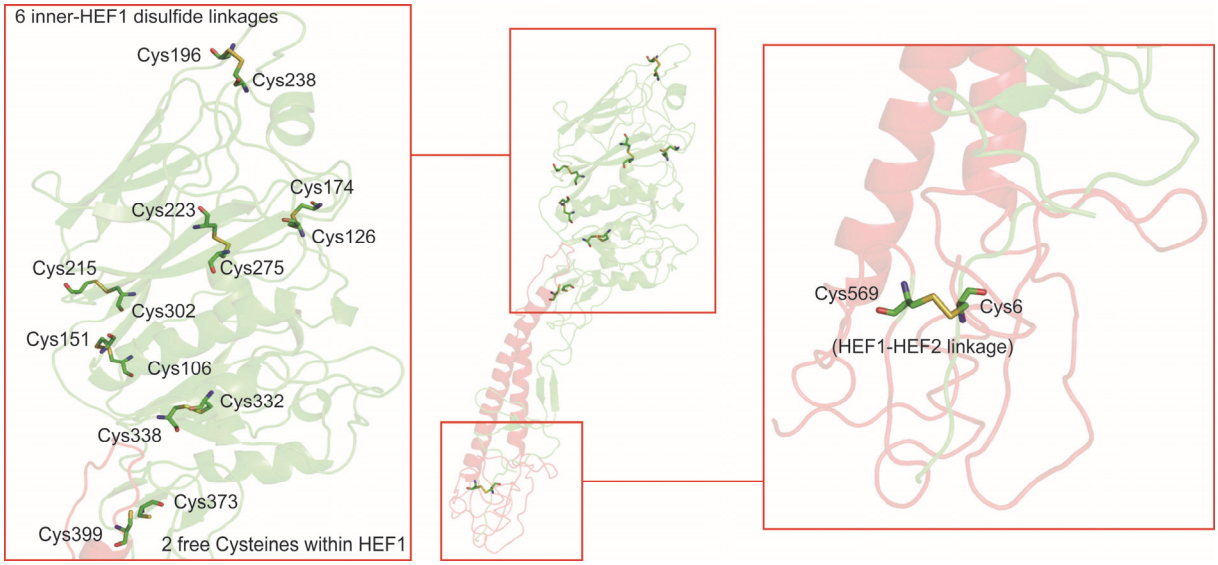

FIG 1.6 Location of intramolecular disulfide linkages in HEF. The middle part shows the secondary structure of a HEF monomer. HEF1 and HEF2 subunits are drawn in red and green, respectively. The left part shows the head domain which contains six disulfide linkages and also two free cysteines. The right part shows the location of the only disulfide linkage between HEF1 and HEF2. The figure was created with PyMol from PDB file 1FLC.

When HEF from C/JHB/1/66 was expressed from cDNA in the absence of the other viral proteins, conversion into the 100 kDa form was either very inefficient or not observed at all suggesting that the interaction of HEF with other viral proteins is required for folding (79). Expressed HEF is not transported to the cell surface, which is in line with the established paradigm that proper folding is a prerequisite for exit of proteins from the ER and hence transport to the plasma membrane (70). The defect in disulfide bond formation and surface transport was partially overcome by either deleting its short cytoplasmic tail (Arg-Thr-Lys),

replacing it by the longer cytoplasmic tail of influenza A virus HA or exchanging the two basic amino acids to acidic or hydrophobic residues (79, 81).

In contrast, HEF proteins from the strainsC/California/78, C/Ann Arbor/1/50 and C/Taylor/1233/47 were efficiently transported to the plasma membranein the absence of other viral proteins (72, 82). In addition, conversion of an 80 kDa to a 100 kDa band was not obvious by SDS-PAGE, although heterogeneity of bands after non-reducing SDS-PAGE suggests that remodeling of disulfide bonds also occurs (72). The reason for this strikingly different behavior of HEF proteins is unknown, but either subtle amino acid differences between HEF proteins of different virus strains or between the cloned HEF-gene and the gene present in virus particles of C/JHB/1/66 have been discussed.

There are also other indications that folding of HEF is more complicated than folding of HA. Whereas HAs from several Influenza A virus strains have passed the medial-Golgi (determined as acquisition of Endo-H resistant carbohydrates), around 15 minutes after synthesis and are rapidly ($t_{1/2}$:30 min) and completely transported to the cell surface (83), intracellular transport of HEF is slow and incomplete. Half times of more than 60 minutes for acquisition of Endo-H resistant carbohydrates and exposure at the cell surface have been reported and only a fraction (70%) of all synthesized molecules appear at the cell surface (72). In addition, HEF exhibits intrinsic temperature sensitivity. Expression levels of HEF at the plasma membrane are two times higher at 33°C compared to 37°C and, probably as a consequence, membrane fusion is more efficient at 33°C than at 37°C. Since trimerization of HEF is also reduced at 37°C the underlying cause of reduced cell surface exposure is slower and less efficient folding of HEF at higher temperatures (84) which is reminiscent of temperature sensitive mutants of HA of influenza A virus (85).

The temperature sensitivity of HEF is probably an adaption of the virus to replicate only in the upper respiratory tract that has, due to contact with inhaled air before it is warmed up, a lower temperature than the lower respiratory tract. In the lab (cell culture and chicken embryos) influenza C virus is also amplified at 33°C where it grows to higher titers than at 37°C (30, 86-88). However, other proteins also influence the temperature preference for virus replication since the polymerase also exhibits a higher activity at 33°C than at 37°C (89).

1.4.3.4 Proteolytic cleavageof HEF protein

After synthesis of the precursor HEF0a yet unknown protease hydrolyses the peptide bond between Arg432 and Ile433, which is located in the stem region of the trimeric spike and thus

in a similar position as the cleavage site in HA (69, 78, 90, 91). The resulting subunits HEF1 and HEF2 remain covalently connected bya single disulfide linkage, which is also located in the stalk region of the protein. Proteolytic cleavage is an essential prerequisite for the membrane fusion activity of HEF (and also of HA) since it enables the protein to get activated by low pH (43, 92, 93).

HEF proteins from all influenza C virus strains contain a monobasic cleavage site and are in this respect similar to HAs from human, porcine, equine and low pathogenic avian Influenza A viruses (60, 94). Polybasic cleavage sites that are present in HA of highly pathogenic avian influenza A viruses and processed by the ubiquitous protease furin are not found in any HEF protein. Consequently, replication of Influenza C virus is limited to the site of virus infection, the respiratory tract. Spread to other tissues or even systemic infection, as observed for highly pathogenic avian influenza virus having a multibasic cleavage site between HA1 and HA2, does not occur with influenza C virus (95, 96). Multiple replication cycles of Influenza C virus in tissue culture are enabled by addition of trypsin, whereas embryonated eggs produce infectious virus with cleaved HEF (78, 80).

The enzyme catalyzing proteolytic cleavage of HEF has not been identified so far, but one (or several) of the proteins responsible for cleavage of HAs with monobasic cleavage sites might be promising candidates (97). Since both HA and HEF can be cleaved by trypsin at similar concentrations *in vitro* (5~20 µg/ml) it seems likely that HA and HEF are also cleaved by the same (or very similar) enzymes inside cells (80, 98).

1.4.3.5 S-acylation and raft-localization of HEF

Another common modification of viral glycoproteins is the covalent attachment of fatty acids, usually palmitate (C 16:0) in a thioester-type linkage to cysteine residues located either at the cytosol-facing end of the transmembrane region or in the cytoplasmictail (99, 100). HEF of influenza C virus is unique in this aspect, since it contains mainly stearic acid (101, 102) (Figure1.7). This longer chain fatty acid (C 18:0) was initially identified by chromatographic determination of HEF-bound, [^{3}H]-labelled fatty acids, but results were recently confirmed by mass-spectrometry with C-terminal anchoring fragments of HEF purified from virus particles (103). These studies revealed also that influenza B virus HA possessing two cytoplasmic cysteines contains only palmitate, whereas HAs of influenza A virus having one transmembrane and two cytoplasmic cysteines contain both palmitate and

stearate, but the latter is exclusively attached to the cysteine positioned in the transmembrane region (101, 103-107) (Figure1.7). It was originally proposed that the different length of the cytoplasmic tails of HA (11 aa) and HEF (3 aa) could be the reason for different fatty acid selection (102), but a recent comprehensive mutagenesis study with HA revealed that the location of a cysteine relative to the transmembrane region is the decisive factor for selective attachment of stearate (108). Enzymes that attach palmitate and stearate to HA or HEF (or to other viral glycoproteins) have not been identified so far, but likely candidates are members of the family of DHHC-proteins, polytopic membrane proteins with the Glu-His-His-Cys motif in one of their cytoplasmic loops, that are known to acylate cellular proteins (109).

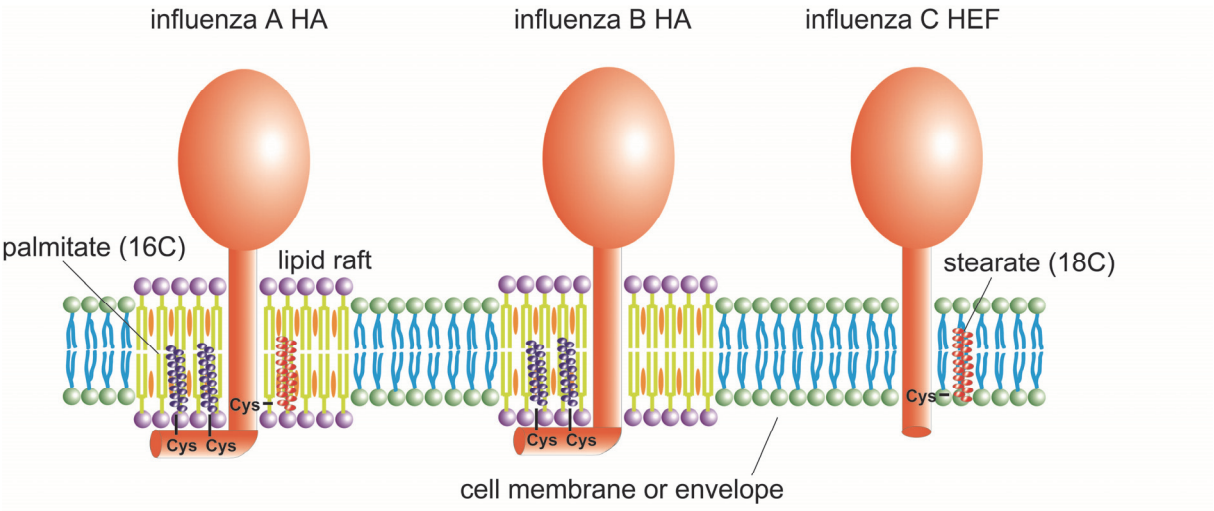

FIG 1.7 Different acylation and lipid raft association of HA and HEF protein. HAs of influenza A virus contain one stearate attached to a cysteine positioned at the end of the transmembrane region and two palmitates attached to cytoplasmic cysteines. HA of Influenza B virus possesses two palmitates attached to cytoplasmic cysteines. HEF of influenza C virus has only one stearate attached to a transmembrane cysteine. Whereas HA of Influenza A and B virus are associated with membrane rafts, cholesterol- and sphingolipid-enriched nanodomains of the plasma membrane, HEF is thought to localize to the bulk phase of the plasma membrane.

Acylation of HA of influenza A virus is essential for virus replication, since (depending on the virus strain) either virus mutants with more than one acylation site deleted show drastically impaired growth or could not be created at all by reverse genetics (110-112). Recombinant virus lacking the acylation site of HEF could be rescued, but viral titers were reduced by one log relative to wild type Flu C (our unpublished results). The resulting virus particles have a regular protein composition and no changes in their morphology were obvious by electron microscopy, but their hemolytic activity is reduced indicating a defect in membrane fusion. This is in accordance with results on several HA subtypes showing that (i) the stearoylated cysteine at the end of the transmembrane span is less important for virus

replication compared to the two cytoplasmic palmitoylatedcysteines and that (ii) acylation affects opening of a fusion pore (111, 113, 114). However, for H2 subtype HA it was reported that acylation does not influence HA´s membrane fusion activity, but plays an essential role for virus particle assembly (110, 112).

Several studies illuminated the essential role of palmitoylation for association of HA with rafts, cholesterol and sphingolipid-enriched nanodomains on the cellular plasma membrane that serves as the viral assembly and budding site (115-118) (Figure 1.7). Interestingly, HEF is apparently not a component of rafts, at least it does not associate with detergent-resistant membranes, their controversial biochemical correlate indicating that virus particles buds from the bulk phase of the plasma membrane (119).

1.4.4 Regular arrangement of HEF spikes in virus particles

Electron microscopy revealed another unique feature of Influenza C virus particles not observed for Influenza A and B virions. HEF trimers on the surfaces of both spherical and filamentous particles are arranged in a reticular structure that has been described to consist mainly of hexagons (37, 41, 76). The regular polymeric reticular structure can be observed not only on the surface of intact viral particles, but also when HEF is removed from the membrane, either by limited proteolytic digestion or by spontaneous release (43). These results indicate (i) that the hexagonal arrangement is an intrinsic feature of HEF and does not require other viral proteins such as M1 and (ii) its formation likely involves lateral interaction between the ectodomains of HEF; the TMR and cytoplasmic tail are not required to maintain the structures. Which amino acids form lateral interactions between HEF trimers and which function it serves for virus replication has not been investigated. One might speculate that the formation of a regular arrangement of HEF trimers on the plasma membrane might induce membrane curvature, i.e. it acts like an extrinsic coat that might help to sculpt a virus particle out of the membrane. However, the lateral arrangement of exclusively hexagons would result in the formation of a flat structure without any curvature. Thus, in order to create and cover a spherical particle, HEF must form a precisely defined arrangement of pentagons and hexagons.

Virus budding might be reinforced by the matrix protein M1 that has been shown to form virus-like particles when expressed in the absence of other viral proteins (39). M1 might execute a pushing force by oligomerization at the inner site of the plasma membrane. How these two assumed activities of HEF and M1 are coupled is not obvious since the cytoplasmic

tail of HEF is very short, only three amino acids, and might thus not be able to bind to M1 with high affinity.

1.4.5 Receptor binding activity of HEF

HA of Influenza A and B virus and HEF of influenza C virus use different sialic acid derivatives as receptor (Figure1.8). HEF binds to 9-O-Acetyl-N-acetylneuraminic acid (9-O-Ac-NeuAc), which can be present on both glycolipids and glycoproteins to function as viral receptor (46, 61, 120, 121). Likewise, HEF binds to its receptor regardless of whether 9-O-Ac-NeuAc is attached via an α-2,3 or α-2,6 linkage to the following galactosyl residue (61). In contrast, HA uses terminal N-acetylneuraminic acid (NeuAc) and the glycosidic bond of NeuAc influence the host specificity. Avian influenza viruses usually bind to NeuAc-α2,3-Gal while mammalian influenza viruses usually bind to NeuAc-α2,6-Gal (122, 123). The unique receptor specificity of influenza C virus has been used as an efficient tool to detect 9-O-Ac-NeuAc on the surface of various cells (124-126).

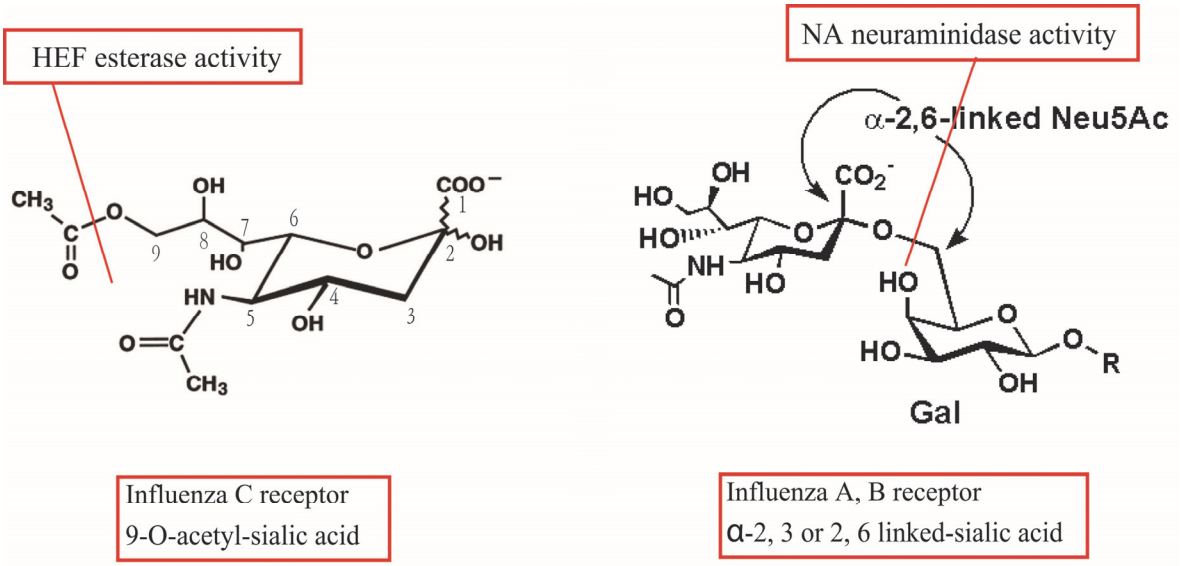

FIG 1.8 Cellular receptors and receptor-destroying activity of Influenza C virus and Influenza A and B virus. The structure of cellular receptors for HEF from Influenza C virus (9-O-acetyl-N-acetylneuraminic acid) and HA from influenza A and B virus (N-acetylneuraminic acid) are shown. Both sialic acid derivatives are the terminal sugars in carbohydrate chains attached to glycolipids or glycoproteins located at the cellular surface. Subtypes of influenza A virus HA discriminate between a α2-6 and α2-3 linkage to the second galactosyl residue, a property that (partially) explains species specificity. HEF of Influenza C virus apparently recognizes 9-O-acetyl-N-acetylneuraminic acid independent of its linkage to the next sugar. HEF has also esterase activity that cleaves acetyl from the C9 position. In influenza A and B virus the receptor-destroying activity is performed by the NA protein, which hydrolyzes the glycosidic bond between sialic acid and galactosyl residues. The cleaved bonds are indicated by a red line.

There is some evidence that the abundance of 9-O-Ac-NeuAc in cultured cells influences the tropism of Influenza C virus. A mutant of Influenza C virus was generated that has the ability to replicate in a subline of Madin-Darby canine kidney cells, MDCK II cells, which is resistant to infection by the parent virus. This mutant has an amino acid exchange from threonine to isoleucine at position 270 (284including the 14 amino acid long signal peptide, see figure1.4 for the location of Thr 270 in the crystal structure of HEF) that apparently increases the affinity of HEF for its receptor (127). Using reverse genetics it was recently confirmed that the exchange from threonine to isoleucine is necessary and sufficient to enable Influenza C virus to grow in MDCK II cells (88).

The crystal structure shows that HEF binds to 9-O-Ac-NeuAc in a similar pattern as HA binds to NeuAc. The binding elements consist of an α-helix, a loop, and an extended strand (Figure1.9A). The key residues for binding HEF to 9-O-Ac-NeuAcare shown in Figure1.9B. Tyr127, Thr170, Gly172, Tyr227 and Arg292 form hydrogen bonds with hydroxyl-groups of the ligand, and some other residues form the structural support of the receptor binding site. The HEF binding site also contains a unique hydrophobic pocket that accommodates the acetyl methyl group (69).

Some Coronaviruses, such as the prototype member mouse hepatitis virus (MHV) and human and bovine coronavirus, contain an hemagglutinin esterase (HE) protein that also uses 9-O-Ac-NeuAc as receptor (128-130). The crystal structure of HE from bovine coronavirus revealed that the ligand is bound in an opposite orientation compared to HEF and HA (131) (Figure1.9C).

1.4.6 Membrane fusion activity of HEF

Membrane fusion between the viral envelope and endocytic vesicles is the crucial step to release the viral genome into the cytoplasm of the cell (73, 132). There are two essential requirements for both HEF and HA to catalyze membrane fusion: (i) The precursor proteins HEF0 and HA0, must be cleaved into the subunits HEF1 (HA1) and HEF2 (HA2). (ii) The proteins must then be exposed to acidic pH to become fusogenic. This was initially demonstrated for influenza viruses by a simple membrane fusion assay, hemolysis of erythrocytes that occurs only if virus particles containing cleaved HA or HEF are exposed to acidic pH (92, 93, 133-136). Biochemical assays subsequently revealed that low pH initiates a conformational change since molecules become susceptible to proteolytic digestion (133).

The low pH is thought to cause protonation of specific amino acids that triggers the following large scale rearrangement of the proteins. Histidines might play this role since their pKas match the pH of endosomes (5.5– 6). For HA of influenza A virus specific histidine residues have been identified (137), but similar studies have not been performed with HEF. In both influenza A and C virus threshold pH values that initiate membrane fusion differ from strain to strain by about 0.7 pH units. This does not necessarily mean that different histidines are the relevant target of protonation, but that (between strains) variable amino acids in the vicinity of a specific histidine affect its pKa. For influenza C virus pH values required to cause hemifusion (measured as lipid mixing, range of 5.6-6.1) are 0.3-0.6 pH units higher than pH values for full fusion (measured by hemolysis, range of 5.1-5.7) (133).

Interestingly, kinetic studies with influenza C virus revealed a lag phase before onset of fusion that is not observed with Influenza A and B virus (133). It is likely that the lag phase reflects dispersion of the lateral arrangement of HEF spikes on the viral membrane that might hinder HEF´s conformational change. Accordingly, when virus particles are treated with low pH before electron microscopy, HEF spikes are less well ordered and the typical hexagonal structure disappeared (67).

The molecular details of the subsequent refolding of HEF have not been revealed, but it is believed that they are similar to the well characterized conformational changes of HA that were elucidated by a comparison of the crystal structure of HA at neutral pH with the structure of a HA fragment after low pH treatment (138). The first conformational change removes the fusion peptide from its buried location at the bottom of the stalk and exposes it at the surface of the molecule such that it can insert into the endosomal membrane ("jackknife mechanism"). A second conformational change then bends the ectodomain thereby drawing the fusion peptide towards the transmembrane region. This leads to a close apposition of viral and endosomal membranes, hemifusion with exchange of lipids, opening of a fusion pore and eventually complete merger of both lipid bilayers. The second conformational change requires so-called "heptad repeats", amphipathic helices which interact to form a stable 6-helix coiled coil domain (73, 139-141) (Figure1.10B and 1.10C). With the software "Multicoil Scoring Form" (http://groups.csail.mit.edu/cb/multicoil/cgi-bin/multicoil.cgi), a highly probable heptad repeats domain was found between amino acids 500 and 540, residues that encompass the long α-helix of HEF2. They are thus in a similar position as the heptad repeats that form the six-helix bundle coiled-coil in the low pH structure of HA (Figure1.10A). This region of HEF thus might convert from a long, uninterrupted helix into two smaller, antiparallel helices,

which are connected by a loop and form the coiled-coil domain that stabilizes the fusion conformation (138) (Figure1.10B and 1.10C).

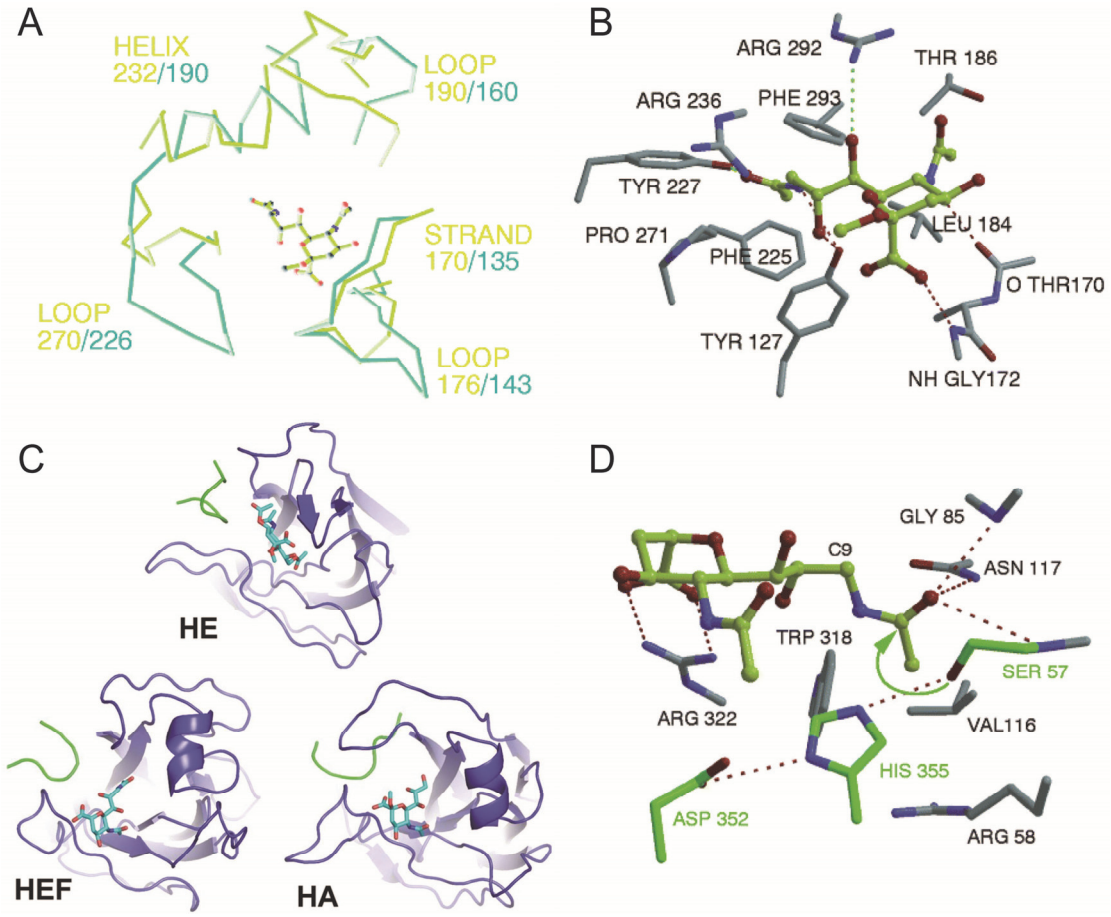

FIG 1.9 Structures of receptor binding site and esterase site of HEF, HA and HE. (A) Superimposing of HEF and HA receptor binding sites complexed with ligand (9-acetamidosialicacid α-methyl glycoside). The yellow-green lines and the light blue lines represent the binding elements of HA and HEF, respectively. (B) Structure of HEF binding sites complexed with the receptor. Key residues forming hydrogen bonds with the ligand are shown. (C) Comparison of the receptor binding topology of the hemagglutinin-esterase (HE) protein of coronavirus, HEF and HA with their ligands. The bound ligands are αNeu4,5,9Ac32Me in HE, αNeu5,9Ac22Me in HEF and αNeu5Ac2Me in HA are shown in stick representation. The ligand is bound to HE in an opposite orientation compared to HEF and HA. (D) Structure of the esterase active site of HEF. Key residues forming hydrogen bonds with the ligand are shown. (A) (B) (D) were taken from reference (Rosenthal et al., 1998) and (C) from reference (Zeng et al., 2008) with permission.

The fusion peptides of HA and HEF have similar, but also different features. The first 23 amino acids of HA2 (GLFGAIAGFI**E**GGWTGMI**D**GWYG, sequence of H1 subtype) is highly conserved between subtypes and contains hydrophobic, aromatic, but also some negatively charged residues. It is also characterized by GxxG and GxxxG motifs that are

known to mediate interactions between transmembrane segments. In a lipid environment the fusion peptide of HA forms a boomerang-like structure (aa 1-20) or a (tighter) helical hairpin (aa 1-23) (142, 143). The sequence at the N-terminus of HEF2 (IFGI**DD**LIIGLLFVAIV**E**AGIGG) is not conserved to that of HA2. However, if the first six residues, which are not buried within the trimeric stalk, are not taken into account some sequence homology between HA and HEF is apparent. The fusion peptide of HEF has a similar amino acid composition as that of HA, but glycine residues do not form GxxG or GxxxG motifs. The structure of HEF´s fusion peptide in lipid micelles is not known, but in the HEF trimer it already adopts a loop-like structure.

1.4.7 Receptor hydrolysis (esterase) activity of HEF

In accordance with its receptor binding specificity, HEF is an esterase that cleaves acetyl from the C9 position of terminal 9-O-Ac-NeuAc residues to release virus particles from infected cells (46, 62, 130) (Figure1.8). The esterase activity of HEF belongs to the class of serine hydrolase, where the –OH group of a serine residue performs a nucleophilic attack on the carbonyl-group of the substrate. Since the –OH group is not sufficiently nucleophilic it is activated by two other amino acids that together build the typical catalytic triad of serine hydrolases, the amino acids serine, histidine and aspartic acid. The base histidine polarizes and deprotonates the –OH-group of serine to increase its reactivity whereas aspartic acid aligns and polarizes the histidine (charge relay system) (144-146).

Crystallography in the presence of two non-hydrolysable receptor analogues of HEF revealed that serine 57, aspartic acid 352 and histidine 355 (numbering of HEF excluding the signal peptide) are the key residues for the acetylesterase activity of HEF (69) (Figure1.9D). Prior to that it has already been shown that mutation of Ser57 and His355 completely abolished the enzymatic activity of HEF, essentially confirming the data from crystallography, but mutation of other residues in the vicinity, i.e. Asp 247, Asn 266 and His 354 also affected the hydrolytic activity of HEF (146).

Ser57 is positioned for nucleophilic attack on the carbonyl carbon of the 9-O-Ac-NeuAc group. The carbonyl oxygen of the substrate points into an ‘oxyanion hole’ formed by the side chain of Asn117 and the NH -groups of Gly85 and Ser57 (69) Arg322 of HEF forms two hydrogen bonds with the sialoside carboxylate group (Figure1.9D). The structure of the esterase site is quite similar between HEF and coronavirus HE. The catalytic triad of HE consists of the same amino acids, i.e. Ser40, His329 and Asp326; Ser40 also forms an oxyanion hole with the sidechains of Gly75 and the NH group of Asn104 (131).

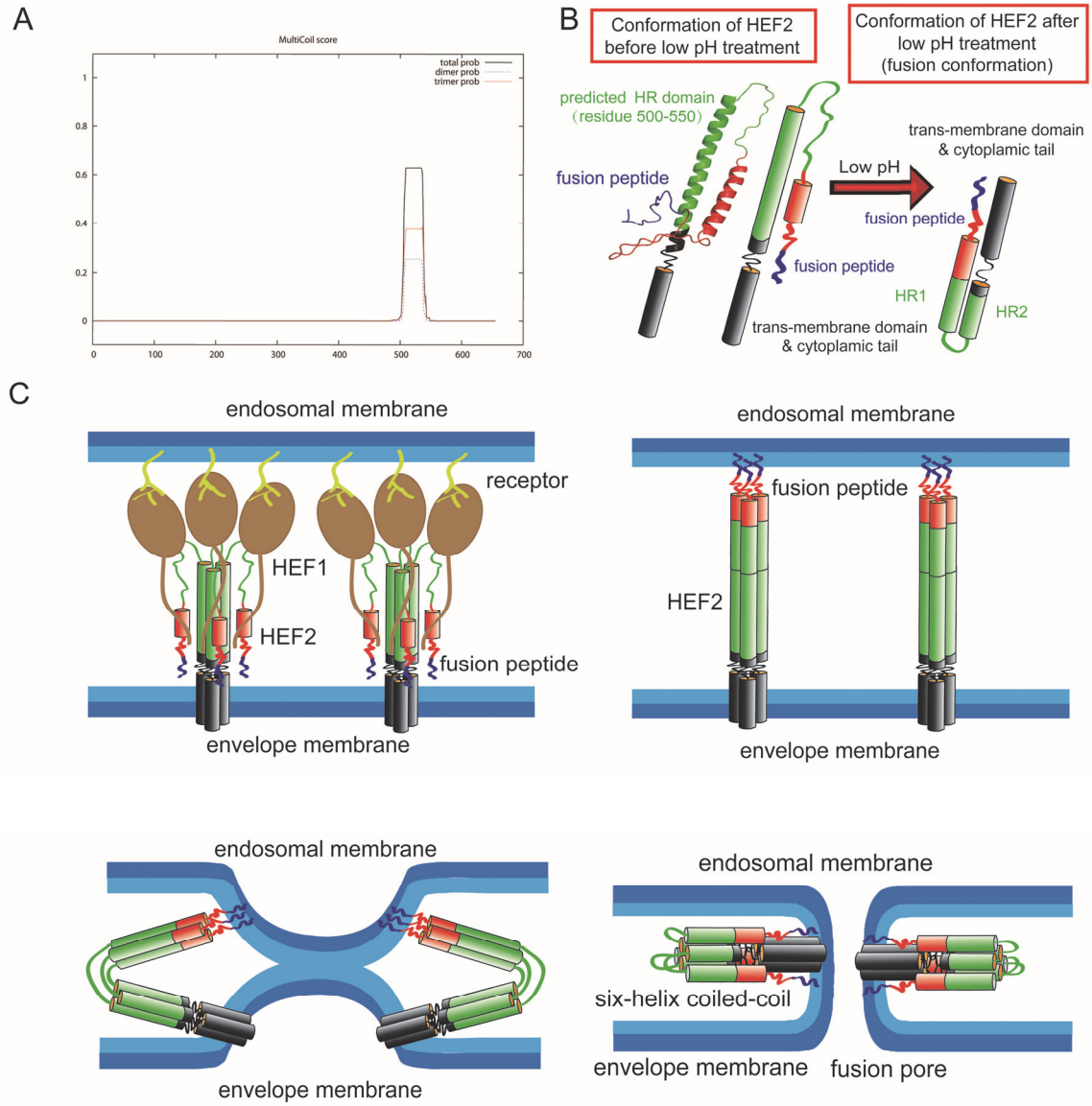

FIG 1.10 Probable mechanism for HEF-mediated membrane fusion. (A) Prediction of a heptad repeat (HR) in HEF by online software "multicoils scoring form"; (B) Probable conformational change of HEF2 during membrane fusion. Left part: Structure of the HEF2 subunit at neutral pH. The HR is located in the long α-helix of HEF2 and thus in a similar position as the HR in HA. Right part: hypothetical structure of the HEF2 subunit at acidic pH. (C) Hypothetical scheme for the HEF-catalyzed membrane fusion mechanism. Upper left part: HEF binds to its receptor via its HEF1 subunit (brown) and is endocytosed. Upper right part: Acidification of the endosome causes a conformational shift in HEF2. The fusion peptide, which was (partially) buried in the stalk is exposed and inserts into the endosomal membrane. Lower, left part: The middle part of the HR domain (green) changes its conformation from a helix to a loop, which causes bending of the molecule and close apposition of viral and cellular membrane allowing the exchange of lipids (hemifusion). Lower, right part: Interactions between the fusion peptide and the TMR of HEF might cause opening of a fusion pore.

1.5 The other proteins of influenza C virus

According to sequencing analysis, as well as protein function, the other proteins of influenza C are all equivalent to their analogues of influenza A virus. PB1, PB2 and P3 are coded by the longest 3 gene segments of influenza C virus, forming RNA polymerase to perform transcription and replication of the influenza C virus genome (89, 147, 148). The P3 protein was not indicated PA as its analogue of influenza A because it does not display any acid charge features at a neutral pH (45).

NP is coded by the fifth gene segment (47). It localizes the same position in cells as influenza A NP and undergoes a molecular maturation during transportation to the nucleus (149). It is essential to the transcription and replication processes of an artificial vRNA flanked by the noncoding regions (148).

The sixth gene segment coded M1 and CM2 with an mRNA splicing way, which was introduced in a front chapter. M1 is the matrix protein and is involved in the budding and morphogenesis processes of the virus (38-40, 150). Studies showed that an amino acid at residue 24 of the M1 protein is responsible for cord formation (39, 40).The analogue of influenza A M2 in influenza C is CM2 (49, 151), which is also a proton channel to modulate the pH, whose transmembrane domain can be substitute for that of the influenza A virus M2 protein (51, 152). CM2 consist of 3 domains: a 23-residue N-terminal extracellular domain, a 23-residue transmembrane domain and a 69-residue cytoplasmic domain (151, 153). In infected cells, CM2 forms disulfide-linked dimers and tetramers (Cys1, Cys6 and Cys20). It is modified by N-glycosylation (Asp11), palmitoylation (Cys65) and phosphorylation (Ser78, Ser103, Ser108 and Pro104) (151, 154). None of the above post translational modification was essential to the transport of CM2 to the cell surface but glycosylation is important for efficient replication of influenza C virus (155). CM2 has a potential role in the genome packaging and uncoating processes of the virus replication cycle (156). The palmitoylation of CM2 is dispensable to influenza C virus replication (157) and the oligomerization by disulfide-bonding was not essential but required for efficient virus replication (158).

NS1 and NS2 of influenza C virus were coded by the seventh vRNA via an mRNA splicing way (52-54). NS1 protein was reported to possess the abilities to counteract RIG-I-mediated IFN signaling and upregulates the splicing of viral mRNAs (159, 160). Influenza C NS2 possesses nuclear export activity as influenza A NS2/NEP and is incorporated into virions (161, 162). When exchange one or both of the 5'/3' non-coding sequence of influenza C vRNA segment with that of influenza A NS vRNA, neither chimeric influenza A or influenza

C virus was able to be rescued, suggesting that non-coding sequences playing an role for type specificity (163).

1.6 Reverse genetics of influenza C virus

Reverse genetics is defined as the generation of virus entirely from cloned cDNA (164). Two earlyforms of reverse genetics systems for influenza A virus were established in 1989 and 1994, respectively (165, 166). In the first system, a foreign gene flanked by noncoding sequences of the NS gene was cloned into a plasmid behind a T7 RNA polymerase promoter, and then the construct was transfected into cells to transcribevirus-like RNA, which was mixed with purified polymerase and NP proteins to reconstitute vRNPs. These artificially generated RNPs were transfected into cells that were infected with a helper influenza virus, and then recombined virus with the foreign gene was rescued together with wt virus (165). In the second system, a plasmid containing cloned influenza virus cDNAs was transfected into cells flanked by RNA polymerase I promoter (pol I) and terminator sequences, followed by helper influenza virus infection, led to the viruses rescuing. These systems rely on helper-virus infection and strong selection systems are necessary to distinguish the modified virus from the wt helper virus.

In 1999, a 12-plasmid reverse genetics system for influenza A was established (167). The eight genome cDNAs were inserted between promoter and terminator sequences of RNA polymerase I in pHH21 plasmids, co-transfected with four pCAGGS/MCS plasmids expressing PB2, PB1, PA and NP proteins into cells. Then the virus was rescued (167). Based on the same strategy, 11-plasmid reverse genetics systems for influenza C virus were established (88, 150).

In the year 2000, an 8-Bidirectional-plasmid reverse genetics system was developed (168). In the bidirectional pHH21 plasmids, a human pol I promoter/cDNA/mouse pol I terminator sequence was flanked by a human pol II and a bovine poly A signal, in a reverse direction. RNA pol I is a cellular enzyme that transcribes ribosomal RNA that lacks both a 5’ cap and a 3’ poly (A) tail (4); RNA pol II transcript mRNA and most snRNA and microRNA (169, 170). Therefore, the same cDNA could be a template for both negative-sense vRNAs and positive-sense mRNAs (168). This 7-bidirectional-plasmid system for influenza C virus was established by ReinhardVlasak et al (30).

Reinhar Vlasak’s 7-plasmid reverse genetics system was used in the present study (Figure 1.11). The seven influenza C virus cDNA segments were ligated into the two Bsm BI

restriction sites on pPMV plasmid leading to nucleotide-exact insertion between pol I terminator and promoter for vRNA replication. The sequence poI I promoter /cDNA/pol I terminator was flanked with CMV promoter and SV40 poly (A) in an opposite direction. mRNA is synthesized by CMV promoter and SV40 poly (A) signal (30). Influenza C virus was rescued after co-transfection these 7 plasmids into Vero cells or MDCK I cells.

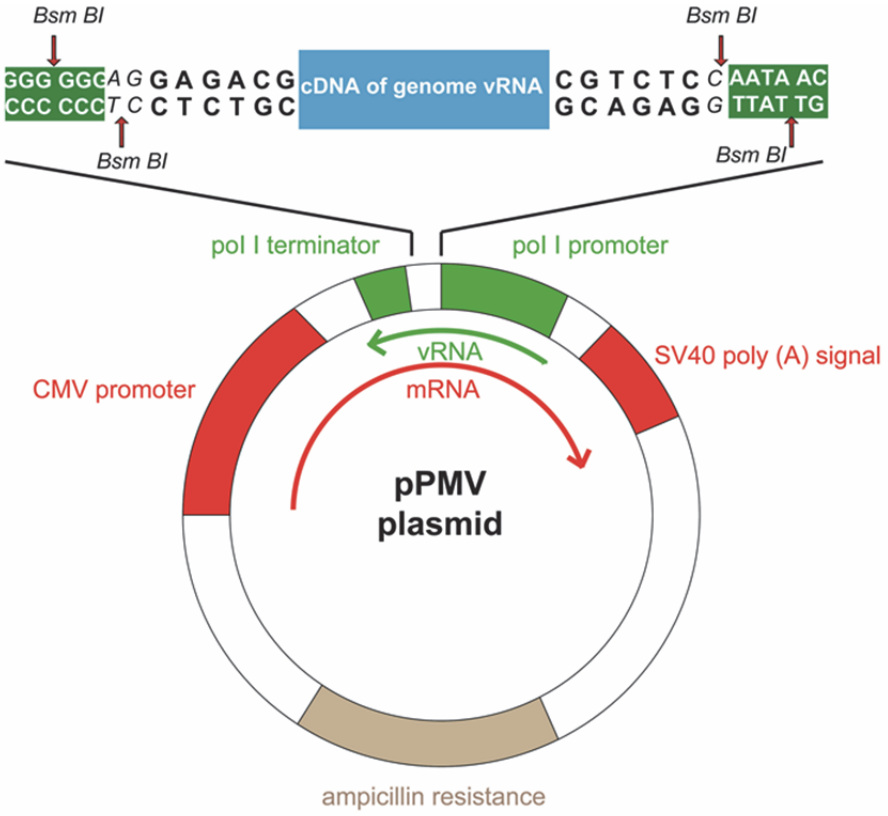

FIG 1.11 Construction of pPMV plasmid from ReinharVlasak's 7-plasmid influenza C reverse genetics system. cDNA segment of complete sequence of influenza C virus genome vRNA segment is inserted between pol I terminator and promoter through two Bsm BI restriction sites, forming a replicon for genome vRNA segment replication. The sequence poI I promoter /cDNA/pol I terminator was flanked with CMV promoter and SV40 poly (A) in an opposite direction, forming a scripton for mRNA synthesis to translate into viral protein.

1.7 Why study Influenza C virus

Although Influenza C virus is currently not a serious threat to humans, it might be nevertheless fruitful and revealing to study its biology. Whereas the receptor-binding and receptor-destroying activities of HEF are now well characterized and its fusion activity is likely to be similar to that of HA, the mechanism of virus assembly and budding is largely unexplored and might be different for influenza A and C virus. If it is confirmed by more sophisticated methods that HEF does not associate with membrane rafts(119), it is likely that influenza A and C virus bud at different sites of the apical plasma membrane, membrane rafts

in the case of influenza A virus (171, 172) and the bulk phase or other domains in the case of influenza C virus. Since rafts are believed to enrich viral proteins and deplete many cellular proteins they represent the first concentration step in the assembly of a virus particle that contains very little cellular proteins (118). One might speculate that the regular arrangement of HEF trimers might substitute for the concentration of HA in rafts, i.e. its formation might displace cellular proteins from the viral assembly site. A regular arrangement of hexagons and pentagons might then help to shape a virus particle out of the plasma membrane.

For influenza A virus it has been demonstrated that virus scission is achieved by the M2 protein that is targeted to the edge of the assembly site and inserts an amphiphilic helix into the inner leaflet to induce membrane curvature (173). Whether CM2 plays a similar role for release of influenza C virus has not been investigated, but the bioinformatic tool heliquest (http://heliquest.ipmc.cnrs.fr/) predicts the presence of an amphiphilic helix at the beginning of the cytoplasmic tail of CM2. The recent developments of reverse genetics systems for influenza C virus make some of the mentioned questions amenable to experimental verification (30, 88, 150). Thus, further studies might reveal common and different principles of influenza virus budding that might be helpful to combat the disease.

2. Aim of the thesis

The only spike protein of influenza C virus, the hemagglutinin-esterase-fusion glycoprotein HEF possesses receptor binding, receptor hydrolysis and membrane fusion activities, combining both functions of Hemagglutinin (HA) and Neuraminidase (NA) of influenza A and B virus (46). All hemagglutinating glycoproteins of Influenza virus are S-acylated at conserved cysteine residues, but their location within the molecule, the types and numbers of attached fatty acids are different between viruses from influenza A, B and C genus (101, 104): HA of influenza A virus contain one stearate, a saturated fatty acid with 18 carbon atoms, attached to a cysteine positioned atthe cytosol-facing end of the transmembrane region andtwo palmitates, a shorter saturated fatty acid containing 16 carbon atoms, attached to cysteines located in the cytoplasmic tail (104); HA of Influenza B virus possess two palmitates attached to cytoplasmic cysteines, whereas HEF of influenza C virus having only one transmembrane cysteine is stearoylated (101) (Figure 1.7). Several studies illuminated the essential role of palmitoylation of HA for virus replication, its association with lipid rafts (115-117), itsmembrane fusion activity (105, 111, 113, 114, 174), as well as virus particles assembly (110, 112). Compared to well-studied palmitoylation of HA, little is known about the role of stearoylation of HEF for influenza C virus replication.

To illuminate the role of S-acylation of HEF forvirus replication, I used a reverse genetics system to rescue an influenza C virus containing non-stearoylated HEF protein. In the mutant, the stearoylatedcysteine was mutated into a serine to block stearoylation. Then I compared the growth kinetics of mutant and wild type virus to see whether acylation influences virus propagation.

If acylation of HEF affects virus replication, the next aim was to determine its influence on the various activities of HEF during virus entryas well as assembly and budding of virus particles. The kinetics of transport of wild typeand non-acylationHEF to the plasma membrane, the site of virus budding, were compared by metabolic labeling and immunoprecipitation. To analyze whether the mutation of HEF affects recruitment of HEF or other components into virus particles, their protein composition was compared with that of wild type virus by SDS-PAGE and Coomassie-staining. Sine defects in virus budding are often accompanied by the formation of aberrantly formed virus particles, the morphology of virions was analyzed by electron microscopy. Finally, to determine whether stearoylation of

HEF plays a role during virus entry, the membrane fusion activity of wild type and mutant virus was compared.

3. Materials

3.1 Kits

PureYield™ Plasmid Maxiprep System	Promega GmbH
Invisorb® Spin Plasmid Mini Two	STRATEC Biomedical AG
Invisorb® Fragment Clean Up	STRATEC Biomedical AG
Invisorb® Spin DNA Extraction	STRATEC Biomedical AG
Invisorb® Spin Virus RNA Mini Kit	STRATEC Biomedical AG
QIAGEN® OneStep RT-PCR Kit	QIAGEN

3.2 Bacteria and cells

DH5α Competent E.coli cells	life technologies
Vero	ATCC number: CCL-81
MDCK I	ECACC number: 00062106
0.5%& 2% (v/v) human erythrocytes	
0.5%& 2% (v/v) chicken erythrocytes	

3.3 Apparatuses

Centrifuge 5417R	Eppendorf
L7-65 Ultracentrifuge	Beckman
SW 28 Swinging-Bucket Rotor	Beckman
SW 55Ti Rotor	Beckman
TLA-100.2 Ultracentrifuge Rotor	Beckman

Sorvall™ RC6 Plus Superspeed centrifuge	Thermo Scientific
SLA-1500 Rotor	Thermo Scientific
Vacuum Controller CVC 300	Brandtech Scientific
Eluator™ Vacuum Elution Device	Promega GmbH
NanoDrop 1000 Spectrophotometer	Thermo Scientific
Master cycler® gradient thermal cycler	Eppendorf
IQTM5 Real-Time PCR Detection System	BIO-RAD
Heracell™ 240i CO2 Incubators	Thermo Scientific
MODEL 583 GEL DRYER	BIO-RAD
TriStar LB 941 Multimode Microplate Reader	Berthold Technologies
Cary Eclipse Fluorescence Spectrophotometer	Agilent Technologies
Biometra Power Pack P25	Biomitra
Mini gel-Twin electrophoretic apparatus	Biometra
Kodak X-Omat Art Film	Sigma-Aldrich
X-ray film cassette	KIRAN
T75 cell culture flask	Corning
35 mm cell culture dish	Corning
96-well plate	Corning
2×8 mm magnetic stir bar	Sigma-Aldrich

3.4 Enzymes and regents

Phusion DNA Polymerases	Thermo Scientific
Dpn I restriction endonuclease	New England Biolabs
Liposfectamine 2000	life technologies
TPCK-trypsin	life technologies
EDTA- trypsin	life technologies
DPBS without Ca^{2+} and Mg^{2+}	PAN-biotech
Phosphate – buffered saline pH 7.4	
3% formaldehyde solution	
crystal violet	
Starving medium (MEM medium plus EBSS solution without methionine, cysteine and glutamine)	Promega GmbH
serum-free Opti-MEM medium	Invitrogen
200 mM L-glutamine	life technologies
PerkinElmer EasyTag Express Protein Labeling Mix, [^{35}S]	PerkinElmer
RIPA lysis buffer	
Protein A-sepharose	life technologies
MES buffered physiological saline (50 mM MES)	
1 M salicylate	
fixing solution (10% ethanol, 10% acetic acid)	
NaAc buffer (150 mMNaCl, 10 mM Na-Acetate buffer, pH 7.4)	

20% Triton X100 (v/v)	
Blood cell lysis buffer (5mM NaH2PO4, pH7.4, with 2% protease inhibitor PMSF)	
1, 1'-bis (4-anilino) naphthalene-5,5'-disulfonic acid (bis-ANS)	Sigma-Aldrich
Octadecylrhodamine B chloride (R18)	life technologies

3.5 Antibodies

Polyclonal antibody against influenza C virus	Rabbit serum
Monoclonal antibody 8B3A5 against HEF protein	Mice serum
Monoclonal antibody 8J3B4 against HEF protein	Mice serum

4. Method

4.1 Maxi preparation of bidirectional plasmids for influenza C virus reverse genetics

7-pPMV-plasmid reverse genetics system for influenza C virus was built and generously provided by Reinhar Vlasak (30). Details on construction of pPMV plasmid were introduced in section 1.7 (Figure 1.11).

Thaw competent cells on ice, and then add 1 µl 100 ng/µl pPMV plasmid into 100 µlXL-10E. coli competent cell and mix gently by pipetting up and down. Place the mixture on ice for 30 min then heat shock at 42°C in water bath for 60 seconds. Place mixture on ice for at least 2 min then add 900 µl antibiotic free LB mediato the tube and shake the tube at 37°C for 60 minutes at a speed of 200 rpm. Spread 50–100 µl of the cells onto the plates containing 100 µg/ml Ampicillin. Incubate the plates at 37°C overnight. On the second day, pick up single colony into 100 ml LB media containing 100 µ g/ml Ampicillin and shake at 37°C for 22h at a speed of 200 rpm. Pellet cells at 5,000 × g for 10 minutes then discard the supernatant. Cell pellet is resuspend thoroughly in 12ml of Cell Resuspension Solution by vortexing or pipetting. Add 12ml of Cell Lysis Solution. Invert gently 3–5 times to mix thenincubate for 3 minutes at room temperature.Add 12ml of Neutralization Solution and Invert gently 10–15 times to mix.Centrifuge the lysate at 14,000 × g for 20 minutes at room temperature using a fixed angle rotor.

Assemble the blue PureYield^{TM} Clearing Column and white PureYield^{TM} Maxi Binding Column in a stack, with the clearing column on top. Place this column stack on the vacuum manifold. Pour one half of the lysate into the blue PureYield^{TM} Clearing Column. Apply maximum vacuum until the lysate has passed through both the clearing and binding columns. Add the remaining lysate and maintain vacuum until the liquid has through both columns. Slowly release the vacuum. Then remove and discard the blue PureYield^{TM} Clearing Column, leaving the PureYieldTM Maxi Binding Column on the vacuum manifold. Add 5 ml of Endotoxin Removal Wash to the PureYieldTM Maxi Binding Column, apply a vacuum and allow the solution to be pulled through the column. Add 20ml of Column Wash to the binding column, and allow the vacuum to pull the solution through the column. Dry the membrane by applying a vacuum for 5 minutes. If the top of the membrane in the binding column does not appeardry, continue the vacuum for an additional 5 minutes. If more than six samples are being dried at once, increase the initialdrying time to 10 minutes as additional samples can reduce vacuum strength. Remove the PureYield™ Maxi Binding Column from the vacuum

manifold, and tap the tip of the column on a paper towelto remove any remaining ethanol. Place a 1.5ml microcentrifuge tube into the base of the Eluator™ Vacuum Elution Device, securing the tubecap in the open position. Assemble the Eluator™ Vacuum Elution Device, and insert the DNA binding column into the device, making sure that thecolumn is fully seated on the collar. Place the elution device assembly onto a vacuum manifold. Add 1ml of Nuclease-Free Water to the DNA binding membrane in the binding column. Wait 1 minute. Apply maximumvacuum for 1 minute or until all liquid has passed through the column. Remove the microcentrifuge tube and save for DNA quantitation by Nanodrop.

4.2 Constructing pPMV plasmid with non-acylated HEF sequence by site-directed mutagenesis

Applying a site-directed mutagenesis method, the stearoylated Cysteine on HEF transmembrane domain (638Cys) was mutated into a Serine to block stearoylation (Figure 4.1). A pair of primers was designed and synthesized:

HEF-C-S-U	5'-CTCTGGGATCGCCATCAGCAGAACTAAATGAT-3'
HEF-C-S-D	5'-ATCATTTAGTTCTGCTGATGGCGATCCCAGAG-3'

Site-directed mutagenesis was performed by a two-step PCR method. For the first step of PCR, the following regent were mixed thoroughly:

5×Pusion HF buffer	10μl
Template (100 ng/μl pPMV- HEF plasmid)	1μl
10mM dNTPs	2 μl
Phusion polymerase	0.5μl
ddH2O	36.5 μl

The above mixture was distributed into 2 PCR tubes equally, then add 2μl of primer HEF-C-S-U into tube No. 1 and add 2μl of primer HEF-C-S-Dinto tube No. 2, respectively. Then the first PCR was performed as the following program:

Cycle 1 × 1	Step1: 98 ℃	30s
Cycle 2 × 3	Step 2: 98 ℃	10 s
	Step 3: 57 ℃	30 s
	Step 4: 72℃	3 min
Cycle 3 × 1	Step 5: 4℃	hold

After the first PCR, 25 μl products from both tube No. 1 and tube No. 2 were transfered into a new PCR tube. 0.5μl Phusion polymerase was added into the tube and mixed thoroughly. Then the second step PCR was performed as following program:

Cycle 1 × 1	Step1: 98 ℃	30 s
Cycle 2 × 30	Step 2: 98 ℃	10 s
	Step 3: 57 ℃	30 s
	Step 4: 72℃	3 min
Cycle 3 × 1	Step 5: 4℃	hold

Add 1 μl *Dpn* I restriction endonuclease into PCR product and incubate at 37 ℃ for 2 h to digest the remaining wt plasmid, then use 25μl to transformed XL-10 competent E. coli cells. Cast the transformed bacteria on an ampicillin resistant LB plate and incubated overnight at 37 ℃. Then pick single colonies into 3 ml ampicillin resistant LB medium, incubate at 37 ℃ at a speed of 200 rpm overnight. Extract plasmid using invisorb® Spin Plasmid Mini Two kit

and send plasmid to company for sequencing. Finally, maxiprepare was performed for the mutant pPMV plasmids.

4.3 Generation of mutant and wt influenza C viruses by reverse genetics

Reverse genetics was performed as previously described (Figure 4.2) (30). 90% confluent Vero cells in 35 mm cell culture dish were transfected with seven pPMV plasmids which contain seven influenza C virus gene fragments respectively. Vero cells were transfected by total amount of 4μg bidirectional plasmids mixture (all plasmids are added at the same amount) with Liposfectamine 2000 (Invitrogen) according to the manufacturer's instructions. Six hours post transfection, cells were washed twice with PBS and added with 3 ml serum-free Opti-MEM medium (Invitrogen). Add TPCK-trypsin at a final concentration of 2μg/ml. Then incubate the cells in 33℃. TPCK-trypsin is added to the medium every second day. 4 to 7 days after transfection, supernatants were collected as the first generation of rescued viruses. 90% confluent MDCK I cells in 35 mm cell culture dish were infected with 200 μl above supernatant then maintained in 3μl serum-free Opti-MEM medium. Cells were incubated in 33℃ and added TPCK-trypsin at a final concentration of 2μg/ml every second day. About 72h post-infection, as soon as the cytopathic effect became visible, the supernatant were collected as the second generation of virus. Hemagglutination (HA) test were performed with 0.5% (v/v) human erythrocytes. Use Invisorb® Spin Virus RNA Mini Kit to isolate virus vRNA as manufacturer's instruction. A pair of primers were designed and synthesized：

HEF-target-U	5'-GCCATCAGAGATCTAAC-3'
HEF-target-D	5'-CTGTACAAAATATTGAC-3'

Use the above primers and QIAGEN®OneStep RT-PCR Kit to perform RT-PCR as follow：

5×QIAGEN®OneStep RT-PCR Buffer	10μl
Template (vRNA)	1μl
10 mM dNTPs	2 μl
HEF-target-U	0.5 μl

HEF-target-D	0.5 µl
QIAGEN®OneStep RT-PCR Enzyme Mix	2 µl
ddH2O	34µl

Cycle 1 × 1	Step1: 50℃	30 min
Cycle 2× 1	Step 2: 95℃	15 min
Cycle 3 × 30	Step 3: 94℃	30 s
	Step 4: 57 ℃	30 s
	Step 5: 72℃	30s
Cycle 4 × 1	Step 6: 4℃	hold

The PCR product was sent for sequencing.

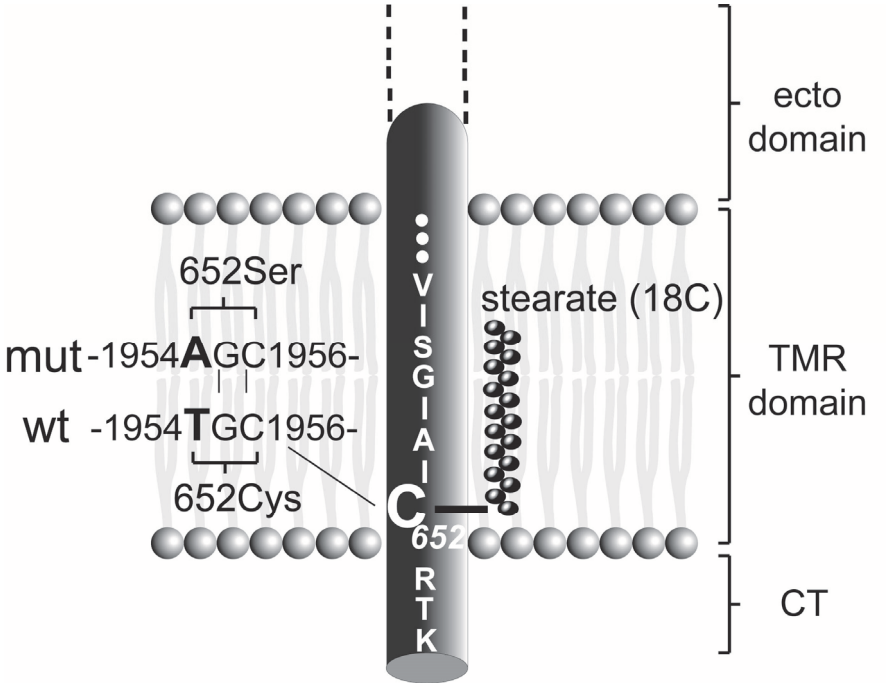

FIG 4.1 Construct of non-stearoylation HEF mutant through site-directed mutagenesis. Location of the attachment site for stearate at the cytosol-facing end of the transmembrane region of HEF. The TGC triplet encoding cysteine was changed to AGC in order to remove the acylation site.

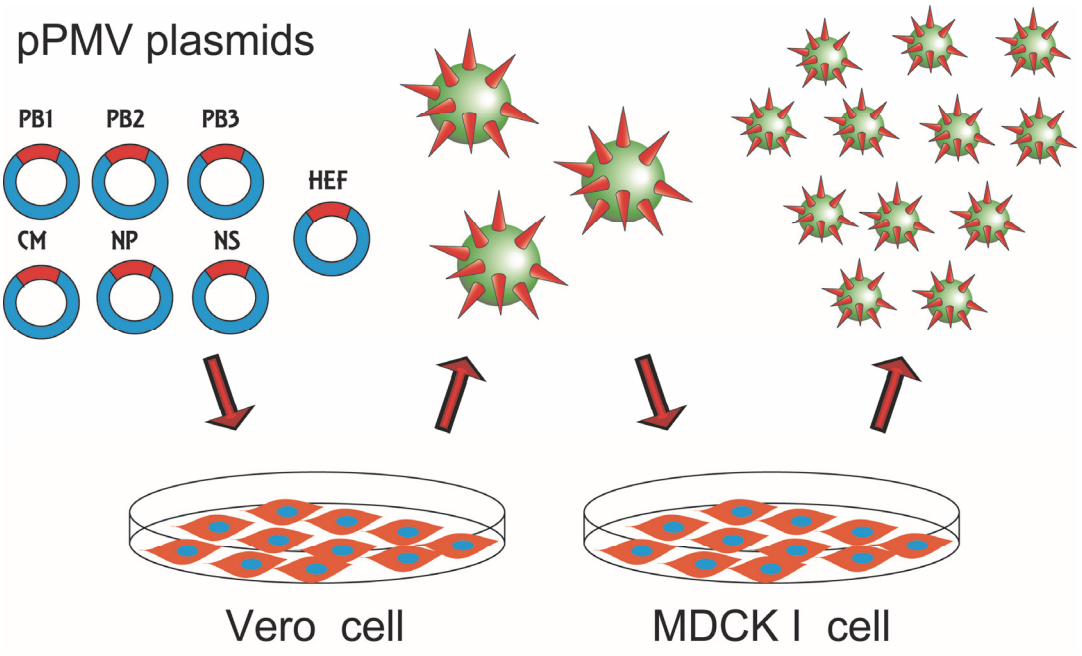

FIG 4.2 Rescue influenza C viruse by 7-pPMV-plasmid reverse genetics system. Co-ransfect seven pPMV plasmids containing influenza C virus genome cDNA into Vero cells.After incubated under 33℃ for 4-7 days, supernatant was taken out and added into MDCK I cells. 3-5 days after incubated under 33℃, CPE was observed and virus was able to be detected.

4.4 Determination of infectious titers of viruses by $TCID_{50}$

The infectious titer of the wt and mutant viruses were determined by TCID50 according to previously reported method. Briefly, 100 ul virus stock was add to 900 ul serum-free Opti-MEM medium, mix thoroughly to get the 1:10 diluted virus. 100μl 10^{-1} virus was added into 900 ul serum-free Opti-MEM medium and mixed thoroughly to get the 1:100 diluted virus. The gradual dilution procedure was repeated to get serial dilutions of viruses from 10^{-1} to 10^{-11}. 80~90% confluent MDCK I cells in 96-well plates were washed by PBS buffer twice. Then add diluted viruses into 96-well plates by100 μl per well and 8 wells for each dilution. The plates were incubated under 33 ℃ for 1h, then supernatant was removed and the cells were washed twice with PBS. 100 ul of serum-free Opti-MEM medium with 2 μg/ml TPCK-trypsin was added to each well. Then the plates were incubated under 33℃ for 5~7 days. Every second day, 25 ulOpti-MEM medium with high concentration TPCK-trypsin was added to each well to keep the final concentration of the new added TPCK-Trypsin at 2 ug/ml. Then the supernatant was removed and washed once with PBS buffer, 50 ul 3% formaldehyde solution was added to each well and incubated for 5 min at room temperature to fix the cells. The fixed cell layer was stained by crystal violet and the TCID 50 titer of wt and mutant strains were calculated through Reed &Muench method.

4.5 Compare growth kinetics of wt and mutant strains

90% confluent MDCK I cells in 2 100 mm dishes were washed twice with PBS buffer, then were infected with wt and mutant strains at a m.o.i. of 0.005, respectively, incubated in serum-free Opti-MEM medium with 2ug/ml TPCK-Trypsin under 33 ℃. At 12 h, 24 h, 48 h, 72 h and 96 h post infection, 100 ul samples were taken out and stored in −80 ℃. Determine the TCID 50 titer of each sample as described above. The titer of each sample was plotted against its time point, therefore the growth kinetics of wt and mutant strains was able to be compared. The result came from 3 independent experiments.

4.6 Continuous passages of the mutant and wt strains

90% confluent MDCK cells in 35 mm dishes were washed twice with PBS buffer, then 200 μl supernatant from P2 generation mutant or wt was added. Incubated under 33℃ for 60 min. Removed viruses, then washed the cells with PBS buffer twice. Add 3 ml serum-free Opti-MEM medium to each dish and add TPCK-trypsin at a final concentration of 2μg/ml. Incubate cells under 33℃ for 72h. During incubation, the same concentration of TPCK-trypsin was added at 36h post infection. 72h p. i. , collect the supernatant, centrifuged at 3000 rpm for 5min. Take 200 ul supernatant to extract v-RNA with Invisorb® Spin Virus RNA Mini Kit. Then use QIAGEN®OneStep RT-PCR Kit, primer HEF-target-U and primer HEF-target-D to perform RT-PCT. Send the extracted PCR fragments to Company for sequencing.Continuously passaged the virus six times to P7 generation, and RT-PCR were performed during every passage to confirm the stability of the non-acylated mutant strain.

4.7 Competitive growthof wt and mutant viruses

The competition experiment was performed to test whether the non-acylated HEF reduce the competitive fitness of the mutant virus compared with the wild type virus. When co-infected MDCK I cells with wt and mutant strains at a very small M.O.I. value, if the mutant strain exhibits a selective disadvantage, it would rapidly be eliminate by the wt strain (Figure 4.3).

90% confluent MDCK I cells cultured in 100 mm dishes were co-infected with wt and non-acylated mutant strains at a ratio of 1:1 and 1:5 (total m.o.i. was 0.005). At 24h, 48h, 72h post infection, 200 ul supernatant were taken from dishes and RT-PCR were performed. All the PCR products were sent to Company for sequencing. The competitive growth of wt and mutant strains was able to be detected within the peak-wave chart of sequencing results. Note

the differences in the peak heights and areas in the chromatograms should not be interpreted in a precise quantitative manner.

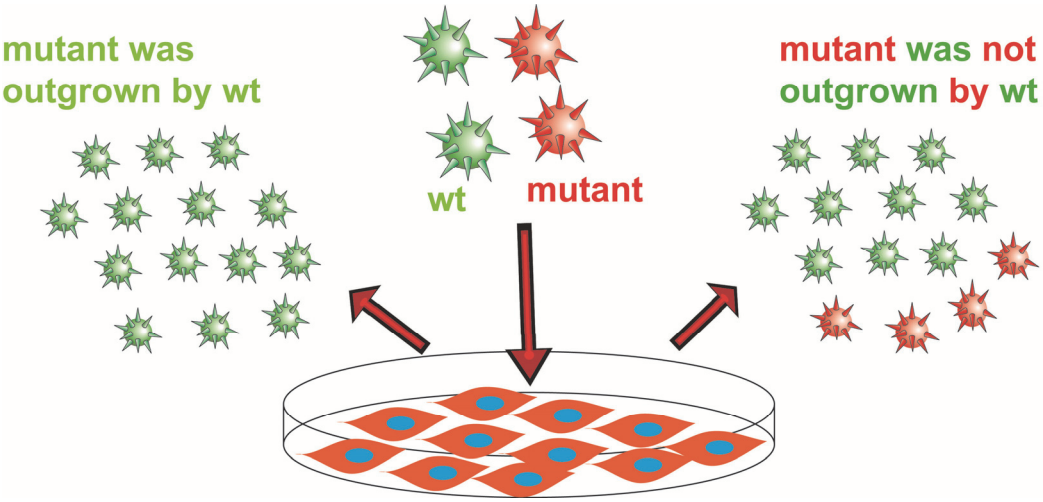

FIG 4.3 Competitive experiment of wt and mutant influenza C viruses. MDCK I cells were co-infected with wt and mutant strains at a low M.O.I. , if the mutant strain exhibits a selective disadvantage, it would rapidly be eliminate by the wt strain; If the non-acylation mutation on HEF does not bring shortcoming to competitive fitness, mutant virus would be able to be detected at different time points accompanying wt virus.

4.8 Comparison of protein composition between wt and mutant viruses by SDS-PAGE

The protein components of the wt and mutant virus strains virus particles were compared to assess whether the non-acylated mutation on HEF protein influence the virus particle composition by SDS-PAGE.

The viral particles used for SDS-PAGE were harvested as follow: 90% confluent MDCK I cells cultured in 150 mm dishes were infected with wt and mutant strains at an m.o.i. of 0.5, respectively. After 48 hours incubation at 33 ℃, the supernatant was collected. The supernatants were centrifuged at 3000 rpm for 10 min to remove floating cells. Then supernatants without any treated or treated with 10 μg/ml TPCK-Trypsin at 37 ℃ for 1 h were ultra-centrifuged at 28000 rpm for 2 hours. Supernatant were removed and the pellets were dissolved by 50 ul reducing or non-reducing SDS-PAGE loading buffer, respectively.

Then electrophoresis on 15% SDS-PAGE under reducing and non-reducing condition was performed and the gels were stained with Coomassie brilliant blue.

4.9 Electron microscope of the viral particles

To determine whether acylation have an influence on the structure of viral particles, viruses were visualized by negative staining transmission electron microscope and Cryo-transmission electron microscope.

The viral particles used for SDS-PAGE were harvested as follow: 90% confluent MDCK I cells cultured in 150 mm dishes were infected with wt and mutant strains at an m.o.i. of 0.5, respectively. After 48 hours incubation at 33 ℃, the supernatant was collected. The supernatants were centrifuged at 3000 rpm for 10 min to remove floating cells. Then supernatants were ultra-centrifuged at 28000 rpm for 2 hours. Supernatant were removed and the pellets were resuespended with 500 μl PBS buffer. Samples were sent for electron microscopy imaging.

To perform the transmission electron microscopy (TEM) 5 μl virus suspension in PBS were pipetted onto a hydrophilised (by 60 s glow discharging at 8 W in a BALTEC MED 020 device) carbon covered microscopical copper grid (400 mesh). After 30 seconds a piece of filter paper was used to remove excess fluid. Subsequently, 5 μl of the contrast enhancing heavy metal stain solution (1% Phosphotungstic acid, pH 7.4) were applied and blotted again after 45 s. After air-drying a standard holder was used to transfer the sample into a Tecnai F20 TEM microscope (FEI Company, Oregon) equipped with field emission gun and operating at 160 kV. Micrographs were recorded with an FEI Eagle 4k x 4k CCD camera using the twofold binning mode.

To perform the Cryo-TEM, virus sample droplets (5μl) were applied to hydrophilisedperforated (hole diameter of 1μm) carbon film-covered 200 mesh grids (R1/4 batch of Quantifoil, MicroTools GmbH, Jena, Germany). The excessive fluid was removed with a piece of filter paper until an ultrathin film of the sample solution remained spanning the holes of the carbon film. Immediately after blotting, the samples were vitrified by plunging the grids (held by a forceps) into liquid ethane using a guillotine-like apparatus. The vitrified samples were subsequently transferred under liquid nitrogen into a Tecnai F20 TEM (FEI Company, Oregon) by the use of a Gatan tomography cryo-holder (Model 914). Microscopy was carried out at a 94 K sample temperature using the low-dose protocol of the microscope.

4.10 Testing antibodies for metabolic labeling & immunoprecipitation

One polyclonal rabbit antibody against influenza C JJ50 strain and 2 monoclonal antibodies against JJ50 HEF protein, 8B3A5 and 8J3B4, were generously provided by Reinhar Vlasak. Metabolic labeling & immuneprecipitation was carried out to select the optimal antibody and its usingamount for the experiment.

90% confluent MDCK cells in 9 35 mm cell culture dishes were infected with wt virus at an m.o.i. of 0.5 for 1 h. After 24 hour incubation at 33 ℃, supernatant was removed and the cells were washed twice by PBS. Add 950 ul starving medium (MEM medium plus EBSS solution without methionine, cysteine and glutamine) and 20 ul 200 mM L-glutamine per dish and cells were incubated for 1 hour at 33 ℃. Then, transfer the dishes to the isotope lab and add 5 ul ^{35}S-methionine (50 uCi) to each dish. Then incubate the dishes in the incubator in the isotope lab for 1h. The medium was removed and washed once with PBS. Added 600 ul ice-cold RIPA buffer and then incubated for 15 min on ice. Transferred lysates into Eppendorf reaction tubes and centrifuged for 20 min at a speed of 14000 rpm/min at 4 ℃. Transfer the supernatant into 9 new tubes. Add 8B3A5 antibody 2 µl, 1 µl, 0.5 µl, 8J3B4 antibody 2 µl, 1 µl, 0.5 µl, polyclonal antibody2 µl, 1 µl and 0.5 µl into the above 9 tubes, respectively. The tubes were shook overnight on shaker in the cold room. At the second day, added 50 µl of a 1:1-slurry of protein A-sepharose in RIPA to each lysate and incubate for 2.5 h at 4 ℃ on the shaker. Centrifuged the samples at 3000 rpm for 3 min, took off supernatant and re-suspended pellet in 1 ml RIPA, vortexed and centrifuged again. Repeat this washing procedure 4 times. After the last washing, took off the supernatant as completely as possible. Add 30 µl 4× loading buffer into the samples to re-suspend the pellet. Heat at 95 ℃ for 5 min and then loaded the samples into 15% polyacrylamide gel and electrophoresis was carried out. After the SDS-PAGE, the gel was transferred into fixing solution (10% ethanol, 10% acetic acid) and shook overnight. Poured away fixing solution and washed the gel twice for 15 min each with aquadest. Then replace with 1 M salicylate for 30 min to 1 hour.The gel was dried and placed into a film cassette and put an X-ray film on it. Incubate at −80 ℃ for 3 to 5 days. Then develop the film.

4.11 Cell membrane transport kinetics of wt and non-acylated HEF

Cell surface transport kinetics of wt and non-acylation HEF were examined by metabolic labeling &immune precipitation as previously described with slight modification (72). In this experiment, HEF0 which has been transported on surface is able to be cleaved into HEF1 and

HEF2 by adding TPCK-trypsin, while HEF0 which has not arrived at surface is not cleaved. Proportion of cleaved HEF0, i.e. surface HEF protein, can be calculated from comparison between HEF0 and HEF1 amount (Figure 4.4).

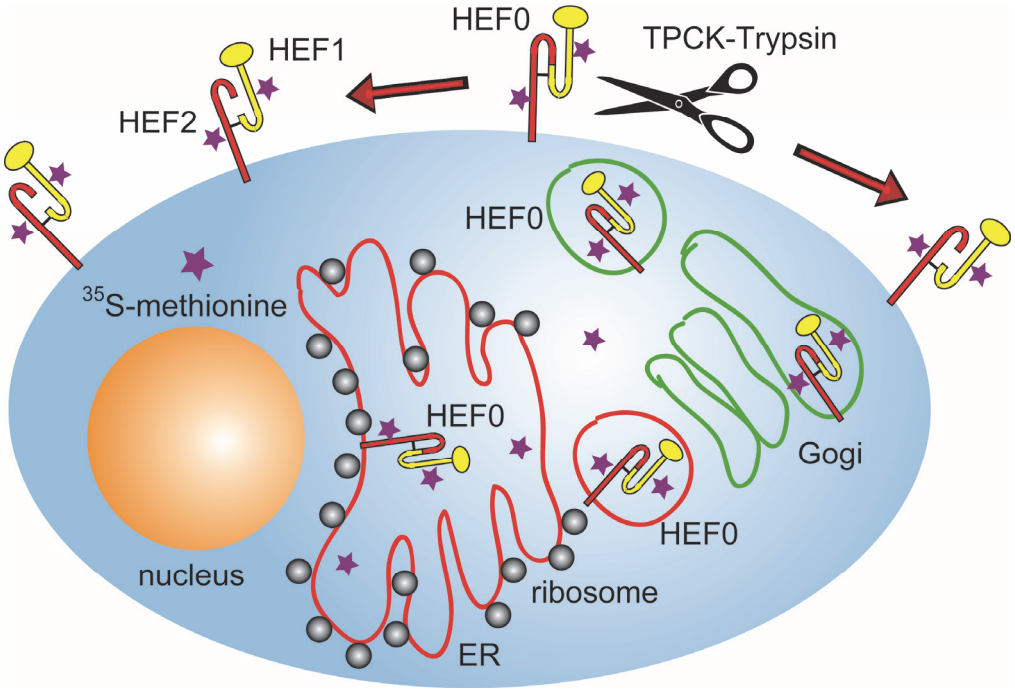

FIG 4.4 Cell membrane transported HEF0 is cleaved into HEF1 and HEF2 by TPCK-Trypsin. HEF0 which has been transported on surface is able to be cleaved into HEF1 and HEF2 by adding TPCK-trypsin, while HEF0 which has not arrived at surface is not cleaved. When metabolically labeled by ^{35}S-methionine, proportion of cleaved HEF0, i.e. surface transported HEF protein, can be calculated from comparison between HEF0 and HEF1 amount.

90% confluent MDCK cells in 35 mm cell culture dishes were washed twice with PBS buffer, and then infected with wt and mutant strains, respectively, at a m.o.i. 0.5 for 1 h. After 24 hour incubation at 33 ℃, supernatant was removed and the cells were washed twice by PBS. Add 950 ul starving medium (MEM medium plus EBSS solution without methionine, cysteine and glutamine) and 20 ul 200 mM L-glutamine per dish and cells were incubated for 1 hour at 33 ℃. Then, transfer the dishes to the isotope lab and add 5 ul ^{35}S-methionine (50 uCi) to each dish. Incubate the dishes in the incubator in the isotope lab for 1 min, 30 min, 60 min, 90 min, 120 min, and 180 min, respectively. 10 min prior to the indicated times, TPCK-Trypsin was added to the media at a concentration of 15 ug/ml to cleave cell surface HEF0 into HEF1 and HEF2 subunits. After the indicated labelling time, the medium was removed and washed once with PBS. Added 600 ul ice-cold RIPA buffer and then incubated for 15

min on ice. Transferred lysates into Eppendorf reaction tubes and centrifuged for 20 min at a speed of 14000 rpm/min at 4 ℃. Took the supernatant into a new tube and added 0.5 ul HEF monoantibody and shook overnight on shaker in the cold room. At the second day, added 50 ul of a 1:1-slurry of protein A-sepharose in RIPA to each lysate and incubate for 2.5 h at 4 ℃ on the shaker. Centrifuged the samples at 3000 rpm for 3 min, took off supernatant and re-suspended pellet in 1 ml RIPA, vortexed and centrifuged again. Repeat this washing procedure 4 times. After the last washing, took off the supernatant as completely as possible. Add 30 ul 4× loading buffer into the samples to re-suspend the pellet. Boiled at 95 ℃ for 5 min and then loaded the samples into 15% polyacrylamide gel and electrophoresis was performed. After the SDS-PAGE, the gel was transferred into fixing solution (10% ethanol, 10% acetic acid) and shook overnight. Poured away fixing solution and washed the gel twice for 15 min each with aqua dest. Then place it into 1 M salicylate for 30 min to 1 hour. The gel was dried and placed into a film cassette and put an X-ray film on it. Incubate at −80 ℃ for 3 to 5 days. Then the film was developed. The film was further analyzed by analysis software.

4.12 Hemolysis assay of mutant influenza C virus with non-acylation HEF and wt virus

To determine whether the non-acylation mutation at HEF protein influence the membrane fusion activity or not, a serial hemolysis assays were carried out in a pH-dependence, a time-dependence and a viral titer-dependence way, respectively (Figure 4.5).

To perform the pH-dependent hemolysis assay, added 50uL hemagglutining titer 6virus into 100 uL 2% chicken erythrocytes, mixed gently, then incubated the mixture in 4 ℃ for 30min; Centrifuged the mixture at a speed of 1500 rpm/min for 1min, then removed the supernatant and re-suspended the erythrocytes with MES buffered physiological saline (50 mM MES) at pH 4.5, 4.75, 5.0, 5.25, 5.5, 5.75, 6.0, 6.5 and 7.0, then incubated samples in 37 ℃ for 60 min; After the incubation, re-suspended the erythrocyte very gently, then centrifuged the samples at a speed of 1500 rpm/min for 1min. Transported 50uL supernatant into wells of 96-well plate and added 200uL PBS into the same well; Determined the OD value of each well at wavelength 405 nm through micro plate reader. Plotted the OD values against pH values and then compare the trend lines between wt and mutant strains.

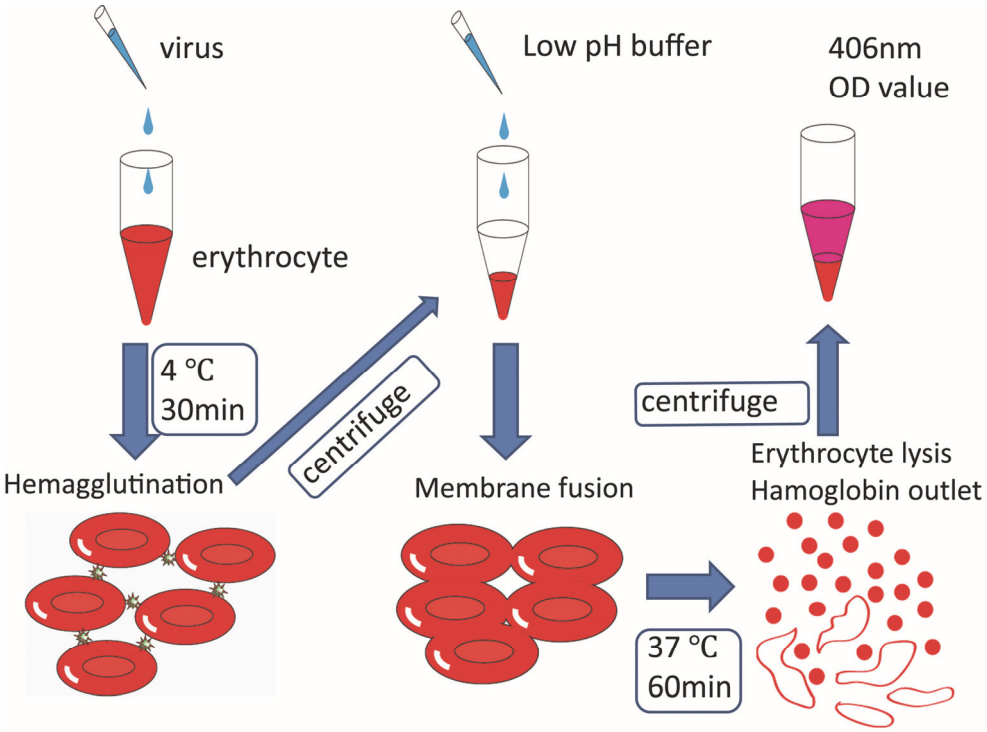

FIG 4.5 Technological process of influenza C virus hemolysis experiment. Virus at a certain titer was added into 2% chicken erythrocytes, then the mixture was incubated in 4 ℃ for 30 min to give rise to hemagglutination; The mixture was centrifuged at a speed of 1500 rpm/min for 1 min, then remove the supernatant and re-suspended the erythrocytes with MES buffered physiological saline (50 mM MES) at pH 4.5, 4.75, 5.0, 5.25, 5.5, 5.75, 6.0, 6.5 and 7.0 (in pH-independent hemolysis experiment) or at pH5.25 (in time-dependent and titer-dependent hemolysis experiments), then incubated samples in 37 ℃ for 60 min (in pH-independent and titer-dependent hemolysis experiments) or for 10 min, 30 min, 60 min, 90 min, 120 min and 180 min, respectively (in time-dependent hemolysis experiments); After the incubation, the mixture was re-suspended very gently, then was centrifuged at a speed of 1500 rpm/min for 1min. Transported 50uL supernatant into wells of 96-well plate and added 200uL PBS into the same well; Determined the OD value of each well at wave length 405 nm through micro plate reader.

Time-dependent hemolysis assay was similar to above assay with slightly modification. Added 50uL hemagglutining titer 6 virus into 100uL 2% chicken erythrocytes, mixed gently, then incubated the mixture in 4 ℃ for 30min; Centrifuge the mixture at a speed of 1500 rpm/min for 1min, then remove the supernatant and re-suspended the erythrocytes with MES buffered physiological saline (50 mM MES) at pH 5.25, and incubated samples in 37 ℃ for 10 min, 30 min, 60 min, 90 min, 120 min and 180 min, respectively. At the indicated time points, re-suspended the erythrocyte very gently, then centrifuged the samples at a speed of 1500 rpm/min for 1min. Transported 50uL supernatant into wells of 96-well plate andadded 200uL PBS buffer into the same well; Determine the OD value of each well at wavelength

405 nm through micro plate reader. Plotted the OD values against incubation time and then compare the trend lines of wt and mutant strains.

Titer-dependent hemolysis assay was similar to above 2 assays with slightly modification. Added 50uL virus of different hemagglutining titer at 8, 16, 32, 64, 128, 256 and 512 into 100uL 2% chicken erythrocytes, mixed gently, then incubated the mixture in 4 ℃ for 30min; Centrifuged the mixture at a speed of 1500 rpm/min for 1min, then removed the supernatant and re-suspended the erythrocytes with MES buffered physiological saline (50 mM MES) at pH 5.25, and incubated samples in 37 ℃ for 60min. Then re-suspended the erythrocytes very gently, then centrifuged the samples at a speed of 1500 rpm/min for 1min. Transported 50uL supernatant into wells of 96-well plate and added 200uL PBS buffer into the same well; Determine the OD value of each well at wavelength 405 nm through micro plate reader. Plotted the OD values against hemagglutining titer and then compare the trend lines of wt and mutant strains.

4.13 pH dependent binding of fluorophore bis-ANS to wt and mutant strain

Binding of the fluorophore 1,1'-bis(4-anilino)naphthalene-5,5'-disulfonic acid (bis-ANS) (invitrogen) to virus particles at various pH values was done as described for influenza A virus (42). Bis-ANS (3.25 uM final concentration) was added to 1 ml pre-warmed MES-buffer (50 mM MES buffered physiological saline, adjusted to a pH of 4.5, 4.75, 5.0, 5.25, 5.5, 5.75, 6.0, 6.5 or 7.0 with NaOH). The suspension was transferred to a cuvette and stirred continuously with a 2×8 mm magnetic stir bar. The bis-ANS fluorescence was measured (excitation wavelength 400 nm, emission 490 nm) at 37°C in a Cary Eclipse Fluorescence Spectrophotometer (Agilent Technologies) until the base line was stable. Then 10 µl virus (cleared cell culture supernatant adjusted with PBS to 1 mg/ml) was injected into the cuvette and the fluorescence intensity was recorded for 4 min with a time resolution of 1 s.

5. Results

5.1 Generation of mutant and wt influenza C viruses by reverse genetics

After transfecting Vero cells with seven pPMV plasmids containing influenza C genome cDNA segments, no obvious cytopathic effect (CPE) was observed 3-5 days post transfecting. The supernatant did not possess hemagglutination (HA)titer (data not shown). Use the supernatant to infect MDCK I cell, CPE was observed at 72 hpost infection and the supernatant showed a hemagglutination (HA) titer of 2^8 for both mutant and wt viruses to 0.5 % human erythrocytes (Figure 5.1A). Then RT-PCR and sequencing results confirmed the existing of wt and mutant virus in the supernatant (Figure 5.1B).

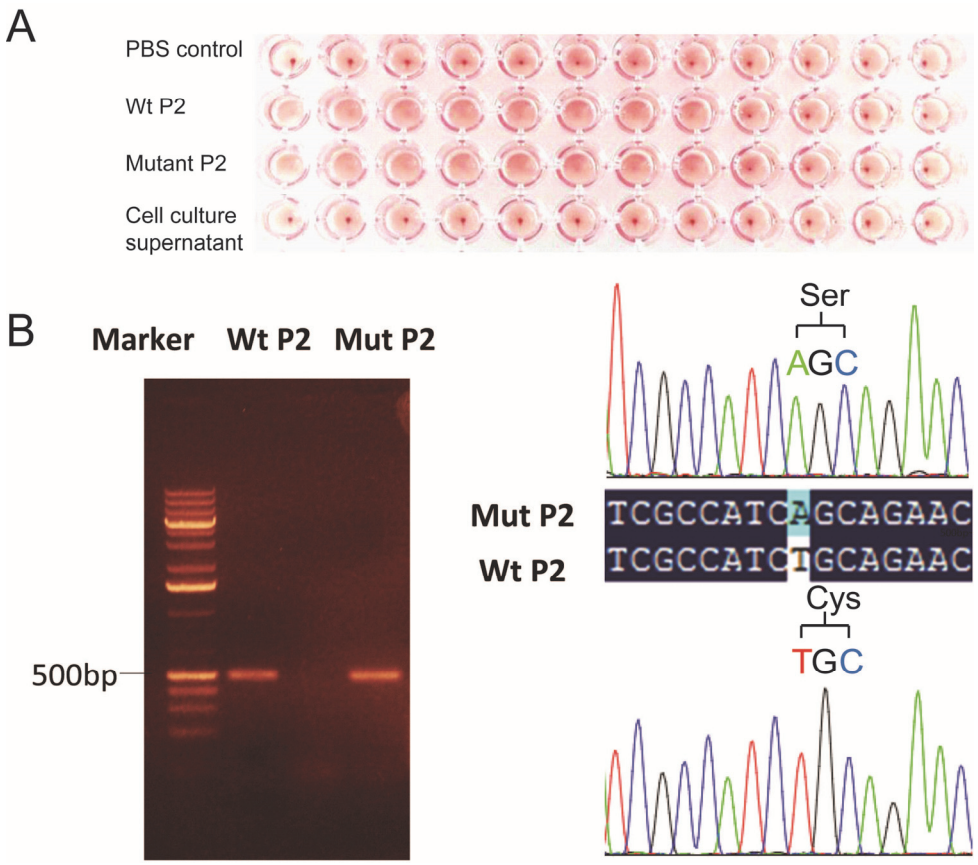

FIG 5.1 Rescue of wt and mutant viruses were confirmed by hemagglutination (HA) test, RT-PCR and sequencing. (A) P2 generation of wt and mutant viruses showed a hemagglutination (HA) titer of 2^8; (B) Use the extractive vRNA from supernatant as template, RT-PCR was carried out. In agarose gel electrophoresis, target segment ~500 bp was observed. The sequencing results confirmed the existence of wt and mutant strains.

5.2 Growth kinetics of wt and mutant strains

Next we compared the production of infectious particles of mutant and wild type (wt) virus under multiple cycle growth conditions. MDCKI cells were infected with wt and mutant strains at an m.o.i. of 0.005 and incubated in the presence of trypsin at 33 ℃, the optimal growth temperature of influenza C virus. At 12, 24, 48, 72, 96 and 144 hours post infection an aliquot of the cell culture supernatant was removed and the infectious titer was determined by a TCID 50 assay. Plotting the titer of each sample from three independent infection experiments against its time point revealed that growth of the mutant was reduced by about one log, especially at early time points (Figure5.2). The results are consistent with published data on acylation mutants of various HA subtypes where exchange of the stearyolated cysteine at the end of the TMR caused a small growth defect, whereas deletion of the palmitoylated cysteines reduced virus titers by several logs or the corresponding infectious virus particles could even not be rescued (110-112).

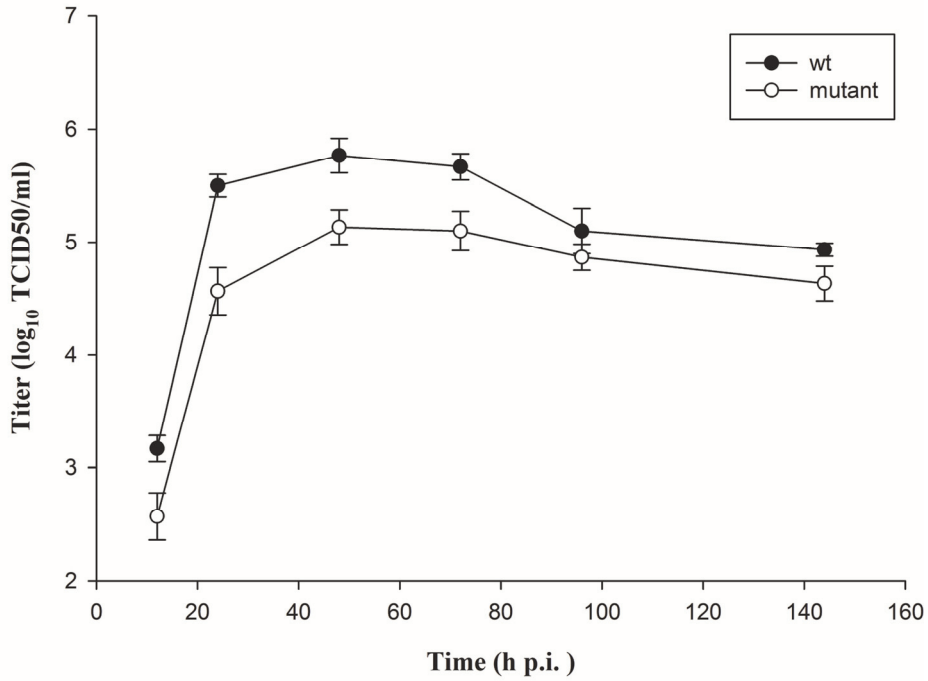

FIG 5.2 Growth kinetics of wt and mutant influenza C viruses. MDCK I cells were infected with wt and mutant virus at m.o.i. of 0.005 and incubated in the presence of trypsin at 33 ℃. At 12 h, 24 h, 48 h, 72 h, 96 h and 144 h post infection, aliquots were removed from the cell culture supernatant and the TCID 50 titer was determined. The titer of each sample is plotted against its time point. The graph shows the mean including standard deviation from three different experiments.

5.3 Continuous passages of the mutant and wt strains

Due to the high error rate of the viral RNA polymerase a one nucleotide exchange can rapidly revert back to wild-type if the resulting virus has a growth advantage. To test its stability the mutant virus was serially passaged seven times under multiple cycle growth conditions, RNA was extracted from virus particles and reverse transcribed. Sequencing of the RT-PCR products shows that the nucleotide substitution is still present in the HEF gene (Figure5.3).

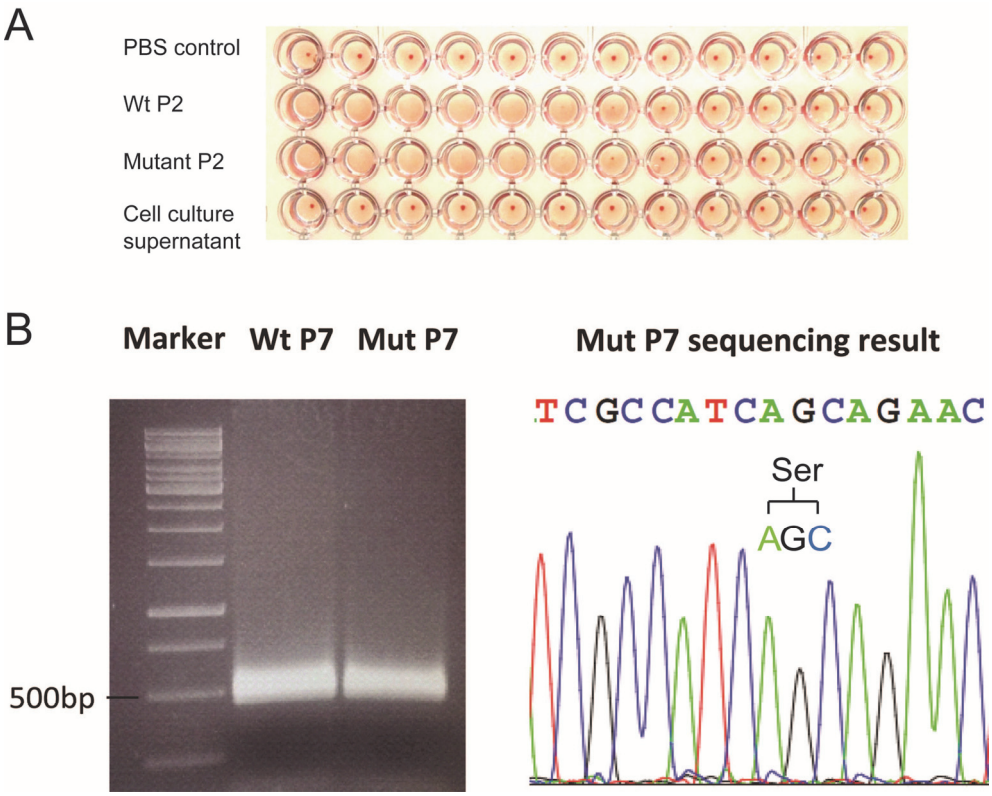

FIG 5.3 Continuous passages of the wt and mutant influenza C viruses. (A) HA-assay of wild type and mutant virus particles after 7 times continuously passages. Both viruses grow to a titer of 2^7. (B) Use the extractive vRNA from supernatant as template, RT-PCR was carried out. In agarose gel electrophoresis, target segment ~500 bp was observed; Mutant virus was serially passaged seven times in MDCK I cells and the HEF gene was sequenced. No reversion to the wild type triplet was observed.

5.4 Competitive growth of wt and mutant viruses

We next hypothesized that mutating HEF might reduce the competitive fitness of the virus compared to the wild type virus. If the latter exhibits a selective advantage, it would rapidly eliminate the mutant one. To test this, we co-infected MDCKI cells under multiple cycle

growth conditions (total m.o.i.: 0.005) with mutant and wild type virus at a ratio of 1:1, removed aliquots from the cell culture supernatant at 24h, 48h and 72h p.i. and sequenced the RT-PCR products (Figure5.4). The sequencing chromatograms showed that both wild-type and mutant nucleotide species were present at each time point, reflected by superimposed peaks for the respective bases. Although differences in the peak heights and areas in the chromatograms should not be interpreted in a precise quantitative manner, it is also obvious that peak heights did not change within the time frame of the experiment (72 h). The same result was obtained if wild-type and mutant virus was mixed at a ratio of 1:5ratio (Figure 5.4).

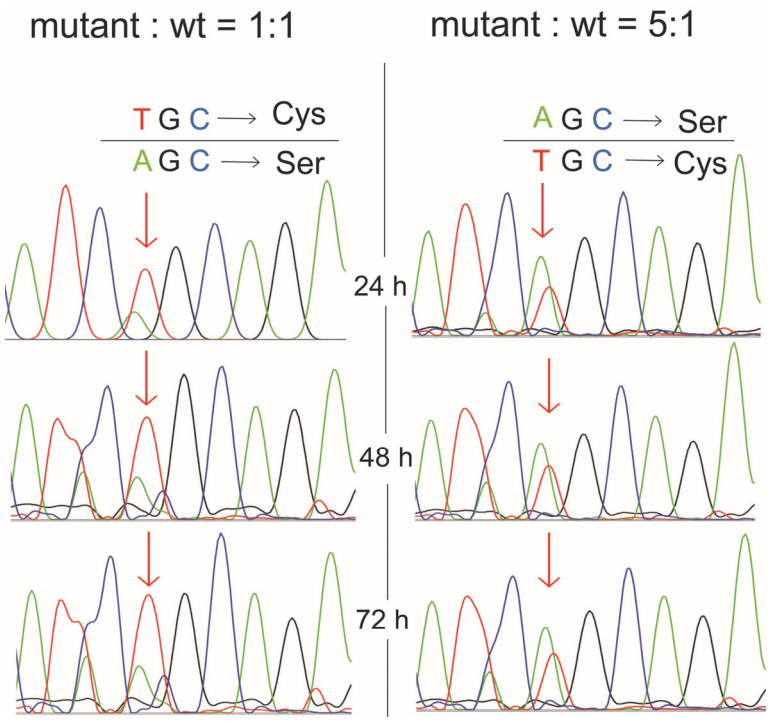

FIG 5.4 Competitive experiments of wt and mutant influenza C viruses. MDCK I cells were co-infected with a 1:1 or 1:5 mixture of wt and non-acylated mutant (total m.o.i. of 0.005). At 24h, 48h, 72h post infection an aliquot of the supernatant was removed and the HEF gene was sequenced. Within the peak-wave charts of the sequencing chromatogram the signal for wt (TGC→stearoylated cysteine at position 638) and for mutant (AGC→non-stearoylated serine at position 638) was observed at each time point.

5.5 Protein composition of wt and mutant viruses by SDS-PAGE

To assess whether the mutation in HEF also influences the viral protein composition we amplified wild type and mutant virus in the absence of trypsin under one cycle growth conditions (m.o.i. = 0.5) in MDCKI cells, purified virus particles and analyzed their protein composition by SDS-PAGE and Coomassie staining (Figure5.5). Both after reducing and

non-reducing SDS-PAGE three major bands are present in the gel, uncleaved HEF0, NP and M1 that represent the main components of influenza C virus particles. As already described, uncleaved HEF exhibits a higher SDS-PAGE mobility at non-reducing compared to reducing conditions. More importantly, the band pattern of wild type and mutant virus is almost identical indicating that acylation of HEF does not affect the protein composition of virus particles.

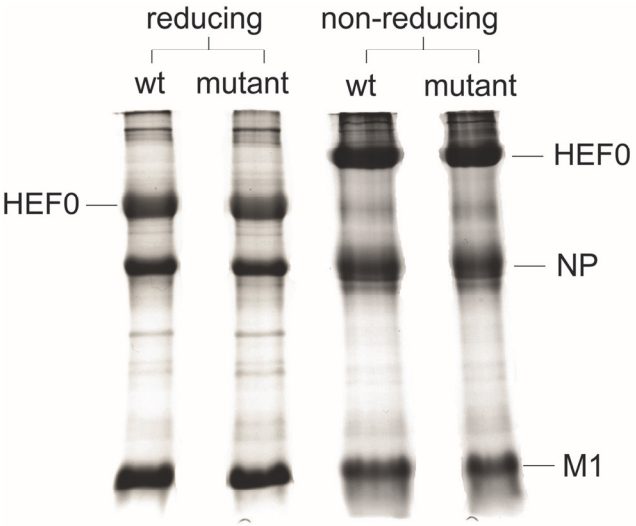

HEF0 : NP : M1

	reducing	non-reducing
wt	1 : 1,03 : 1,03	1 : 0,9 : 0,87
mutant	1 : 1,04 : 1,03	1 : 0,9 : 0,87

FIG 5.5 Protein composition of wt and mutant influenza C virus particles. MDCK I cells were infected with wt and mutant virus at an m.o.i. of 1. After 48 hours incubation at 33 ℃ in the absence of trypsin, virus particles were prepared from cleared cell culture supernatants by ultra-centrifugation and subjected to reducing or non-reducing SDS-PAGE and Coomassie staining. Uncleaved HEF0 has a different SDS-PAGE mobility under reducing and non-reducing conditions as described previously . The density of individual bands (HEF0, NP, M1) was quantified, normalized (HEF0 = 1) and protein ratios were calculated.

5.6 Electron microscope of the viral particles

Influenza A virus mutants with defects in virus assembly and budding have been reported to release particles with aberrant morphology. We first employed transmission electron microscopy (TEM) to evaluate the morphology of wild type influenza C virus particles and the density and arrangement of HEF spikes on their surface. Using contrast enhancing heavy metals as staining solution (negative staining) we could visualize the typical regular arrangement of HEF trimers in a hexagonal lattice (Figure5.6A). Hexagonal arrangements are best visible if the whole surface of the virion is embedded within the staining material (Figure 5.7). We observed both long filamentous virions and spherical particles with diameters between 75 and 200 nm confirming that influenza C particles are pleomorphic. Some

deformed particles were also present, but deviations from the ideal spherical shape may simply due to drying during sample preparation. Therefore we used for the first time cryo-TEM to visualize the virus in its hydrated state. Sections of cryo-electron micrographs (Figure 5.6B) revealed a higher ratio of ideal spherical virions confirming the partly destructive influence of negative staining (Figure5.8). The hexagonal arrangement of HEF spikes can also be detected by cryo-TEM, although not clearly on each particle. It is in the nature of projection images that the lattice pattern is only very prominent when the densities on the front and on the rear side of the virus are nearly in superposition. Occasionally, very long filamentous particles with a length of up to few micrometers and a small diameter (about 36 nm without spikes) were observed (Figure 5.9).

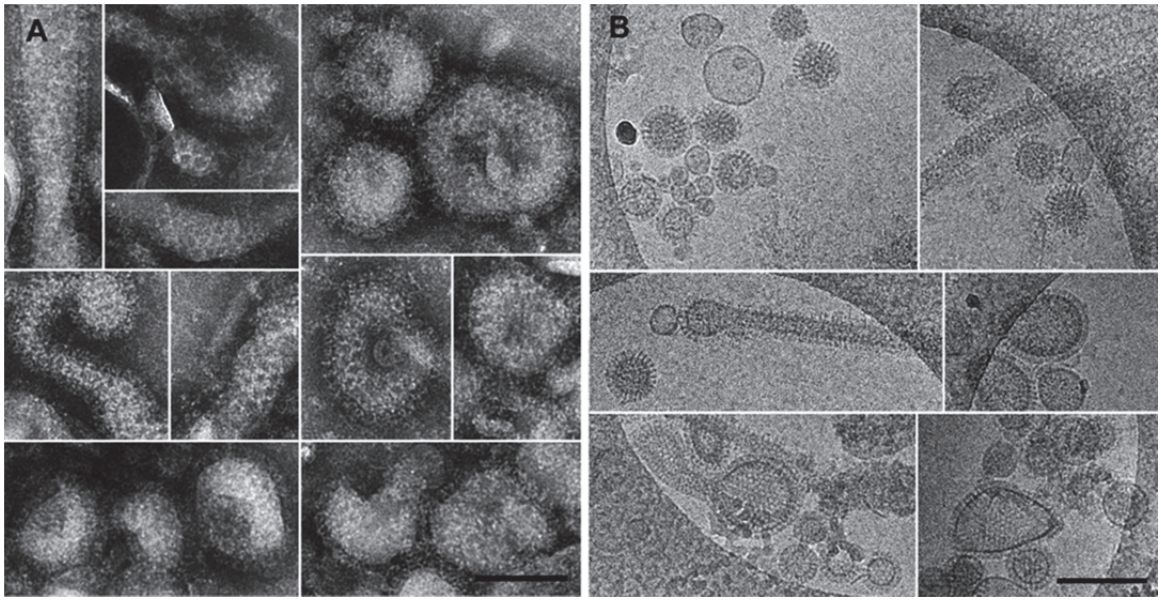

FIG 5.6 Electron microscopy of wild-type Influenza C virus particles. (A) Sections of negative stain micrographs illustrating the hexagonal arrangement of HEF spikes. The scale bar corresponds to 100 nm. (B) Sections of cryo-TEM micrographs illustrating the varying morphology of virus particles. Scale bar corresponds to 200 nm.

Having established TEM and cryo-TEM methodology for influenza C virions we next visualized particles having a non-acylated HEF protein. TEM revealed that the hexagonal arrangement of HEF spikes is preserved in the mutant (Figure5.10A and B). Particles having an aberrant morphology were not observed with Cryo-TEM. Wild type and mutant particles showed no obvious difference in morphology, both filamentous and spherical particles are present at a similar ratio and the diameter and length of particles is also comparable. Note also that the viral surface is completely covered with spike projections indicating that lack of acylation does not affect recruitment of HEF into virus particles.

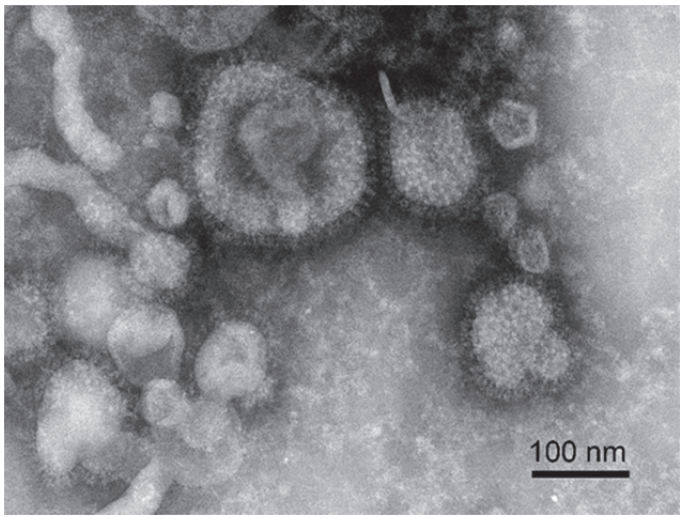

FIG 5.7 Electron micrograph of negatively stained wild type influenza C virions. Note the hexagonal arrangement of surface projections, which is only clearly visible if particles are completely embedded in the staining solution [containing phosphotungstic acid, 1% (w/v)], such as in the right part of the figure.

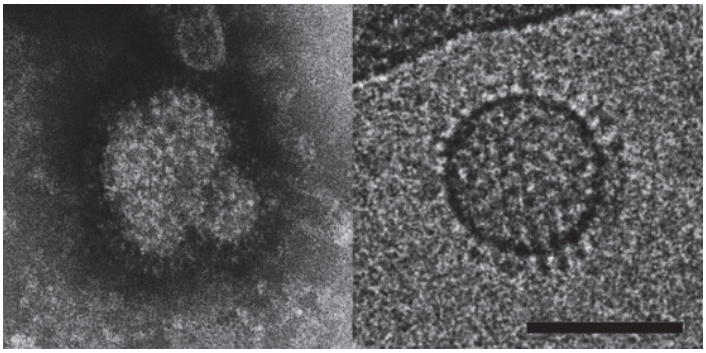

FIG 5.8 Comparison of negative stain and Cryo-TEM of wild type influenza C virus. Scale bars correspond to 100 nm.

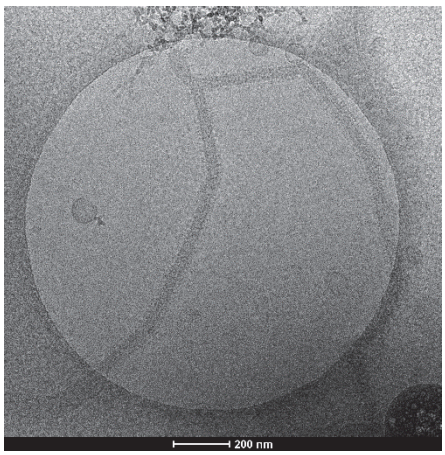

FIG 5.9 Cryo-TEM of influenza C virus (wild type). Filamentous viruses with lengths in the µm range were observed frequently, but also for virions containing non-acylated HEF (not shown).

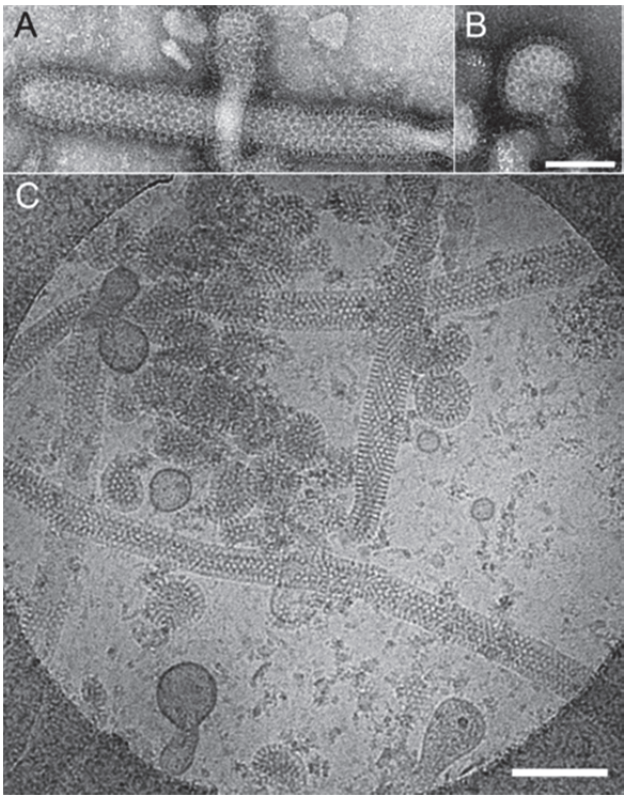

FIG 5.10 Electron microscopy of Influenza C virus with non-acylated HEF. (A, B) negative stain micrographs and (C) cryo-TEM. Virus shape (filamentous and spherical) as well as hexagonal arrangement of HEF remains unchanged compared to wily type virus. Scale bars correspond to 100 nm.

In sum, no evidence was obtained that removal of the acylation site from HEF affects the morphology of virus particles, the density of spikes on the viral surface or their lateral arrangement in hexagonal structures.

5.7 Antibody selectionfor metabolic labeling &immunoprecipitation

By metabolic labeling &immunoprecipitation, 3 antibodies were tested for the next experiment. Samples immunoprecipitated by monoclonal antibody 8B3A5 did not show any bands on X-ray film; Samples immunoprecipitated by monoclonal antibody 8J3B4 showed bands on X-ray film at all three testing amount: 2 µl, 1 µl, 0.5 µl, and the clear 0.5 µl band illuminated that this amount was enough for the following experiments; For samples immunoprecipitated by polyclonal rabbit antibody, only 2 µshowed light bands for HEF and NP proteins, and the other amount were not able to detect visible bands (Figure 5.7). This film illuminated that mono antibody 8J3B4 should be selected for immunoprecipitation and the proper amount for each sample should be 0.5 µl.

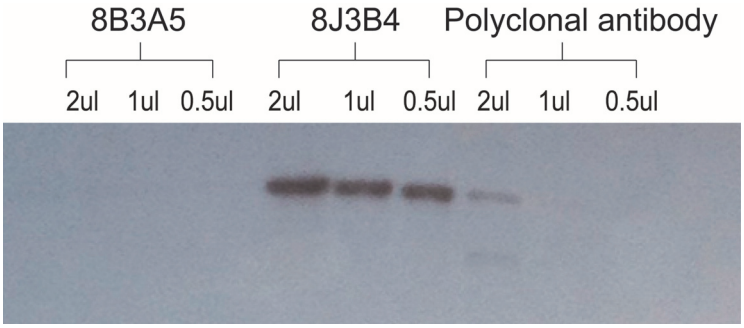

FIG 5.11 Antibodies selection by metabolic labeling &immunoprecipitation. MDCK I cells infected by wt influenza C virus were metabolic labeled by ^{35}S-methionine for 1 h. Add 8B3A5, 8J3B4 and polyclonal rabbit antibody at amounts of 2 µl, 1 µland 0.5 µl to each cell lysis sample to precipitate radioactive labeled viral proteins. In the developed x-ray film, the first three channel for antibody 8B3A5 did not show any visible bands; In channel 4 to 6 for antibody 8J3B4, clear HEF bands were able to be observed; In channel 7 to 9 for polyclonal antibody, light HEF and NP bands were able to be observed only in high amount of antibody (2 µl). In conclusion, mono antibody 8J3B4 was available for immunoprecipitation and the proper amount for each sample should be 0.5 µl.

5.8 Transport of wt and non-acylation mutant HEF to the plasma membrane

We compared transport of wild type and non-acylated HEF to the plasma membrane by cell surface trypsinization. The enzyme cleaves HEF into its subunits HEF1 and HEF 2, but only if HEF is exposed at the cell surface (72). Virus-infected MDCKI cells were metabolically labeled with ^{35}S-methionine for different periods of time; i. e. 30, 60, 90, 120 or 180 minutes. Ten minutes prior to the end of the labeling period trypsin was added, cells were lysed in the presence of protease inhibitors and HEF was subjected to immunoprecipitation, SDS-PAGE and fluorography (Figure 5.12). Two bands representing the HEF1 subunits became visible in the fluorogram only after 90 minutes of labeling indicating that intracellular transport of HEF is slow in comparison to many other viral glycoproteins, such as HA. The amount of HEFI greatly increases with longer labeling time, whereas the band representing the HEF0 precursor remains (almost) constant. An identical band pattern was observed for non-acylated HEF and densitometric quantification of bands revealed no difference in the HEF0/HEFI ratios between wild type and mutant virus. The result indicate that removal of acylation sites does not affect plasma membrane transport of HEF, which is in line with other studies on non-acylated HA from various influenza A virus strains.

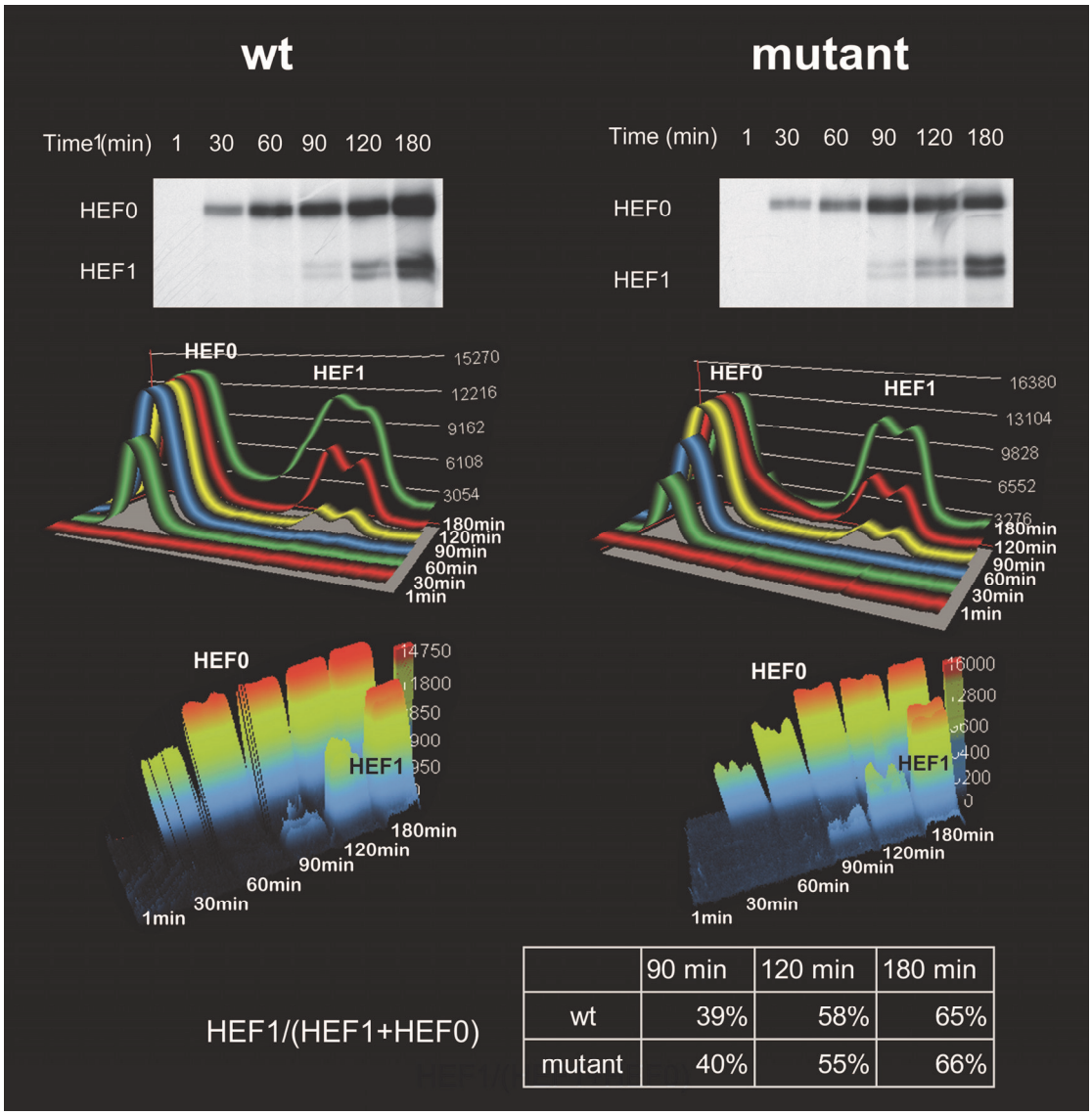

	90 min	120 min	180 min
wt	39%	58%	65%
mutant	40%	55%	66%

FIG 5.12 Removal of acylation site from HEF does not affect its surface transport. Cell surface trypsinisation assay. MDCK I cells were infected with wt and mutant viruses and labeled 24 hours post infection with ^{35}S-methionine for 1min, 30 min, 60 min, 90 min, 120 min and 180 min, respectively. 10 min prior to the end of the labeling period, trypsin was added to a final concentration of 15ug/ml. HEF was then immunoprecipitated from cellular lysates and subjected to SDS-PAGE and fluorography. Density of HEF0 (uncleaved precursor) and HEFI bands were analyzed by Bio1D software and proportion of cleaved HEF0 at different time points was calculated.

5.9 Hemolysis assays of wt and mutant influenza C virus

For HAs of various influenza influenza A and B subtypes it was reported that deletion of acylation sites causes defects in membrane fusion. More precisely, non-acylated HA expressed on the surface of transfected cells is able to cause hemifusion (mixing of lipids) with fluorescently labelled erythrocyte ghosts, but opening of the fusion pore, demonstrated as diffusion of a soluble fluorophore from the ghost into HA-expressing cells, was disturbed.

However, although widely used, these assays have disadvantages with respect to quantification of the date. The amount of HA present at the cell surface, which is known to affect the extent of membrane fusion, can neither be controlled nor precisely determined in transfected cells. Likewise, since fusion is recorded microscopically as distribution of a fluorophore on the surface or inside cells, the kinetics and magnitude can only roughly be estimated. Since virus particles containing non-acylated HEF are infectious they might have a reduction, but not a complete blockade of membrane fusion and thus a better quantifiable assay is required. We therefore used hemolysis assays, which allow adjusting the amount of virus by means of their HA-titer and to record membrane fusion precisely by measuring the release of hemoglobin. In addition, hemolysis requires opening of a fusion pore, not just mixing of lipids, which is, based on published results with HA, unlikely to be disturbed by removal of acylation sites.

In a first set of experiments we compared hemolysis of wild type and mutant virus as a function of the virus concentration. Culture supernatants of virus-infected cells, adjusted to an HA-titer from 2^3 to 2^9, were adsorbed to chicken erythrocytes, the pH was adjusted to 5.5, erythrocytes with bound virus were incubated for 60 min at 37°C and hemoglobin release was determined. For wild-type virus our data essentially confirm previous results, i.e. hemolysis already occurred at an HA-titer of 2^3, the extent of hemolysis correlated with the HA-titer until it saturates at a titer of 2^8 (Figure 5.13A). Importantly, hemolysis produced by virus containing non-acylated HA is reduced by ~50% at low HA-titers (2^3 to 2^6), the difference between wild–type and mutant virus decreased at higher titers until at a HA-titer of 2^9 both viruses cause the same amount of hemolysis. Thus, the mutant exhibits a defect in hemolysis which can be compensated by using more viruses.

Next we analyzed the kinetics of hemolysis with viruses adjusted to a HA-titer of 2^6 and pH to 5.5. As described before wild type virus exhibits a ~ 30 minutes long lag phase with little hemolysis (Figure 5.13B), which is not seen with Influenza influenza A and B virus. Release of hemoglobin then increases linearly until it reaches saturation after ~90 minutes of incubation. The lag phase is more pronounced with the mutant virus, it lasts for ~60 minutes, increases then rapidly, but never reaches complete saturation, even after 180 minutes of incubation. At each time point hemolysis induced by the mutant virus is reduced compared to wild type virus, by ~50% at early time points, but later the difference between wild type and mutant becomes smaller.

Finally, we compared hemolysis of wild type and mutant virus at various acidic pH values between 4.5 and 7 (Figure 5.13C). In accordance with published data, wild type virus starts to cause release of hemoglobin at pH 6, its amount increased linearly until at pH 5.25 it levels off to reach saturation at pH5. At pH values below 5.0 erythrocytes spontaneously hemolyse, as observed previously. Experiments with the mutant virus exhibit the same curve shape for hemoglobin release, but to accomplish the same amount of hemolysis more acidic pH values (~0.3 units) are required. At pH 5 both viruses caused the same amount of hemoglobin release indicating that a defect in hemolysis can be compensated by more acidic pH values. In sum, virus containing non-acylation HEF revealed a defect in hemolysis which could be compensated by adding more viruses, performing the assay at more acidic pH value or incubating samples for longer time periods.

5.10 Binding of fluorophore bis-ANS to wt and non-acylation HEF at low pH condition

Since acylation apparently does not affect budding of virus particles, the reduction in viral titers might be due to disturbed virus entry by membrane fusion, which requires a cleaved HEF protein and its activation by mildly acidic pH. Although not elucidated in such detail as for HA of influenza A virus, the conformational change is thought to remove the hydrophobic fusion peptide from its buried location at the bottom of the stalk and exposes it at the surface of the trimer. Subsequent bending of the molecule draws the fusion peptide towards the transmembrane region leading to a close apposition of viral and endosomal membranes, hemifusion with exchange of lipids, opening of a fusion pore and eventually complete merger of both lipid bilayers.

To analyze whether acylation of HEF affects its conformational change we used the water soluble fluorophore 1,1'-bis(4-anilino)naphthalene-5,5'-disulfonic acid (bis-ANS), which is virtually non-fluorescent in aqueous solutions, but becomes strongly fluorescent when it is bound to hydrophobic sites in proteins. With influenza A virus a dramatic increase of the bis-ANS fluorescence intensity was observed at low pH, which was mainly attributed to an enhanced binding of the fluorophore to hydrophobic sites of the HA ectodomain. When we performed the same assay with influenza C virus (1mg/ml), a fivefold higher fluorescence intensity was recorded at pH 4.5 relative to pH 7.0, which is in perfect agreement with published results on influenza A virus. When normalized fluorescence intensities recorded at the end of incubation (3 minutes) are plotted against the pH-value, they increased linear with

acidification (Figure5.14A). A threshold pH-value for bis-ANS binding, as reported for HA, is not obvious for HEF. The kinetics of the individual binding experiments showed at each pH-value a rapid increase of the fluorescence intensity immediately after addition of bis-ANS to the virus. At neutral pH the fluorescence intensity then remains constant with time, but at acidic pH, starting at pH 5.5, a further slower increase is seen (Figure5.14A). The same kinetics and curve shapes were recorded with mutant virus and the second, slower increase also begins at pH 5.5 (Fig. 4B). In addition, no difference in the normalized fluorescence intensities was detectable between wild type and mutant virus at each pH suggesting that removal of acylation sites does not affect binding of bis-ANS and hence the conformational change of HEF (Fig. 4C).

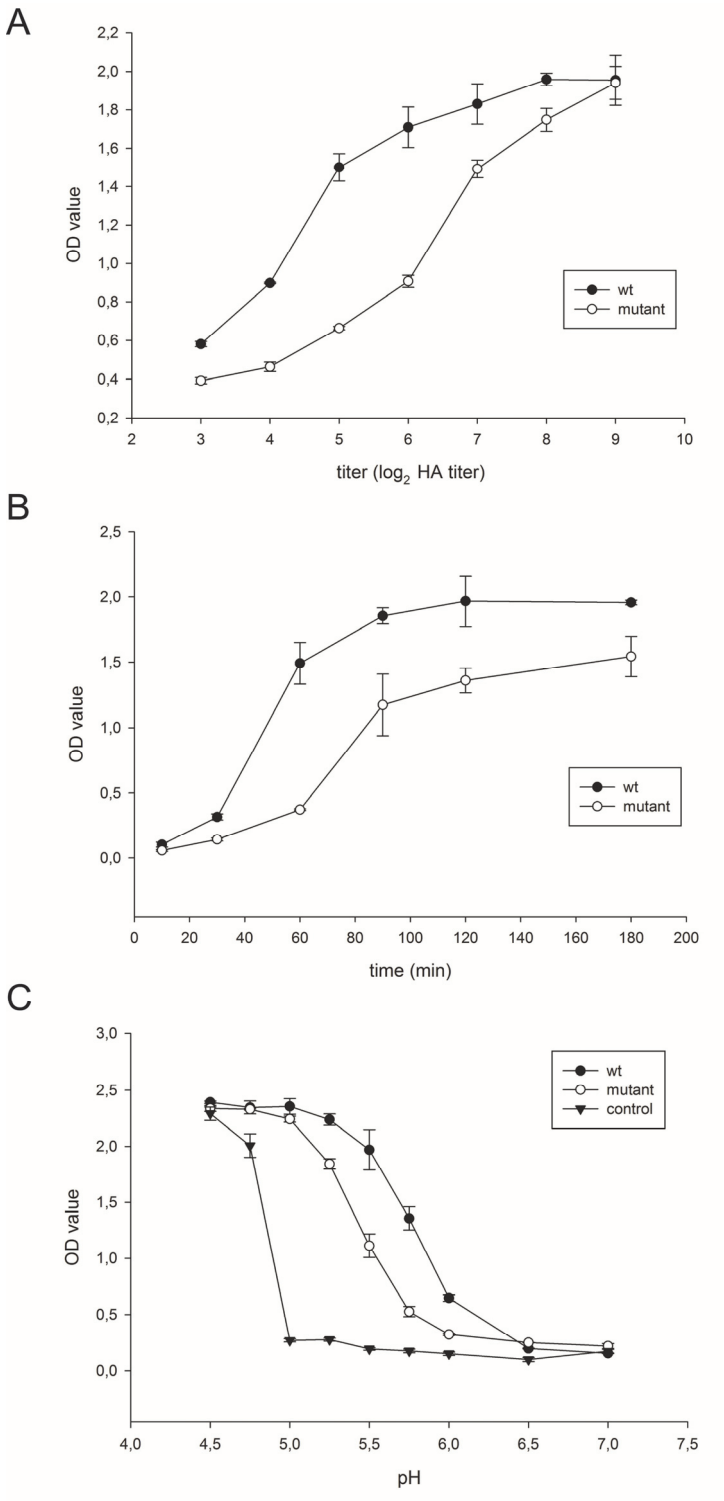

FIG 5.13 Removal of the acylation site from HEF affects hemolytic activity of virus particles. (A) Titer-dependence: Virus particles (wt and mutant) were adjusted to the indicated HA-titers, adsorbed to chicken erythrocytes and pelleted. Samples were adjusted to pH 5.5 and incubated for 60 min at 37°C. Released hemoglobin (OD 405) is plotted against the virus titer.(B) Time dependence: Virus particles were adjusted to an HA titer of 26, adsorbed to chicken erythrocytes and pelleted. Samples were adjusted to pH 5.5 and incubated for the indicated time periods at 37°C. Released hemoglobin (OD 405) is plotted against the virus titer.(C) pH-dependence: Virus particles were adjusted to an HA titer of 26, adsorbed to chicken erythrocytes and pelleted. Samples were adjusted to the indicated pH and incubated for 60 min at 37°C.

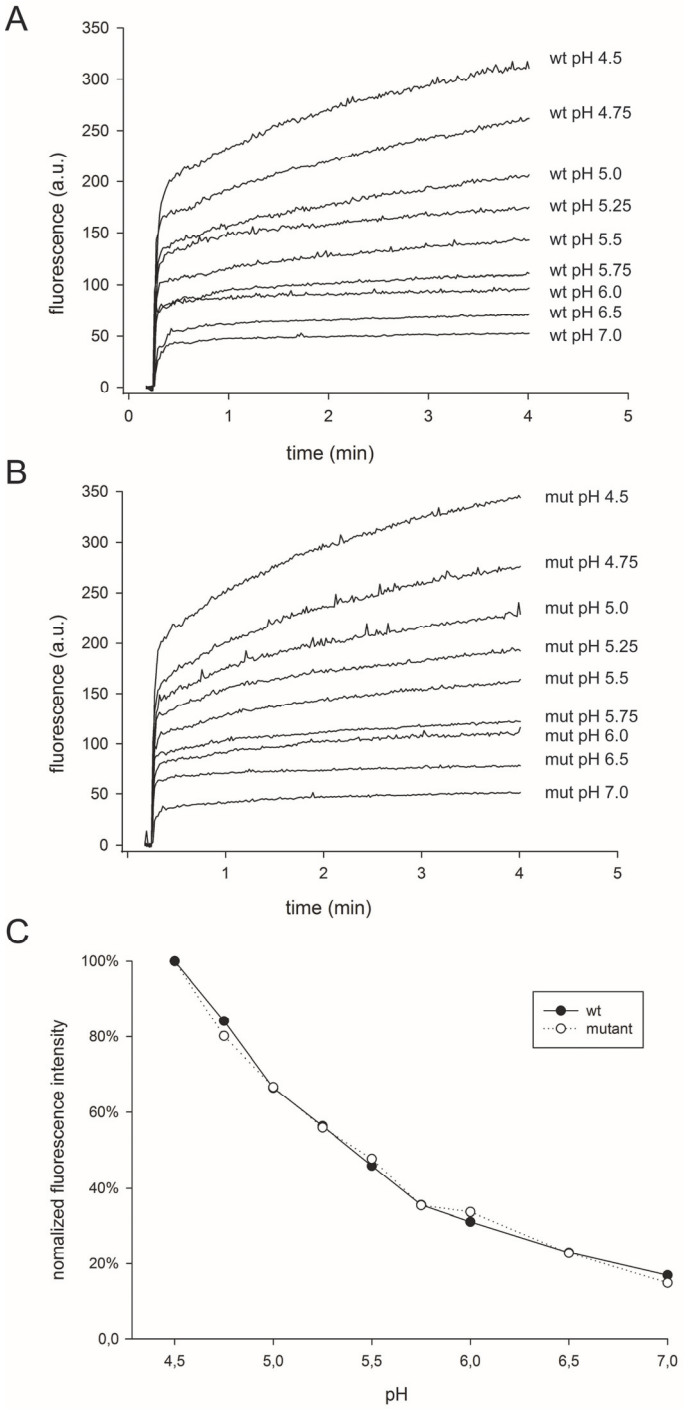

FIG 5.14 Binding of bis-ANS to virus particles at different pH values. (A, B) Time course of the fluorescence intensity continuously recorded at various pH values. A: wild type, B: mutant virus. Fluorescence intensity in arbitrary units (a. u.) is plotted against time. Note that the fluorescence intensity increases immediately upon addition of virus particles at each pH value, but its extent depends on the acidification. Starting with pH 5.5 there is a further, but slower increase, which is more pronounced at more acidic pH. (C) Normalized fluorescence intensities (value after incubation for four minutes at pH 4.5 = 100%) are plotted against the pH. No difference between wild type and mutant virus particles is apparent suggesting that the conformational change of HEF is not affected by removal of acylation sites.

6. Discussions

Here we have analyzed the effect of removal of the single acylation site of HEF on virus replication and various activities of the protein. We have shown that influenza C virus having a non-acylated HEF protein could be rescued (Figure 5.1), the mutation was stable upon serial passage (Figure 5.3) and the virus had no competitive fitness defect (Figure 5.4), but infectious virus titers were reduced by one order of magnitude in growth experiments (Figure 5.2). This is consistent with studies on HA of several influenza A virus strains where exchange of the stearoylated cysteine reduced virus titers by ~ one log, but much more (two to five logs) if palmitoylated cytoplasmic cysteines were replaced (110-112). Thus, to generalize published results on S-acylation of hemagglutinating glycoproteins of influenza viruses it appears that palmitate attached to the cytoplasmic tail is more important for virus replication than stearate linked to the end of the TMR.

The stability of the mutation and the rather marginal effect of removal of the fatty acid binding site on virus replication allowed us to study its consequences for the function of HEF during each aspect of the viral life cycle. Acylation does not affect the kinetics of surface transport of HEF (Figure 5.12), a result that is again in line with studies on intracellular transport of non-acylated HA mutants of influenza A and B virus as well as other viral glycoproteins .

Both transmission and cryo-electron microscopy revealed that the morphology of virus particles was unaltered by the mutation (Figure 5.10). Mainly spherical particles, but also (sometimes very long) filamentous ones were observed in both cases. Acylation of HEF also plays no role for formation and maintenance of the hexagonal structures on the viral surface, which are typical for influenza C viruses (41-43, 76). This is consistent with published data that the regular polymeric reticular structures can still be observed when HEF is removed from the membrane, either by limited proteolytic digestion or by spontaneous release (43), indicating that lateral interactions of the ectodomains shape the hexagonal structures.

Comparing the protein composition of virus particles revealed no difference between wild type and mutant virions; the ratios of the major structural proteins HEF, NP and M1 were identical in Coomassie-stained gels (Figure 5.5). Cryo-EM also confirmed that recruitment of

HEF into virions is not compromised since wild type and mutant virus particles are both densely packed with spike proteins. In accordance, HEF is not associated with detergent-resistant membranes (119); the biochemical correlates of rafts, in contrast to HA which is targeted to rafts by fatty acylation (115-119). Acylation of HEF does also not affect incorporation of M1 into virus particles, as has been reported for HA of the Udorn-strain of influenza A virus (111). However, the effect of removal of the stearoylation site at the end of the TMR of HA on the viral protein composition was much less pronounced than exchange of cytoplasmic palmitoylation sites (105, 111). It is also noteworthy in this regard that the cytoplasmic tail of HEF is composed of only three amino acids and thus might be too short to recruit M1 to the assembly site. In sum, acylation of HEF apparently does not influence any of the functions of HEF involved in virus assembly and budding.

To study a possible role of acylation of HEF during virus entry we compared the membrane fusion activity of wild type and mutant virus. Having shown that both wild type and mutant virus particles contain the same amount of HEF we adjusted virus particles to the same HA-titer and performed hemolysis assays with erythrocytes. Hemolysis has the advantage that the release of content (and thus opening of a fusion pore) is measured, since hemifusion is unlikely to be disturbed in non-acylated HEF, at least if one assumes that the fusion mechanism of HA and HEF is very similar.

Virus containing non-acylated HEF revealed a defect in hemolysis, both the kinetics as well as the extent of fusion was reduced relative to wild type virus (Figure 5.13). Compromised fusion activity after removal of acylation sites was also reported for HA from a variety of influenza A and B virus strains, but removal of stearoylation sites had a lower effect than exchange of palmitoylation sites (105, 111, 114).

The fusion defect of non-acylated HEF could be compensated by adding more viruses or by incubating samples for longer time periods. We conclude that non-acylated HEF exhibits membrane fusion activity (as expected since mutant viruses replicate), but the fusion efficiency is apparently reduced. Mutant viruses also cause the same amount of hemoglobin release as wild type at more acidic pH values. Since acylated and non-acylated HEF bind the same amount of the fluorescent hydrophobic dye bis-ANS at each pH (Figure 5.14), the pH threshold for the conformational change catalyzing membrane fusion is probably not affected

by the mutation. We rather assume that if virus particles contain non-acylated HEF more spikes must be activated to initiate a productive fusion event that allows genome release.

One can only speculate on the mechanism how protein-bound stearate improves HEF´s fusion efficiency. A feature of the post fusion structure of HA (and other viral and cellular fusogens) is spatial proximity of the two membrane-associated elements (175). It was therefore suggested that the fusion peptide and the transmembrane anchor interact, possibly to cause opening of a fusion pore. Stearate attached to the end of the TMR of HEF might facilitate this interaction thereby enhancing pore formation. Alternatively, since small fusion pores flicker (open and close repetitively) prior to their irreversible opening and enlargement (176), the fatty acid might help to trap the fusion pore in an open state which would also increase the efficiency of membrane fusion.

Why does a reduction in the membrane fusion activity of HEF decreases virus replication? Although cell entry of influenza C virus has hitherto not been investigated in detail, its similarity to influenza A virus suggests that it also occurs mainly by clathrin-mediated endocytosis (177). Virus particles thus hijack the endosomal vesicular pathway for their transportation from the plasma membrane to a perinuclear region. On the one hand, viruses should join the endosomal pathway as long as possible to release their genome in the vicinity of the nucleus, where transcription and replication occurs. On the other hand, since endosomes are destined to ultimately fuse with the lysosome, viruses must leave this transport pathway in due time to avoid their degradation by proteases. The cue to activate the fusogenic activity of HA and HEF are protons, the concentration of which continuously increases during endosome maturation, i. e. from a pH range of 6.8-6.0 in early endosomes to 6.0-5.0 in late endosomes and to 4.5 in lysosomes (177, 178). Since the optimal pH for fusion is shifted to more acidic values in non-acylated HEF, a fraction of the respective virions might not be able to escape from the endosomal transport pathway prior to formation of the endolysosome and are thus not able to initiate an infection. Single particle tracking of incoming influenza virions that allows observing individual fusion events in real time inside cells might be suitable to test this hypothesis (179).

7. References

1. **Taylor RM.** 1949. Studies on survival of influenza virus between epidemics and antigenic variants of the virus. American journal of public health and the nation's health **39:**171-178.
2. **Taylor RM.** 1951. A further note on 1233 influenza C virus. Archiv fur die gesamte Virusforschung **4:**485-500.
3. **Francis T, Jr., Quilligan JJ, Jr., Minuse E.** 1950. Identification of another epidemic respiratory disease. Science **112:**495-497.
4. **Matsuzaki Y, Abiko C, Mizuta K, Sugawara K, Takashita E, Muraki Y, Suzuki H, Mikawa M, Shimada S, Sato K, Kuzuya M, Takao S, Wakatsuki K, Itagaki T, Hongo S, Nishimura H.** 2007. A nationwide epidemic of influenza C virus infection in Japan in 2004. Journal of clinical microbiology **45:**783-788.
5. **Gouarin S, Vabret A, Dina J, Petitjean J, Brouard J, Cuvillon-Nimal D, Freymuth F.** 2008. Study of influenza C virus infection in France. Journal of medical virology **80:**1441-1446.
6. **Kauppila J, Ronkko E, Juvonen R, Saukkoriipi A, Saikku P, Bloigu A, Vainio O, Ziegler T.** 2014. Influenza C virus infection in military recruits--symptoms and clinical manifestation. Journal of medical virology **86:**879-885.
7. **Matsuzaki Y, Katsushima N, Nagai Y, Shoji M, Itagaki T, Sakamoto M, Kitaoka S, Mizuta K, Nishimura H.** 2006. Clinical features of influenza C virus infection in children. The Journal of infectious diseases **193:**1229-1235.
8. **Joosting AC, Head B, Bynoe ML, Tyrrell DA.** 1968. Production of common colds in human volunteers by influenza C virus. British medical journal **4:**153-154.
9. **Minuse E, Quilligan JJ, Jr., Francis T, Jr.** 1954. Type C influenza virus. I. Studies of the virus and its distribution. The Journal of laboratory and clinical medicine **43:**31-42.
10. **Salez N, Melade J, Pascalis H, Aherfi S, Dellagi K, Charrel RN, Carrat F, de Lamballerie X.** 2014. Influenza C virus high seroprevalence rates observed in 3 different population groups. The Journal of infection **69:**182-189.
11. **Calvo C, Garcia-Garcia ML, Borrell B, Pozo F, Casas I.** 2013. Prospective study of influenza C in hospitalized children. The Pediatric infectious disease journal **32:**916-919.
12. **Manuguerra JC, Hannoun C, Aymard M.** 1992. Influenza C virus infection in France. The Journal of infection **24:**91-99.
13. **Muraki Y, Hongo S.** 2010. The molecular virology and reverse genetics of influenza C virus. Japanese journal of infectious diseases **63:**157-165.
14. **Ohwada K, Kitame F, Sugawara K, Nishimura H, Homma M, Nakamura K.** 1987. Distribution of the antibody to influenza C virus in dogs and pigs in Yamagata Prefecture, Japan. Microbiology and immunology **31:**1173-1180.
15. **Manuguerra JC, Hannoun C.** 1992. Natural infection of dogs by influenza C virus. Research in virology **143:**199-204.
16. **Manuguerra JC, Hannoun C, Simon F, Villar E, Cabezas JA.** 1993. Natural infection of dogs by influenza C virus: a serological survey in Spain. The new microbiologica **16:**367-371.
17. **Youzbashi E, Marschall M, Chaloupka I, Meier-Ewert H.** 1996. [Distribution of influenza C virus infection in dogs and pigs in Bavaria]. Tierarztliche Praxis **24:**337-342.
18. **Brown IH, Harris PA, Alexander DJ.** 1995. Serological studies of influenza viruses in pigs in Great Britain 1991-2. Epidemiology and infection **114:**511-520.
19. **Yamaoka M, Hotta H, Itoh M, Homma M.** 1991. Prevalence of antibody to influenza C virus among pigs in Hyogo Prefecture, Japan. The Journal of general virology **72 (Pt 3):**711-714.
20. **Horimoto T, Gen F, Murakami S, Iwatsuki-Horimoto K, Kato K, Akashi H, Hisasue M, Sakaguchi M, Kawaoka Y, Maeda K.** 2014. Serological evidence of infection of dogs with human influenza viruses in Japan. The Veterinary record **174:**96.

21. **Guo YJ, Jin FG, Wang P, Wang M, Zhu JM.** 1983. Isolation of influenza C virus from pigs and experimental infection of pigs with influenza C virus. The Journal of general virology **64 (Pt 1):**177-182.
22. **Muraki Y, Hongo S, Sugawara K, Kitame F, Nakamura K.** 1996. Evolution of the haemagglutinin-esterase gene of influenza C virus. The Journal of general virology **77 (Pt 4):**673-679.
23. **Matsuzaki Y, Mizuta K, Sugawara K, Tsuchiya E, Muraki Y, Hongo S, Suzuki H, Nishimura H.** 2003. Frequent reassortment among influenza C viruses. Journal of virology **77:**871-881.
24. **Speranskaia AS, Mel'nikova NV, Belenkin MS, Dmitriev AA, Oparina N, Kudriavtseva AV.** 2012. [Genetic diversity and evolution of the influenza C virus]. Genetika **48:**797-805.
25. **Tada Y, Hongo S, Muraki Y, Sugawara K, Kitame F, Nakamura K.** 1997. Evolutionary analysis of influenza C virus M genes. Virus genes **15:**53-59.
26. **Peng G, Hongo S, Muraki Y, Sugawara K, Nishimura H, Kitame F, Nakamura K.** 1994. Genetic reassortment of influenza C viruses in man. The Journal of general virology **75 (Pt 12):**3619-3622.
27. **Hause BM, Ducatez M, Collin EA, Ran Z, Liu R, Sheng Z, Armien A, Kaplan B, Chakravarty S, Hoppe AD, Webby RJ, Simonson RR, Li F.** 2013. Isolation of a novel swine influenza virus from Oklahoma in 2011 which is distantly related to human influenza C viruses. PLoS pathogens **9:**e1003176.
28. **Collin EA, Sheng Z, Lang Y, Ma W, Hause BM, Li F.** 2014. Co-circulation of two distinct genetic and antigenic lineages of proposed influenza D virus in cattle. Journal of virology.
29. **Collin EA, Sheng Z, Lang Y, Ma W, Hause BM, Li F.** 2015. Cocirculation of two distinct genetic and antigenic lineages of proposed influenza d virus in cattle. Journal of virology **89:**1036-1042.
30. **Pachler K, Mayr J, Vlasak R.** 2010. A seven plasmid-based system for the rescue of influenza C virus. Journal of molecular and genetic medicine : an international journal of biomedical research **4:**239-246.
31. **Krossoy B, Hordvik I, Nilsen F, Nylund A, Endresen C.** 1999. The putative polymerase sequence of infectious salmon anemia virus suggests a new genus within the Orthomyxoviridae. Journal of virology **73:**2136-2142.
32. **Gammelin M, Altmuller A, Reinhardt U, Mandler J, Harley VR, Hudson PJ, Fitch WM, Scholtissek C.** 1990. Phylogenetic analysis of nucleoproteins suggests that human influenza A viruses emerged from a 19th-century avian ancestor. Molecular biology and evolution **7:**194-200.
33. **Yoon SW, Webby RJ, Webster RG.** 2014. Evolution and ecology of influenza a viruses. Current topics in microbiology and immunology **385:**359-375.
34. **Bean WJ, Schell M, Katz J, Kawaoka Y, Naeve C, Gorman O, Webster RG.** 1992. Evolution of the H3 influenza virus hemagglutinin from human and nonhuman hosts. Journal of virology **66:**1129-1138.
35. **Saitou N, Nei M.** 1986. Polymorphism and evolution of influenza A virus genes. Molecular biology and evolution **3:**57-74.
36. **Suzuki Y, Nei M.** 2002. Origin and evolution of influenza virus hemagglutinin genes. Molecular biology and evolution **19:**501-509.
37. **Waterson AP, Hurrell JM, Jensen KE.** 1963. The fine structure of influenza A, B and C viruses. Archiv fur die gesamte Virusforschung **12:**487-495.
38. **Nishimura H, Hara M, Sugawara K, Kitame F, Takiguchi K, Umetsu Y, Tonosaki A, Nakamura K.** 1990. Characterization of the cord-like structures emerging from the surface of influenza C virus-infected cells. Virology **179:**179-188.
39. **Muraki Y, Washioka H, Sugawara K, Matsuzaki Y, Takashita E, Hongo S.** 2004. Identification of an amino acid residue on influenza C virus M1 protein responsible for formation of the cord-like structures of the virus. The Journal of general virology **85:**1885-1893.

40. **Nishimura H, Hongo S, Sugawara K, Muraki Y, Kitame F, Washioka H, Tonosaki A, Nakamura K.** 1994. The ability of influenza C virus to generate cord-like structures is influenced by the gene coding for M protein. Virology **200:**140-147.
41. **Flewett TH, Apostolov K.** 1967. A reticular structure in the wall of influenza C virus. The Journal of general virology **1:**297-304.
42. **Apostolov K, Flewett TH.** 1969. Further observations on the structure of influenza viruses A and C. The Journal of general virology **4:**365-370.
43. **Herrler G, Nagele A, Meier-Ewert H, Bhown AS, Compans RW.** 1981. Isolation and structural analysis of influenza C virion glycoproteins. Virology **113:**439-451.
44. **Desselberger U, Racaniello VR, Zazra JJ, Palese P.** 1980. The 3' and 5'-terminal sequences of influenza A, B and C virus RNA segments are highly conserved and show partial inverted complementarity. Gene **8:**315-328.
45. **Yamashita M, Krystal M, Palese P.** 1989. Comparison of the three large polymerase proteins of influenza A, B, and C viruses. Virology **171:**458-466.
46. **Herrler G, Durkop I, Becht H, Klenk HD.** 1988. The glycoprotein of influenza C virus is the haemagglutinin, esterase and fusion factor. The Journal of general virology **69 (Pt 4):**839-846.
47. **Nakada S, Creager RS, Krystal M, Palese P.** 1984. Complete nucleotide sequence of the influenza C/California/78 virus nucleoprotein gene. Virus research **1:**433-441.
48. **Yamashita M, Krystal M, Palese P.** 1988. Evidence that the matrix protein of influenza C virus is coded for by a spliced mRNA. Journal of virology **62:**3348-3355.
49. **Pekosz A, Lamb RA.** 1998. Influenza C virus CM2 integral membrane glycoprotein is produced from a polypeptide precursor by cleavage of an internal signal sequence. Proceedings of the National Academy of Sciences of the United States of America **95:**13233-13238.
50. **Hongo S, Sugawara K, Muraki Y, Matsuzaki Y, Takashita E, Kitame F, Nakamura K.** 1999. Influenza C virus CM2 protein is produced from a 374-amino-acid protein (P42) by signal peptidase cleavage. Journal of virology **73:**46-50.
51. **Stewart SM, Pekosz A.** 2012. The influenza C virus CM2 protein can alter intracellular pH, and its transmembrane domain can substitute for that of the influenza A virus M2 protein and support infectious virus production. Journal of virology **86:**1277-1281.
52. **Nakada S, Graves PN, Desselberger U, Creager RS, Krystal M, Palese P.** 1985. Influenza C virus RNA 7 codes for a nonstructural protein. Journal of virology **56:**221-226.
53. **Nakada S, Graves PN, Palese P.** 1986. The influenza C virus NS gene: evidence for a spliced mRNA and a second NS gene product (NS2 protein). Virus research **4:**263-273.
54. **Alamgir AS, Matsuzaki Y, Hongo S, Tsuchiya E, Sugawara K, Muraki Y, Nakamura K.** 2000. Phylogenetic analysis of influenza C virus nonstructural (NS) protein genes and identification of the NS2 protein. The Journal of general virology **81:**1933-1940.
55. **Crescenzo-Chaigne B, Barbezange C, van der Werf S.** 2008. Non coding extremities of the seven influenza virus type C vRNA segments: effect on transcription and replication by the type C and type A polymerase complexes. Virology journal **5:**132.
56. **Robertson JS.** 1979. 5' and 3' terminal nucleotide sequences of the RNA genome segments of influenza virus. Nucleic acids research **6:**3745-3757.
57. **Cheong HK, Cheong C, Lee YS, Seong BL, Choi BS.** 1999. Structure of influenza virus panhandle RNA studied by NMR spectroscopy and molecular modeling. Nucleic acids research **27:**1392-1397.
58. **Fodor E, Pritlove DC, Brownlee GG.** 1994. The influenza virus panhandle is involved in the initiation of transcription. Journal of virology **68:**4092-4096.
59. **Hsu MT, Parvin JD, Gupta S, Krystal M, Palese P.** 1987. Genomic RNAs of influenza viruses are held in a circular conformation in virions and in infected cells by a terminal panhandle. Proceedings of the National Academy of Sciences of the United States of America **84:**8140-8144.
60. **Herrler G, Klenk HD.** 1991. Structure and function of the HEF glycoprotein of influenza C virus. Advances in virus research **40:**213-234.

61. **Rogers GN, Herrler G, Paulson JC, Klenk HD.** 1986. Influenza C virus uses 9-O-acetyl-N-acetylneuraminic acid as a high affinity receptor determinant for attachment to cells. The Journal of biological chemistry **261:**5947-5951.
62. **Herrler G, Rott R, Klenk HD, Muller HP, Shukla AK, Schauer R.** 1985. The receptor-destroying enzyme of influenza C virus is neuraminate-O-acetylesterase. The EMBO journal **4:**1503-1506.
63. **Gao Q, Brydon EW, Palese P.** 2008. A seven-segmented influenza A virus expressing the influenza C virus glycoprotein HEF. Journal of virology **82:**6419-6426.
64. **Pfeifer JB, Compans RW.** 1984. Structure of the influenza C glycoprotein gene as determined from cloned DNA. Virus research **1:**281-296.
65. **Nakada S, Creager RS, Krystal M, Aaronson RP, Palese P.** 1984. Influenza C virus hemagglutinin: comparison with influenza A and B virus hemagglutinins. Journal of virology **50:**118-124.
66. **Matsuzaki M, Sugawara K, Adachi K, Hongo S, Nishimura H, Kitame F, Nakamura K.** 1992. Location of neutralizing epitopes on the hemagglutinin-esterase protein of influenza C virus. Virology **189:**79-87.
67. **Hewat EA, Cusack S, Ruigrok RW, Verwey C.** 1984. Low resolution structure of the influenza C glycoprotein determined by electron microscopy. Journal of molecular biology **175:**175-193.
68. **Zhang X, Rosenthal PB, Formanowski F, Fitz W, Wong CH, Meier-Ewert H, Skehel JJ, Wiley DC.** 1999. X-ray crystallographic determination of the structure of the influenza C virus haemagglutinin-esterase-fusion glycoprotein. Acta crystallographica. Section D, Biological crystallography **55:**945-961.
69. **Rosenthal PB, Zhang X, Formanowski F, Fitz W, Wong CH, Meier-Ewert H, Skehel JJ, Wiley DC.** 1998. Structure of the haemagglutinin-esterase-fusion glycoprotein of influenza C virus. Nature **396:**92-96.
70. **Doms RW, Lamb RA, Rose JK, Helenius A.** 1993. Folding and assembly of viral membrane proteins. Virology **193:**545-562.
71. **Hongo S, Sugawara K, Homma M, Nakamura K.** 1986. The functions of oligosaccharide chains associated with influenza C viral glycoproteins. I. The formation of influenza C virus particles in the absence of glycosylation. Archives of virology **89:**171-187.
72. **Pekosz A, Lamb RA.** 1999. Cell surface expression of biologically active influenza C virus HEF glycoprotein expressed from cDNA. Journal of virology **73:**8808-8812.
73. **Skehel JJ, Wiley DC.** 2000. Receptor binding and membrane fusion in virus entry: the influenza hemagglutinin. Annual review of biochemistry **69:**531-569.
74. **Hongo S, Sugawara K, Homma M, Nakamura K.** 1986. The functions of oligosaccharide chains associated with influenza C viral glycoproteins. II. The role of carbohydrates in the antigenic properties of influenza C viral glycoproteins. Archives of virology **89:**189-201.
75. **Segal MS, Bye JM, Sambrook JF, Gething MJ.** 1992. Disulfide bond formation during the folding of influenza virus hemagglutinin. The Journal of cell biology **118:**227-244.
76. **Compans RW, Bishop DH, Meier-Ewert H.** 1977. Structural components of influenza C virions. Journal of virology **21:**658-665.
77. **Kendal AP.** 1975. A comparison of "influenza C" with prototype myxoviruses: receptor-destroycing activity (neuraminidase) and structural polypeptides. Virology **65:**87-99.
78. **Sugawara K, Ohuchi M, Nakamura K, Homma M.** 1981. Effects of various proteases on the glycoprotein composition and the infectivity of influenza C virus. Archives of virology **68:**147-151.
79. **Szepanski S, Veit M, Pleschka S, Klenk HD, Schmidt MF, Herrler G.** 1994. Post-translational folding of the influenza C virus glycoprotein HEF: defective processing in cells expressing the cloned gene. The Journal of general virology **75 (Pt 5):**1023-1030.
80. **Herrler G, Compans RW, Meier-Ewert H.** 1979. A precursor glycoprotein in influenza C virus. Virology **99:**49-56.

81. **Oeffner F, Klenk HD, Herrler G.** 1999. The cytoplasmic tail of the influenza C virus glycoprotein HEF negatively affects transport to the cell surface. The Journal of general virology **80 (Pt 2):**363-369.
82. **Vlasak R, Krystal M, Nacht M, Palese P.** 1987. The influenza C virus glycoprotein (HE) exhibits receptor-binding (hemagglutinin) and receptor-destroying (esterase) activities. Virology **160:**419-425.
83. **Engel S, de Vries M, Herrmann A, Veit M.** 2012. Mutation of a raft-targeting signal in the transmembrane region retards transport of influenza virus hemagglutinin through the Golgi. FEBS Lett **586:**277-282.
84. **Takashita E, Muraki Y, Sugawara K, Asao H, Nishimura H, Suzuki K, Tsuji T, Hongo S, Ohara Y, Kawaoka Y, Ozawa M, Matsuzaki Y.** 2012. Intrinsic temperature sensitivity of influenza C virus hemagglutinin-esterase-fusion protein. Journal of virology **86:**13108-13111.
85. **Garten W, Will C, Buckard K, Kuroda K, Ortmann D, Munk K, Scholtissek C, Schnittler H, Drenckhahn D, Klenk HD.** 1992. Structure and assembly of hemagglutinin mutants of fowl plague virus with impaired surface transport. Journal of virology **66:**1495-1505.
86. **O'Callaghan RJ, Loughlin M, Labat DD, Howe C.** 1977. Properties of influenza C virus grown in cell culture. Journal of virology **24:**875-882.
87. **Wagaman PC, Spence HA, O'Callaghan RJ.** 1989. Detection of influenza C virus by using an in situ esterase assay. Journal of clinical microbiology **27:**832-836.
88. **Crescenzo-Chaigne B, van der Werf S.** 2007. Rescue of influenza C virus from recombinant DNA. Journal of virology **81:**11282-11289.
89. **Nagele A, Meier-Ewert H.** 1984. Influenza-C-virion-associated RNA-dependent RNA-polymerase activity. Bioscience reports **4:**703-706.
90. **Klenk HD, Rott R, Orlich M, Blodorn J.** 1975. Activation of influenza A viruses by trypsin treatment. Virology **68:**426-439.
91. **Lazarowitz SG, Choppin PW.** 1975. Enhancement of the infectivity of influenza A and B viruses by proteolytic cleavage of the hemagglutinin polypeptide. Virology **68:**440-454.
92. **Kitame F, Sugawara K, Ohwada K, Homma M.** 1982. Proteolytic activation of hemolysis and fusion by influenza C virus. Archives of virology **73:**357-361.
93. **Ohuchi M, Ohuchi R, Mifune K.** 1982. Demonstration of hemolytic and fusion activities of influenza C virus. Journal of virology **42:**1076-1079.
94. **Neumann G, Kawaoka Y.** 2006. Host range restriction and pathogenicity in the context of influenza pandemic. Emerging infectious diseases **12:**881-886.
95. **Stieneke-Grober A, Vey M, Angliker H, Shaw E, Thomas G, Roberts C, Klenk HD, Garten W.** 1992. Influenza virus hemagglutinin with multibasic cleavage site is activated by furin, a subtilisin-like endoprotease. The EMBO journal **11:**2407-2414.
96. **Horimoto T, Kawaoka Y.** 1994. Reverse genetics provides direct evidence for a correlation of hemagglutinin cleavability and virulence of an avian influenza A virus. Journal of virology **68:**3120-3128.
97. **Bottcher-Friebertshauser E, Klenk HD, Garten W.** 2013. Activation of influenza viruses by proteases from host cells and bacteria in the human airway epithelium. Pathogens and disease **69:**87-100.
98. **Nerome K, Nakayama M, Ishida M.** 1979. Established cell line sensitive to influenza C virus. The Journal of general virology **43:**257-259.
99. **Veit M.** 2012. Palmitoylation of virus proteins. Biology of the cell / under the auspices of the European Cell Biology Organization **104:**493-515.
100. **Veit M, Serebryakova MV, Kordyukova LV.** 2013. Palmitoylation of influenza virus proteins. Biochemical Society transactions **41:**50-55.
101. **Veit M, Herrler G, Schmidt MF, Rott R, Klenk HD.** 1990. The hemagglutinating glycoproteins of influenza B and C viruses are acylated with different fatty acids. Virology **177:**807-811.
102. **Veit M, Reverey H, Schmidt MF.** 1996. Cytoplasmic tail length influences fatty acid selection for acylation of viral glycoproteins. The Biochemical journal **318 (Pt 1):**163-172.

103. **Kordyukova LV, Serebryakova MV, Baratova LA, Veit M.** 2008. S acylation of the hemagglutinin of influenza viruses: mass spectrometry reveals site-specific attachment of stearic acid to a transmembrane cysteine. Journal of virology **82:**9288-9292.
104. **Veit M, Kretzschmar E, Kuroda K, Garten W, Schmidt MF, Klenk HD, Rott R.** 1991. Site-specific mutagenesis identifies three cysteine residues in the cytoplasmic tail as acylation sites of influenza virus hemagglutinin. Journal of virology **65:**2491-2500.
105. **Naeve CW, Williams D.** 1990. Fatty acids on the A/Japan/305/57 influenza virus hemagglutinin have a role in membrane fusion. The EMBO journal **9:**3857-3866.
106. **Naim HY, Amarneh B, Ktistakis NT, Roth MG.** 1992. Effects of altering palmitylation sites on biosynthesis and function of the influenza virus hemagglutinin. Journal of virology **66:**7585-7588.
107. **Steinhauer DA, Wharton SA, Wiley DC, Skehel JJ.** 1991. Deacylation of the hemagglutinin of influenza A/Aichi/2/68 has no effect on membrane fusion properties. Virology **184:**445-448.
108. **Brett K, Kordyukova LV, Serebryakova MV, Mintaev RR, Alexeevski AV, Veit M.** 2014. Site-specific S-acylation of influenza virus hemagglutinin: the location of the acylation site relative to the membrane border is the decisive factor for attachment of stearate. The Journal of biological chemistry **289:**34978-34989.
109. **Greaves J, Chamberlain LH.** 2011. DHHC palmitoyl transferases: substrate interactions and (patho)physiology. Trends in biochemical sciences **36:**245-253.
110. **Chen BJ, Takeda M, Lamb RA.** 2005. Influenza virus hemagglutinin (H3 subtype) requires palmitoylation of its cytoplasmic tail for assembly: M1 proteins of two subtypes differ in their ability to support assembly. Journal of virology **79:**13673-13684.
111. **Wagner R, Herwig A, Azzouz N, Klenk HD.** 2005. Acylation-mediated membrane anchoring of avian influenza virus hemagglutinin is essential for fusion pore formation and virus infectivity. Journal of virology **79:**6449-6458.
112. **Zurcher T, Luo G, Palese P.** 1994. Mutations at palmitylation sites of the influenza virus hemagglutinin affect virus formation. Journal of virology **68:**5748-5754.
113. **Sakai T, Ohuchi R, Ohuchi M.** 2002. Fatty acids on the A/USSR/77 influenza virus hemagglutinin facilitate the transition from hemifusion to fusion pore formation. Journal of virology **76:**4603-4611.
114. **Ujike M, Nakajima K, Nobusawa E.** 2004. Influence of acylation sites of influenza B virus hemagglutinin on fusion pore formation and dilation. Journal of virology **78:**11536-11543.
115. **Engel S, Scolari S, Thaa B, Krebs N, Korte T, Herrmann A, Veit M.** 2010. FLIM-FRET and FRAP reveal association of influenza virus haemagglutinin with membrane rafts. The Biochemical journal **425:**567-573.
116. **Levental I, Grzybek M, Simons K.** 2010. Greasing their way: lipid modifications determine protein association with membrane rafts. Biochemistry **49:**6305-6316.
117. **Melkonian KA, Ostermeyer AG, Chen JZ, Roth MG, Brown DA.** 1999. Role of lipid modifications in targeting proteins to detergent-resistant membrane rafts. Many raft proteins are acylated, while few are prenylated. The Journal of biological chemistry **274:**3910-3917.
118. **Veit M, Thaa B.** 2011. Association of influenza virus proteins with membrane rafts. Advances in virology **2011:**370606.
119. **Zhang J, Pekosz A, Lamb RA.** 2000. Influenza virus assembly and lipid raft microdomains: a role for the cytoplasmic tails of the spike glycoproteins. Journal of virology **74:**4634-4644.
120. **Herrler G, Klenk HD.** 1987. The surface receptor is a major determinant of the cell tropism of influenza C virus. Virology **159:**102-108.
121. **Herrler G, Reuter G, Rott R, Klenk HD, Schauer R.** 1987. N-acetyl-9-O-acetylneuraminic acid, the receptor determinant for influenza C virus, is a differentiation marker on chicken erythrocytes. Biological chemistry Hoppe-Seyler **368:**451-454.

122. **Thomas JK, Noppenberger J.** 2007. Avian influenza: a review. American journal of health-system pharmacy : AJHP : official journal of the American Society of Health-System Pharmacists **64:**149-165.
123. **Trebbien R, Larsen LE, Viuff BM.** 2011. Distribution of sialic acid receptors and influenza A virus of avian and swine origin in experimentally infected pigs. Virology journal **8:**434.
124. **Muchmore EA, Varki A.** 1987. Selective inactivation of influenza C esterase: a probe for detecting 9-O-acetylated sialic acids. Science **236:**1293-1295.
125. **Zimmer G, Suguri T, Reuter G, Yu RK, Schauer R, Herrler G.** 1994. Modification of sialic acids by 9-O-acetylation is detected in human leucocytes using the lectin property of influenza C virus. Glycobiology **4:**343-349.
126. **Martin LT, Verhagen A, Varki A.** 2003. Recombinant influenza C hemagglutinin-esterase as a probe for sialic acid 9-O-acetylation. Methods in enzymology **363:**489-498.
127. **Szepanski S, Gross HJ, Brossmer R, Klenk HD, Herrler G.** 1992. A single point mutation of the influenza C virus glycoprotein (HEF) changes the viral receptor-binding activity. Virology **188:**85-92.
128. **Vlasak R, Luytjes W, Spaan W, Palese P.** 1988. Human and bovine coronaviruses recognize sialic acid-containing receptors similar to those of influenza C viruses. Proceedings of the National Academy of Sciences of the United States of America **85:**4526-4529.
129. **Schwegmann-Wessels C, Herrler G.** 2006. Sialic acids as receptor determinants for coronaviruses. Glycoconjugate journal **23:**51-58.
130. **Mayr J, Haselhorst T, Langereis MA, Dyason JC, Huber W, Frey B, Vlasak R, de Groot RJ, von Itzstein M.** 2008. Influenza C virus and bovine coronavirus esterase reveal a similar catalytic mechanism: new insights for drug discovery. Glycoconjugate journal **25:**393-399.
131. **Zeng Q, Langereis MA, van Vliet AL, Huizinga EG, de Groot RJ.** 2008. Structure of coronavirus hemagglutinin-esterase offers insight into corona and influenza virus evolution. Proceedings of the National Academy of Sciences of the United States of America **105:**9065-9069.
132. **Hamilton BS, Whittaker GR, Daniel S.** 2012. Influenza virus-mediated membrane fusion: determinants of hemagglutinin fusogenic activity and experimental approaches for assessing virus fusion. Viruses **4:**1144-1168.
133. **Formanowski F, Wharton SA, Calder LJ, Hofbauer C, Meier-Ewert H.** 1990. Fusion characteristics of influenza C viruses. The Journal of general virology **71 (Pt 5):**1181-1188.
134. **Huang RT, Rott R, Klenk HD.** 1981. Influenza viruses cause hemolysis and fusion of cells. Virology **110:**243-247.
135. **Lenard J, Miller DK.** 1981. pH-dependent hemolysis by influenza, Semliki, Forest virus, and Sendai virus. Virology **110:**479-482.
136. **Maeda T, Ohnishi S.** 1980. Activation of influenza virus by acidic media causes hemolysis and fusion of erythrocytes. FEBS letters **122:**283-287.
137. **Mair CM, Meyer T, Schneider K, Huang Q, Veit M, Herrmann A.** 2014. A histidine residue of the influenza virus hemagglutinin controls the pH dependence of the conformational change mediating membrane fusion. Journal of virology **88:**13189-13200.
138. **Bullough PA, Hughson FM, Skehel JJ, Wiley DC.** 1994. Structure of influenza haemagglutinin at the pH of membrane fusion. Nature **371:**37-43.
139. **Harrison SC.** 2008. Viral membrane fusion. Nature structural & molecular biology **15:**690-698.
140. **Cross KJ, Langley WA, Russell RJ, Skehel JJ, Steinhauer DA.** 2009. Composition and functions of the influenza fusion peptide. Protein and peptide letters **16:**766-778.
141. **Kemble GW, Danieli T, White JM.** 1994. Lipid-anchored influenza hemagglutinin promotes hemifusion, not complete fusion. Cell **76:**383-391.
142. **Han X, Bushweller JH, Cafiso DS, Tamm LK.** 2001. Membrane structure and fusion-triggering conformational change of the fusion domain from influenza hemagglutinin. Nature structural biology **8:**715-720.

143. **Lorieau JL, Louis JM, Schwieters CD, Bax A.** 2012. pH-triggered, activated-state conformations of the influenza hemagglutinin fusion peptide revealed by NMR. Proceedings of the National Academy of Sciences of the United States of America **109:**19994-19999.
144. **Kraut J.** 1977. Serine proteases: structure and mechanism of catalysis. Annual review of biochemistry **46:**331-358.
145. **Herrler G, Multhaup G, Beyreuther K, Klenk HD.** 1988. Serine 71 of the glycoprotein HEF is located at the active site of the acetylesterase of influenza C virus. Archives of virology **102:**269-274.
146. **Pleschka S, Klenk HD, Herrler G.** 1995. The catalytic triad of the influenza C virus glycoprotein HEF esterase: characterization by site-directed mutagenesis and functional analysis. The Journal of general virology **76 (Pt 10):**2529-2537.
147. **Crescenzo-Chaigne B, Naffakh N, van der Werf S.** 1999. Comparative analysis of the ability of the polymerase complexes of influenza viruses type A, B and C to assemble into functional RNPs that allow expression and replication of heterotypic model RNA templates in vivo. Virology **265:**342-353.
148. **Crescenzo-Chaigne B, van der Werf S.** 2001. Nucleotides at the extremities of the viral RNA of influenza C virus are involved in type-specific interactions with the polymerase complex. The Journal of general virology **82:**1075-1083.
149. **Sugawara K, Muraki Y, Takashita E, Matsuzaki Y, Hongo S.** 2006. Conformational maturation of the nucleoprotein synthesized in influenza C virus-infected cells. Virus research **122:**45-52.
150. **Muraki Y, Murata T, Takashita E, Matsuzaki Y, Sugawara K, Hongo S.** 2007. A mutation on influenza C virus M1 protein affects virion morphology by altering the membrane affinity of the protein. Journal of virology **81:**8766-8773.
151. **Pekosz A, Lamb RA.** 1997. The CM2 protein of influenza C virus is an oligomeric integral membrane glycoprotein structurally analogous to influenza A virus M2 and influenza B virus NB proteins. Virology **237:**439-451.
152. **Betakova T, Hay AJ.** 2007. Evidence that the CM2 protein of influenza C virus can modify the pH of the exocytic pathway of transfected cells. The Journal of general virology **88:**2291-2296.
153. **Hongo S, Sugawara K, Nishimura H, Muraki Y, Kitame F, Nakamura K.** 1994. Identification of a second protein encoded by influenza C virus RNA segment 6. The Journal of general virology **75 (Pt 12):**3503-3510.
154. **Li ZN, Hongo S, Sugawara K, Sugahara K, Tsuchiya E, Matsuzaki Y, Nakamura K.** 2001. The sites for fatty acylation, phosphorylation and intermolecular disulphide bond formation of influenza C virus CM2 protein. The Journal of general virology **82:**1085-1093.
155. **Okuwa T, Muraki Y, Himeda T, Ohara Y.** 2012. Glycosylation of CM2 is important for efficient replication of influenza C virus. Virology **433:**167-175.
156. **Furukawa T, Muraki Y, Noda T, Takashita E, Sho R, Sugawara K, Matsuzaki Y, Shimotai Y, Hongo S.** 2011. Role of the CM2 protein in the influenza C virus replication cycle. Journal of virology **85:**1322-1329.
157. **Muraki Y, Okuwa T, Furukawa T, Matsuzaki Y, Sugawara K, Himeda T, Hongo S, Ohara Y.** 2011. Palmitoylation of CM2 is dispensable to influenza C virus replication. Virus research **157:**99-105.
158. **Muraki Y, Okuwa T, Himeda T, Hongo S, Ohara Y.** 2013. Effect of cysteine mutations in the extracellular domain of CM2 on the influenza C virus replication. PloS one **8:**e60510.
159. **Pachler K, Vlasak R.** 2011. Influenza C virus NS1 protein counteracts RIG-I-mediated IFN signalling. Virology journal **8:**48.
160. **Muraki Y, Furukawa T, Kohno Y, Matsuzaki Y, Takashita E, Sugawara K, Hongo S.** 2010. Influenza C virus NS1 protein upregulates the splicing of viral mRNAs. Journal of virology **84:**1957-1966.
161. **Paragas J, Talon J, O'Neill RE, Anderson DK, Garcia-Sastre A, Palese P.** 2001. Influenza B and C virus NEP (NS2) proteins possess nuclear export activities. Journal of virology **75:**7375-7383.

162. **Kohno Y, Muraki Y, Matsuzaki Y, Takashita E, Sugawara K, Hongo S.** 2009. Intracellular localization of influenza C virus NS2 protein (NEP) in infected cells and its incorporation into virions. Archives of virology **154:**235-243.
163. **Crescenzo-Chaigne B, Barbezange C, van der Werf S.** 2013. The Panhandle formed by influenza A and C virus NS non-coding regions determines NS segment expression. PloS one **8:**e81550.
164. **Neumann G, Whitt MA, Kawaoka Y.** 2002. A decade after the generation of a negative-sense RNA virus from cloned cDNA - what have we learned? The Journal of general virology **83:**2635-2662.
165. **Luytjes W, Krystal M, Enami M, Parvin JD, Palese P.** 1989. Amplification, expression, and packaging of foreign gene by influenza virus. Cell **59:**1107-1113.
166. **Neumann G, Zobel A, Hobom G.** 1994. RNA polymerase I-mediated expression of influenza viral RNA molecules. Virology **202:**477-479.
167. **Neumann G, Watanabe T, Ito H, Watanabe S, Goto H, Gao P, Hughes M, Perez DR, Donis R, Hoffmann E, Hobom G, Kawaoka Y.** 1999. Generation of influenza A viruses entirely from cloned cDNAs. Proceedings of the National Academy of Sciences of the United States of America **96:**9345-9350.
168. **Hoffmann E, Neumann G, Kawaoka Y, Hobom G, Webster RG.** 2000. A DNA transfection system for generation of influenza A virus from eight plasmids. Proceedings of the National Academy of Sciences of the United States of America **97:**6108-6113.
169. **Sims RJ, 3rd, Mandal SS, Reinberg D.** 2004. Recent highlights of RNA-polymerase-II-mediated transcription. Current opinion in cell biology **16:**263-271.
170. **Kornberg RD.** 1999. Eukaryotic transcriptional control. Trends in cell biology **9:**M46-49.
171. **Gerl MJ, Sampaio JL, Urban S, Kalvodova L, Verbavatz JM, Binnington B, Lindemann D, Lingwood CA, Shevchenko A, Schroeder C, Simons K.** 2012. Quantitative analysis of the lipidomes of the influenza virus envelope and MDCK cell apical membrane. The Journal of cell biology **196:**213-221.
172. **Rossman JS, Lamb RA.** 2011. Influenza virus assembly and budding. Virology **411:**229-236.
173. **Rossman JS, Jing X, Leser GP, Lamb RA.** 2010. Influenza virus M2 protein mediates ESCRT-independent membrane scission. Cell **142:**902-913.
174. **Melikyan GB, Jin H, Lamb RA, Cohen FS.** 1997. The role of the cytoplasmic tail region of influenza virus hemagglutinin in formation and growth of fusion pores. Virology **235:**118-128.
175. **Harrison SC.** 2015. Viral membrane fusion. Virology **479-480C:**498-507.
176. **Melikyan GB, Niles WD, Peeples ME, Cohen FS.** 1993. Influenza hemagglutinin-mediated fusion pores connecting cells to planar membranes: flickering to final expansion. The Journal of general physiology **102:**1131-1149.
177. **Mercer J, Schelhaas M, Helenius A.** 2010. Virus entry by endocytosis. Annual review of biochemistry **79:**803-833.
178. **Huotari J, Helenius A.** 2011. Endosome maturation. The EMBO journal **30:**3481-3500.
179. **Otterstrom J, van Oijen AM.** 2013. Visualization of membrane fusion, one particle at a time. Biochemistry **52:**1654-1668.

8. Supplemental material

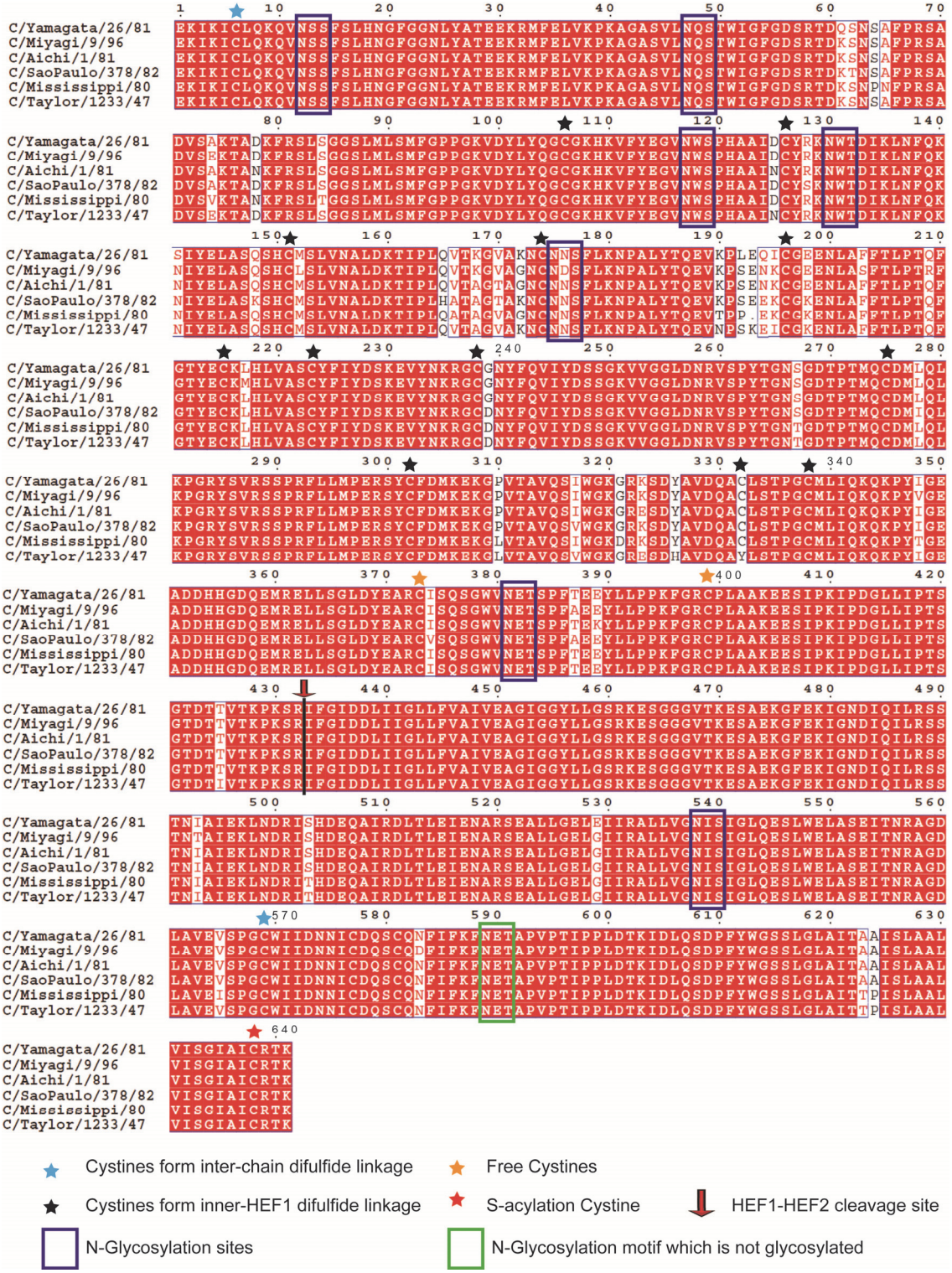

9. Acknowledgements

I am deeply grateful to my supervisor, Dr. Michael Veit, for offering me the precious opportunity to pursuit my Ph.D study in his lab, and for guiding me and motivating me to complete this thesis. I enjoyed great benefits of his profound knowledge, rigorous academic attitude and motivation.

I would also like to thank my co-supervisors, Univ. -Prof. Dr. Nikolaus Osterrieder and Dr. Karsten Tedin for all their valuable supports, comments, suggestions and guidance. It is my great honor to have them as my co-supervisors.

Many thanks to Dr. Christoph Böttcher and Dr. Kai Ludwig for their generous help and exquisite skills on electron microscopy.

Many thanks to all the members of the Michael Veit's group. I thank Bastain Thaa, Ludwig Krabben, Balaji Sinhadri, Ania Wieliczco, Maren de Vries, Katharina Brett, Stefanie Siche, Mingze Zhang and Susanne Kaufer for all the supports and friendship. I appreciate Angelika Thomele, Elke Dyrks and Claudia Tielesch for their help. Many thanks to Fiona Kerlin for her great assistant work for my research and all the interesting cultural communications.

Many thanks to all the members of the Institut für Virologie, FU-Berlin, for all their supports and friendship.

All my heartfelt thanks to my beloved wife, Jing Zhang, who is the pillar of my life and supports me all the time. I am also very thankful to my parents for all their understanding and encouragements.

Last but not least, I am very appreciating the China Scholarship Council (CSC) for financially sponsoring me to study in Germany for these years.

Selbständigkeitserklärung

Hiermit bestätige ich, dass ich die vorliegende Arbeit selbständig angefertigt habe. Ich versichere, dass ich ausschließlich die angegebenen Quellen und Hilfen in Anspruch genommen habe.

Berlin, den June 25, 2015 Mingyang Wang